PREFERENTIAL ESTIMATION

THÈSE N^{O} 4004 (2008)

PRÉSENTÉE LE 22 FÉVRIER 2008

À LA FACULTÉ DES SCIENCES ET TECHNIQUES DE L'INGÉNIEUR

Laboratoire d'Automatique

SECTION DE GÉNIE MÉCANIQUE

ÉCOLE POLYTECHNIQUE FÉDÉRALE DE LAUSANNE

POUR L'OBTENTION DU GRADE DE DOCTEUR ÈS SCIENCES

PAR

Levente Csaba BÓDIZS

Ingénieur en chimie, Université Babeş-Bolyai, Cluj-Napoca, Roumanie
et de nationalité roumaine

acceptée sur proposition du jury:

Prof. P. Xirouchakis, président du jury
Prof. D. Bonvin, directeur de thèse
Prof. B. Merminod, rapporteur
Prof. B. A. Ogunnaike, rapporteur
Prof. B. Srinivasan, rapporteur

ÉCOLE POLYTECHNIQUE
FÉDÉRALE DE LAUSANNE

Lausanne, EPFL
2008

Édesanyám, Gúti Gabriella (1952-2007), és
nagybátyám, Gúti József (1954-2007),
emlékére

Acknowledgments

I would like to express my gratitude towards my teachers for guiding me throughout my professional life. Prof. Dominique Bonvin gave me the opportunity to join the Laboratoire d'Automatique and allowed me to have the right balance of professional and private life. I would like to thank him and Prof. Bala Srinivasan for all the helpful discussions we had and ideas they gave me during my doctoral studies. Dr. Zoltán K. Nagy introduced me to the field of process control during my engineering studies at Universitatea Babeş-Bolyai and had a great influence on my decision to continue my studies at the doctoral level. Cseresznyés Éva and Schwartz István, my chemistry and physics teachers at high-school, Lorántffy Zsuzsanna Református Gimnázium, Oradea, made me enjoy science and decide to take up a career in engineering. My English teachers, Oláh Mária and Galaczi Juli, enabled me to pursue an international career.

I would also like to thank my colleagues at Laboratoire d'Automatique for accepting me and guiding me in all aspects of my stay in Switzerland. I am grateful to Philippe for helping me out when having computer-related problems, and to the 'secrétariat' for their help with administrative issues. I also thank my friends in Lausanne and back home with whom I passed unforgettable moments.

Finally, my special thanks go to my family. My mother, Gúti Gabriella, my father, Bódizs János, and my uncle, Gúti József, loved and helped me throughout my life. I owe them everything I have today. Most of all, I would like to thank my wife, Gabi, for all the joy and support she gave me in the past and will give me in the future.

Abstract

State estimation is a necessary component of advanced monitoring and control techniques, since these techniques often require information that is too expensive or impossible to obtain from direct measurements. The objective of estimation is the reconstruction of the missing information from both the available measurements and prior knowledge in the form of a dynamic model.

Usually, full-state estimation is considered because of the close link between estimation and the state feedback literature. By having an accurate estimate of all states, the entire system can be controlled, provided the system is controllable. However, since in some cases the goal is to control only a subset of the states, knowledge of all states is not required. The objective of this thesis is to estimate accurately a vector of *preferred variables*, whose dimension is much lower than that of the full state vector, while paying no attention to the accuracy of the estimates of the remaining variables. Such a problem might arise, for example, when optimizing a process by tracking active constraints.

Biased estimates are often obtained due to the presence of plant-model mismatch. This mismatch can be regarded as a deterministic disturbance. In addition, the measurements of key variables might be available less frequently than the output measurements. The problem of *preferential estimation* (PE) is formulated as that of eliminating the bias in the estimates of the preferred variables using their infrequent measurements and a full-order model. Hence, the measurements are handled at two time scales. Such a concept has been studied thoroughly in the literature for the purpose of standard estimation, i.e. estimating all states accurately, for which infrequent measurements of all states are needed. The advantage of PE is to require a smaller number of measurements, despite using the full-order model.

The following observer structures are studied in the thesis:

- *Proportional observer*. This structure contains a correction term proportional to errors obtained from the frequent measurements of the output variables. The gains corresponding to this term are computed from the infrequent measurements of the preferred variables, thus leading to a calibration-type approach. It is shown that bias can be eliminated in the preferred variables by an appropriate choice of the gains. Due to the observer structure, a different set of gains is required for each disturbance value. Hence, the gains have to be retuned each time the disturbances change or, since the disturbances are not measurable, each time a new measurement of the preferred variables becomes available.
- *Integral observer*. In addition to the proportional term based on the frequent measurements of the output variables, this structure contains an integral term based on the infrequent measurements of the preferred variables. Hence, this observer has a dual-rate structure. The presence of the integral term guarantees bias elimination in the preferred variables even for varying disturbances, provided the observer is stable. It is shown that stability can be guaranteed, and a procedure for tuning the observer gains is provided. The design parameters in this procedure can also be determined using a calibration-type approach.

To simplify the mathematical developments, PE is formulated for linear time-invariant (LTI) systems. Its performance is investigated both analytically and through simulation. Though the analysis is restricted to LTI systems, the idea extends to more general systems, which is demonstrated via the estimation of biomass and enzyme concentrations in a pilot-scale filamentous fungal fermentation.

Keywords: Estimation, deterministic disturbances, proportional observer, integral observer, filamentous fungal fermentation.

Version abrégée

L'estimation d'état est une composante vitale des techniques de réglage et de surveillance. Toutefois, ces techniques nécessitent des informations qui sont obtenues, soit de manière trop onéreuse, soit manière indirecte et non propice à une utilisation adéquate. Le but de l'estimation est la reconstruction des ces informations manquantes à partir des mesures disponibles en tenant compte au mieux des connaissances a priori formulés comme un modèle dynamique.

De manière générale, l'estimation nécessite la reconstruction de tous les états nécessaires à l'élaboration de la loi de commande. L'obtention de l'ensemble de toutes les variables de l'état conduit, dans la plupart des cas, à un comportement adéquat de la boucle commandée lorsque le système est commandable et que le régulateur est synthétisé de manière adéquate. Cependant, dans certains cas, il est avantageux de ne considérer que la sous partie de l'état réellement nécessaire pour le bon comportement du système bouclé. Ainsi, il est souvent possible d'estimer qu'une partie réduite de l'état. L'objectif de cette thèse est de déduire cet ensemble de variables en observant une collection de variables (dites préférentielles) qui sont inférieurs en nombre par rapport au nombre de variables d'état du système. L'idée maîtresse est de négliger la précision d'estimation des variables complémentaires. Un exemple d'application de cette technique se situe par exemple dans les problèmes d'estimation lors de l'optimisation d'un procédé par la technique de poursuite des conditions nécessaires d'optimalité.

Remarquons que le modèle dynamique disponible fournit souvent des prédictions biaisés en raison de la présence d'erreurs de modélisation. Ces erreurs apparaissent comme des perturbations déterministes. Par ailleurs, les mesures des variables clés sont disponibles à des cadences inférieures à la mesure des variables de sortie. Le problème d'*estimation préférentielle* (EP) est formulé comme l'élimination du biais dans les estimations des variables

préférentielles en utilisant leur mesure respective peu fréquente, ainsi q'un modèle d'état complet. Par conséquant, des mesures disponibles à deux échelles de temps sont utilisés. Un tel concept est abondamment discuté dans la litterature du point de vue de l'estimation standard (ES), c.à.d. du point de vue de l'estimation précise de l'ensemble des états. Cependant, des mesures peu fréquentes de tous les états sont nécessaires pour l'ES. L'avantage de l'EP est qu'elles nécessitent qu'un faible nombre de variables mesurés, malgré l'utilisation d'un modèle d'état complet.

Les observateurs suivants sont étudiés dans cette thèse:

- *Les observateurs de type proportionnel.* Cette structure contient un seul terme de correction qui est proportionnel à l'erreur obtenue à partir des mesures fréquentes des variables de sortie. Les gains correspondants sont calculés en se basant sur des mesures peu fréquentes des variables préférentielles. Ceci conduit à une approche similaire au concept de calibrage. Il est démontré que le biais peut être éliminé dans les variables préférentielles avec un choix de gains appropriés. De part la structure même de l'observateur, chaque perturbation nécessite des gains différents. En conséquence, l'observateur doit être réajusté chaque fois que la perturbation change, ou, lorsque la perturbation n'est pas mesurable, à l'arrivé de chaque nouvelle mesure des variables préférentielles.

- *Les observateurs à effet intégral.* En plus du terme proportionnel basé sur les mesures de sortie disponibles à l'échelle de temps rapide, cette structure contient un terme intégral basé sur les mesures peu fréquentes des variables préférentielles. Le résultat est une structure d'observateur à deux échelles de temps. La présence du terme intégral garantit l'elimination du biais dans les variables préférentielles, même lorsque les perturbations changent (pour autant que l'observateur soit stable). Il est toutefois démontré que la stabilité peut être garantie, et une procédure d'ajustage de gains d'observateur est fournie. Les paramètres d'ajustage sont dans ce cas également déterminés à l'aide d'une approche de calibrage.

Pour simplifier les développements mathématiques, l'EP est formulée pour des systèmes linéaires stationnaires. Sa performance est, d'une part

étudié analytiquement, et d'autre part vérifiée à l'aide de simulations. Bien que l'analyse soit restreinte au cas des systèmes stationnaires, l'idé s'étend également à des systémes plus généraux. Cette généralisation est illustrée et démontrée sur l'estimation des concentrations de biomasse et d'enzyme dans une fermentation de fongus filamenteux exploité dans une installation pilote.

Mots clés: estimation, perturbations déterministes, observateur proportionnel, observateur intégral, fermentation de fongus filamenteux.

Contents

Notation Glossary **xx**

1 Introduction **1**
1.1 A brief historical overview of estimation 2
1.2 Motivation and related work 3
1.3 Contributions made by this thesis 8
1.4 Organization of the thesis 10

2 Preliminaries **13**
2.1 Plant description 14
2.2 Notions of stability and observability 15
2.2.1 Asymptotic stability 15
2.2.2 Observability 16
2.3 Luenberger observer 17
2.3.1 Observer structure 17
2.3.2 Pole placement 18
2.4 Integral observer 19
2.4.1 Need for an integral term 19
2.4.2 Observer structure 21
2.4.3 Integral observability 22
2.5 Kalman filter 23
2.5.1 Observer structure 24
2.5.2 Kalman filter extended with integrators 25
2.6 Dual-rate observers 29
2.6.1 Fast-time-scale correction 31
2.6.2 Slow-time-scale correction 31
2.7 Illustration 32

3 Proportional observer for preferential estimation 45
3.1 Preferential estimation 45
3.1.1 Problem formulation 45
3.1.2 Observers for preferential estimation 46
3.2 Proportional observer P^y 49
3.2.1 Observer structure 50
3.2.2 Convergence of the error dynamics 50
3.2.3 Estimation bias 51
3.2.4 Bias - variance tradeoff 53
3.2.5 Calibration-based tuning 55
3.2.6 Illustration 57
3.2.7 Discussion 65

4 Integral observer for preferential estimation 69
4.1 Observer structure $P^y P^z I^z$ 70
4.2 Observability from the z measurements 71
4.2.1 Observability of a single-rate system ($r = 1$) from z . 71
4.2.2 Observability of a dual-rate system ($r > 1$) from z . . 72
4.3 Convergence of the error dynamics 74
4.4 Estimation bias 81
4.5 Calibration-based tuning 82
4.6 Illustration 84
4.7 Discussion 91

5 Experimental study of a fed-batch filamentous fungal fermentation 95
5.1 Process description and industrial practice 96
5.1.1 Current operation 96
5.1.2 Measurements 98
5.2 Filamentous fungal fermentation model 101
5.2.1 Morphology and rate expressions 101
5.2.2 Mass balance equations 103
5.2.3 Oxygen transfer 104
5.2.4 State-space model used for preferential estimation . . 105
5.3 Observer design 105

5.3.1 Extended Kalman filter based on y_k and z_l measurements – EKF-ZOH . . . 106
5.3.2 Proportional observer based on y_k measurements – P^y 109
5.3.3 Proportional - Proportional Integral observer based on y_k and z_l measurements – $P^y P^z I^z$ . . . 110
5.4 Experimental results . . . 111
5.4.1 Model open-loop prediction capability . . . 111
5.4.2 EKF-ZOH . . . 112
5.4.3 P^y . . . 115
5.4.4 $P^y P^z I^z$ . . . 117
5.5 Discussion . . . 120

6 Conclusions **123**
6.1 Summary . . . 123
6.2 Perspectives . . . 125

A Kinetic expressions, model parameters and notations used in the fed-batch filamentous fermentation model **127**
A.1 Kinetic expressions . . . 127
A.2 Model parameters . . . 127
A.3 Notations . . . 129

Bibliography **133**

Curriculum vitae and list of publications **141**

Notation Glossary

Abbreviations

P^y	Proportional to the error in y
$P^y I^y$	Proportional to the error in y - Integral of the error in y
$P^y P^z I^z$	Proportional to the error in y - Proportional to the error in z - Integral of the error in z
EKF	Extended Kalman Filter
KF	Kalman Filter
KNVD	Kautsky-Nichols-Van Dooren
LO	Luenberger Observer
LSE	Least-Squares Estimation
LTI	Linear Time Invariant
LTV	Linear Time Varying
MIMO	Multiple Input Multiple Output
MISO	Multiple Input Single Output
MLE	Maximum Likelihood Estimation
MSE	Mean Square Error
NCO	Necessary Conditions of Optimality
PE	Preferential Estimation
SE	Standard Estimation
ZOH	Zero-Order Hold

Subscripts, superscripts and indices

$(\cdot)_k$	Fast sampling index
$(\cdot)_l$	Slow sampling index
$\bar{(\cdot)}$	Constant value of a variable

$\hat{(\cdot)}$	Estimate of a variable
$\tilde{(\cdot)}$	Piecewise constant variable

Operators

$(\cdot)^T$	Transpose of a vector or matrix
$(\cdot)^{-1}$	Matrix inverse
Φ	State observer
$\det(\cdot)$	Determinant of a matrix
$\mathrm{diag}(\cdot)$	Diagonal of a matrix
$\mathrm{E}(\cdot)$	Mathematical expectation
$\mathrm{tr}(\cdot)$	Trace of a matrix

Greek symbols

α	Integral state driven by the error in the output y
β	Integral state driven by the error in the preferred variables z
ΔA	Additive error in the state propagation matrix A
ΔB	Additive error in the input matrix B
Δt_j	Time interval for which the disturbance takes the constant value $d_k = \tilde{d}$
γ	A constant, real scalar
λ^*	Desired pole of the observer
ν_l	Measurement noise associated with the preferred variable
ω_k	Unknown input vector
π	Parameter values
Π_e	Sum of mean square errors
Σ_{Π_e}	Sum of total mean square errors
θ	Delay of the slow measurement in terms of number of small sampling periods
$\mathcal{V}_e$	Sum of error variances

Latin symbols

$\bar{e}$	Sum of the absolute value of biases

$\mathcal{N}$	Set of natural numbers
$\Re$	Space of real numbers
$\Re^i$	Space of real i-dimensional vectors
$\Re^{i \times j}$	Space of real $(i \times j)$ - dimensional matrices
A	State propagation matrix of the state space model
A_c	Closed-loop error propagation matrix ($A_c = A - K^y H$)
B	Input matrix of the state space model
D	Unknown input matrix
d_k	Deterministic disturbance vector
e_i	Estimation error of the variable i
H	Measurement matrix of the state space model
I_i	i-dimensional identity matrix
J	Mean-square estimation error
K	Observer gain
K^y	Gain of the term proportional to the error in y
K^z	Gain of the term proportional to the error in z
K^α	Gain of the integral state α
K^β	Gain of the integral state β
k_i	Number of iterations
L	Projection matrix from states to preferred variables
m	Number of preferred variables
n	Number of states
$N(a, A)$	Normal probability distribution with mean a and variance A
n_d	Number of unknown inputs
n_u	Number of inputs
P	Mean-square estimation error
p	Number of ouputs
Q	Process noise covariance
R	Output measurement noise covariance
r	Ratio of large and small sampling times
T	Similarity transformation matrix
t_k	Small sampling time
t_l	Large sampling time

u_k	Input vector
v_k	Output measurement noise
W	Weighting matrix
w_k	Process noise
x_k	State vector
y_k	Output vector
Z	Covariance of the measurement noise associated with the preferred variable
z_l	Vector of preferred variables

List of Figures

2.1 Multirate estimation scheme. The y_k measurements are available at the discrete time instants k, $k = 0, \ldots, r, r+1, \ldots$. The z_l measurements are taken at the time instants l, $l = 0, 1, 2, \ldots$ for which $k = lr$. The z_l measurements are indicated by circles and become available at the time instants marked by crosses, i.e. with a delay of θ small sampling periods. 30

2.2 Comparison of open-loop model prediction and Luenberger observer in Simulation 1. Plant – dash-dotted line (black); open-loop model – solid line (blue); Luenberger observer – dashed line (red). 36

2.3 Comparison of Luenberger and integral observers in Simulation 2. Plant – dash-dotted line (black); Luenberger observer – solid line (blue); Integral observer – dashed line (red). . . . 37

2.4 Comparison of Luenberger observer and Kalman filter in Simulation 3 for one realization of the noises. Plant – dash-dotted line (black); Luenberger observer – solid line (blue); Kalman filter – dashed line (red). 39

2.5 Comparison of KF and combined state and parameter estimation using a KF extended with integrators in Simulation 5 for one realization. Plant – dash-dotted line (black); Kalman filter – solid line (blue); Parameter estimation using the KF – dashed line (red). 41

2.6 Comparison of KF extended with integrators based on infrequent measurements in Simulation 4 for one realization. Plant – dash-dotted line (black); KF-Integral-ZOH observer – solid line (blue); KF-Integral-Switch observer – dashed line (red). 44

3.1 Comparison of the KF-ZOH and KF-Switch observers in Simulation 6 for one realization. Plant – dash-dotted line (black); KF-Switch observer – solid line (blue); KF-ZOH observer – dashed line (red). 62
3.2 Illustration of the best P^y observer on Simulation 6 for $k \in [0, 200]$ for one realization (x_2 and x_3 are the preferred variables). Plant – dash-dotted line (black); KF-ZOH observer – solid line (blue); $P^y - K^y$ observer – dashed line (red). 63
3.3 Comparison of $P^y - K^y$ and the retuned $P^y - K^y$ observer in Simulation 8 for one realization. Plant – dash-dotted line (black); $P^y - K^y$ observer – solid line (blue); $P^y - K^y$ – *retuned* observer – dashed line (red). 64
3.4 Comparison of KF-ZOH and retuned $P^y - K^y$ observer in Simulation 9 for one realization. Plant – dash-dotted line (black); KF-ZOH observer – solid line (blue); $P^y - K^y$ – *retuned* observer – dashed line (red). 66

4.1 Comparison of the KF-Integral-Switch and the $P^y P^z I^z - \lambda$ observers in Simulation 6 (observer tuning) for one realization. Plant – dash-dotted line (black); KF - Integral - Switch observer – solid line (blue); $P^y P^z I^z - \lambda$ observer – dashed line (red). 88
4.2 Comparison of the KF-Integral-Switch and $P^y P^z I^z - \lambda$ observers in Simulation 8 for one realization. Plant – dash-dotted line (black); KF-Integral-Switch observer – solid line (blue); $P^y P^z I^z - \lambda$ observer – dashed line (red). 90
4.3 Comparison of the $P^y P^z I^z - \lambda$ and retuned $P^y - K^y$ observers in Simulation 9 for one realization. Plant – dash-dotted line (black); $P^y - K^y - retuned$ observer – solid line (blue); $P^y P^z I^z - \lambda$ observer – dashed line (red). 92

5.1 Experiment I - Current operation with three phases: Batch operation - biomass growth; Linearly-increasing feed - avoiding oxygen limitation; Constant feed - enzyme production. . 97
5.2 Morphological division of the biomass [1]. 101

5.3 Open-loop model prediction for Experiment I. Plant – solid line and dots (black); Model – dashed line (red). 112
5.4 Open-loop model prediction for Experiment II. Plant – solid line and dots (black); Model – dashed line (red). 113
5.5 Estimates given by the EKF-ZOH for Experiment II. Plant – solid line and dots (black); EKF-ZOH observer – dashed line (red). 114
5.6 Estimates given by the $P^y - K^y$ observer for Experiment II. Plant – solid line and dots (black); P^y observer – dashed line (red). 115
5.7 Estimates given by the $P^y - K^y - retuned$ observer for Experiment II. Plant – solid line and dots (black); $P^y - K^y - retuned$ observer – dashed line (red). 116
5.8 Estimates given by the I^z observer for Experiment II. Plant – solid line and dots (black); I^z observer – dashed line (red). 117
5.9 Estimates given by the $I^z - L^T$ observer for Experiment II. Plant – solid line and dots (black); $I^z - L^T$ observer – dashed line (red). 118
5.10 Estimates given by the $I^z - L^T$ observer with manual tuning for Experiment II. Plant – solid line and dots (black); $I^z - L^T$ observer with manual tuning – dashed line (red). 120

List of Tables

2.1 Simulation scenarios considered for illustrating the single-rate observers. 33
2.2 Measurement model and noise covariance used in the dual-rate observers for Simu-lation 4 in Table 2.1. 34
2.3 Performance of Luenberger and integral observers in Simulation 2 for $k \in [60, 200]$. 36
2.4 Performance of Luenberger observer and Kalman filter in Simulation 3 for $k \in [60, 200]$ over 10 realizations. 38
2.5 Performance of KF, integral observer and KF extended with integrators in Simulation 4 for $k \in [60, 200]$ over 10 realizations. 40
2.6 Performance of KF extended with integrators, based on infrequent measurements in Simulation 4 for $k \in [60, 200]$ over 10 realizations. 43

3.1 Simulation scenarios considered for the P^y observer. 58
3.2 Performance of various P^y observers for Simulation 6 in Table 3.1 for $k \in [60, 200]$ over 10 realizations. 61
3.3 Performance of the KF-ZOH and $P^y - K^y$ observers in Simulation 7 for $k \in [60, 200]$ over 10 realizations. 64
3.4 Performance of the KF-ZOH, $P^y - K^y$ and retuned $P^y - K^y$ observers in Simulation 8 for $k \in [0, 200]$ over 10 realizations. 65

4.1 Performance of the KF-Integral-Switch observer and the integral observers $P^y P^z I^z - man.$, $P^y P^z I^z - \lambda$ and $P^y P^z I^z - K^z$ in Simulation 6 for $k \in [60, 200]$ over 10 realizations. 89
4.2 Performance of the KF-Integral-Switch, $P^y - K^y$ and $P^y P^z I^z - \lambda$ observers in Simulation 7 for $k \in [60, 200]$ over 10 realizations. 89

4.3 Performance of the KF-Integral-Switch, $P^y - K^y - retuned$ and $P^y P^z I^z - \lambda$ observers in Simulation 8 for $k \in [0, 200]$ over 10 realizations. 91
4.4 Performance of the KF-Integral-Switch, $P^y - K^y - retuned$ and $P^y P^z I^z - \lambda$ observers in Simulation 9 for $k \in [0, 200]$ over 10 realizations. 92

5.1 Comparison of observer performances for Experiments I and II. 113

A.1 Model parameter values 128

Chapter 1

Introduction

A basic, if not *the* basic, characteristic of human beings is the desire to dominate the environment in which they are living, in order to increase the quality of their own life. For this reason, farmers are forcing the land to grow useful plants for food production, teachers are educating children in order to shape human society, engineers are forcing machines to work for humans, politicians and managers are fooling or forcing other people to work for them. The first step in achieving the goal of forcing the system (land, child, machine, people) to behave in the desired manner (control) is to acquire sufficient information (measurement), in order to be able to figure out its current properties. For example, it is important for the farmer to know the weather patterns, for the teacher to discuss with the child and observe its behavior in order to understand its personality, for the engineer to measure the physical and chemical properties of the system, for the politician to make polls and surveys, for the manager to conduct marketing studies. Unfortunately, the available measurements do not always contain all the required information about the system. Sticking to the example of the teacher and child, the child is not able to tell the teacher explicitly its personality type. The teacher can only observe signs such as: playing alone, being quiet and passive, never speaking spontaneously, or shouting, always moving, never being able to concentrate, just to mention two extreme cases. However, even with these implicit or incomplete signs (available measurements), the teacher can understand rather well the personality of that particular child by using his own knowledge and previous experience with children (a model of the system). Within the field of control engineering, the method of combining available measurements with a model of the sys-

tem in order to obtain an accurate description of the current properties of the system is called *estimation* and constitutes the subject of this thesis.

1.1 A brief historical overview of estimation

The first work related to estimation is credited to Karl Gauss, a German mathematician, and dates back to 1795 [29, 73]. He invented the least-squares estimation method (LSE) that plays a central role in estimation theory. He used his method to determine the parameters describing the motion of planets and comets from noisy telescopic measurements. The essence of the method is to find the parameters that minimize the square of the deviation of the position predicted by the motion equations and the position measured by a telescope.

Another technique, the maximum likelihood estimation (MLE), was introduced by Ronald Fisher, a British statistician and biologist, in 1912 [27, 58]. In this method, the parameters are determined by maximizing a predefined probability (likelihood) function. The main idea is to find the parameters that are most likely to have produced the data, instead of finding the parameters that describe the data most accurately, as in LSE.

The two aforementioned methods focus on estimating parameters. However, with the technological advances from the beginning of the 20th century, such as telephone and radio, estimating signals, i.e. separating noise from the useful signal (voice), has become increasingly important. In 1941, Andrei Kolmogorov, a Russian mathematician, and in 1942 Norbert Wiener, an American mathematician, independently developed a least-squares estimation technique for signal filtering, which is commonly known as the Wiener filter [83, 73]. This method is based on the original least-squares idea of Gauss, however it incorporates modern mathematics about the description of signals as random processes.

In 1960, Rudolf Kalman, a Hungarian - American system theorist, extended the Wiener filter to the newly developed state-space formulation of systems [48, 47]. Compared to the Wiener filter, the Kalman filter deals with the entire system (states) rather than with the measured signals alone. Besides, in its original formulation, the Kalman filter (KF) uses difference

equations instead of the integral equations of the Wiener filter, thus providing a form more suitable for digital computer implementation. For these reasons, the KF has become a milestone in estimation and, even today, constitutes the backbone of the discipline.

However, least-squares methods are not the only way of reconstructing signals. In 1964, David Luenberger, an American engineer, developed an estimator that, instead of minimizing the squared error at each time instant, as is done in the KF, reduces the estimation error with time until it eventually completely disappears at infinity [53, 6]. The Luenberger observer (LO) was the first one in a series of asymptotic observers, which have since evolved significantly. In general, they are designed to cope with systematic (deterministic) disturbances instead of random (stochastic) ones.

Over the last four decades, a large number of estimation techniques have been developed on the basis of the aforementioned methods [24, 75]. The motivation has been the need to eliminate the effect of both stochastic and deterministic disturbances in the most efficient way possible.

1.2 Motivation and related work

Usually, full-state estimation is considered in the literature because of the close link between estimation theory and full-state feedback [16, 19, 46, 56]. By having an estimate of all states, the entire system can be controlled.

However, since in some cases the goal is to control only a subset of the states, knowledge of all states is not required. The objective of this thesis is to estimate accurately a vector of *preferred variables*, whose dimension is much lower than that of the full-state vector, while paying no attention to the accuracy of the estimates of the remaining variables [11, 12]. Such a problem might arise, for example, when optimizing a process via the tracking of the necessary conditions of optimality (NCO) [77, 76]. This tracking consists of enforcing constraints on states or pushing state-dependent gradients to zero. Usually, at a given time instant only one constraint is active, or only one gradient has to be forced to zero, i.e. the knowledge of only one state or gradient is required, while the estimation accuracy of the other variables is of lesser importance.

For cases where only some of the state variables have to be estimated,

two main approaches are used in the literature, as discussed below.

Reduced-order observers

Reduced-order observers have been proposed mainly for easing the computational burden [44]. In each observer structure, two main steps require most of the computation: i) prediction, where the equations of a dynamic model are propagated in time; and ii) correction, where the observer gains are computed, which may comprise matrix multiplications and inversions. Reduced-order observers have the advantage of being computationally less expensive in one or both of these steps. The following reduction methods are proposed in the literature:

- *Reducing the model order.* The model used for prediction is simplified, thus leading to a model of smaller order for the prediction step. Then, an observer of the same order as the simplified model is used in the correction step. This way, the computational burden is eased in both the prediction and correction steps. There are two main ways of reducing the model order:

  - *Replacing states by their measurements.* In this approach, the order is reduced by simply replacing the measurable states with their measurements and dropping the corresponding equations [52]. The order of such estimators typically corresponds to the difference between the system order and the number of measurements. These techniques have been applied succesfully to chemical reactors [74] and utilized for inferential control purposes [25]. The main drawback is that the reduction in the number of variables to be estimated is generally not significant, due to the small number of measured variables.
  - *Projection.* These methods achieve a much larger reduction in the order of the model than the previous approach [54, 41]. These methods rely on the fact that the most important dynamic characteristics (for a specific purpose) of a complex system can be described by the dominant subspace. Thus, the system can be represented by a dynamic model of dimension equal to that of the dominant subspace. A significant reduction has been reported for

various applications [35]. However, the projection methods often need to be tailored to the application, and there are insufficient guidelines for selecting the appropriate method for a particular application.

A particular case of projection is *decoupling*. Its main idea is to decouple completely the dynamics of a functional of the states, i.e. a particular combination of the states of interest, from that of the rest of the states. Such observers are called functional observers in the literature [2, 22, 39, 78, 86]. However, their existence depends on the possibility of decoupling, which is generally an algebraic matrix equality constraint. Unfortunately, since this condition is often difficult to meet, the applicability of such observers is limited.

- *Reducing the estimator order.* The full-order model is used for prediction. However, the order of the observer used in the correction step is reduced. In this way, the computation of the observer gain is less expensive [9, 36, 40, 60, 71]. Additionally, the prediction step is also made computationally less expensive when the observer structure requires covariance propagation. Thus, reducing the order of the observer might ease the computations in both steps.

  However, in such observers, not all states of the full-order model used for prediction are corrected, since only a reduced-order observer is used in the correction step. Moreover, in contrast to the model-order reduction presented above, reducing the order of the observer alone is not motivated by any physical consideration, such as the presence of a dominant subspace or the possibility of decoupling, but is solely to decrease the computational burden. Hence, the approximations for reducing the order of the estimator are imposed artificially, thereby leading to suboptimal estimates. Though the estimator gains are optimized in order to provide the smallest estimation error in the least-squares sense [44], suboptimality is still present and is manifested in a systematic estimation error called bias.

Hence, each order reduction technique discussed above has some disadvantages that do not allow for accurate estimation of the preferred variables.

Full-order observers

Another way of estimating the preferred variables is to estimate the entire state vector using standard full-state techniques such as Kalman filtering [48, 45, 32] and single out the preferred variables via projection. The drawback of this approach is that the focus is on the accuracy of the entire state vector rather than that of the preferred variables. Consequently, the preferred variables will inherit the accuracy of the state vector, though they could probably be estimated more accurately if attention were focused exclusively on them.

The objective of preferential estimation (PE) is to estimate certain variables more accurately than can be done by state-of-the-art full-state estimation followed by projection. Note that in the case of linear systems with perfect model information and gaussian measurement noise, the optimal solution for estimation problems is the Kalman filter [32]. In such a case, preferential estimation techniques cannot improve the accuracy of the estimates of the selected variables, since the Kalman filter is optimal for the full-state vector and, consequently, also for the preferred variables.

However, systems with perfectly known models and excusively gaussian perturbations are rarely found in the real world. Most often, uncertainty is present in the form of uncertain model parameters, unmodeled dynamics or exogenous disturbance signals. The effect of this uncertainty on the system can be considered as that of unknown inputs. As a result, the estimated states are biased, and the Kalman filter is no longer optimal. To reduce this bias, the following techniques have typically been proposed in the literature:

- *Minimax approach.* This is the classical robust estimation technique, where the estimator is designed for the worst-case scenario in terms of the norm of the uncertainty. It consists in determining (i) the bounds on the unknown inputs that cause maximal bias, and (ii) the estimates that minimize that bias [3, 21, 69]. This is the underlying idea behind interval observers, for which two observers based on the upper and lower bounds of the uncertainty are used [8, 31, 24]. It is guaranteed that the true estimate lies between the values given by the two observers, that is, within the interval defined by them. The disadvantage of the minimax approach is the conservatism caused by the use of a

bound on a signal instead of the signal value itself.

- *Estimation of unknown inputs.* To reduce the conservatism of the previous approach, the unknown inputs can be estimated and used in the state observer. Usually, unknown inputs are estimated by augmenting the state vector with additional state variables and describing their evolution using, for example, random walks. These additional state variables can (i) represent uncertain parameters in cases where it is known which parameters are uncertain, or (ii) directly represent the unknown inputs that are approximated by constants. This approach has been given various names over the decades: Bias estimation [28, 34], garbage collector [23], integral observer [5, 7, 18, 62]. The last of these names is probably the most appropriate, since the way the system is augmented corresponds to adding integrators to the model equations.

- *Decoupling from unknown inputs.* In this approach, an observer, termed unknown input observer, is designed to decouple the dynamics of the states from those of the unknown inputs [20, 33, 38, 65, 79, 82]. The idea is the same as for functional observers. Actually, functional observers can be considered as unknown input observers, where the role of the unknown inputs is played by the dynamics of the 'undesired' states. The same limitation as for functional observers applies.

The study of full-order integral observers capable of rejecting deterministic disturbances in the preferred variables constitutes the focus of this thesis. Elimination of bias in the entire state space, as in SE, requires as many integrators as there are states affected by uncertainty, which, in the worst case, means that n integrators are needed for n states [72, 85]. To implement these integrators requires measurement of all the states affected by disturbances. In contrast, PE will only require as many integrators and measurements as there are preferred states.

Since measurements of the preferred variables can be difficult to obtain at the frequency of the output measurements, they are considered here to be available infrequently, possibly via off-line sensing techniques. Hence, a multirate estimation scheme is studied [75]. In such a scheme, some of the measurements are available less frequently (slow time scale) than the estimates are needed (fast time scale). One way of handling two-time-

scale dynamic systems is to extrapolate the slow measurements for the fast time scale by using some kind of approximations, e.g. zero-order hold or polynomial approximations, and then use a single-rate estimation technique [80, 81, 84, 85]. Another approach is to update the estimates only when the slow measurements become available and meanwhile use the predictions given by the process model corrected with the available fast measurements [4, 63, 67]. In this thesis, the second approach is considered, since it is not influenced by approximation errors.

1.3 Contributions made by this thesis

Formulation of the preferential estimation problem

As was discussed in the previous section, the aim of PE is to improve the accuracy of certain state variables in the presence of uncertainty that can be expressed as deterministic disturbances. However, this improvement is not sought via order reduction as in functional estimation, which is the method found in the literature having the same objective. The reason is to avoid the errors induced by order reduction. PE uses full-order observers that use the most accurate full-order model available. These full-order observers are constructed to provide precise estimates of only the preferred variables, while neglecting the accuracy of the other estimates. To the author's knowledge, this concept has not been studied in the literature and constitutes the main contribution of the thesis, since it avoids the errors associated with order reduction.

In order to ensure the feasibility of PE, infrequent measurements of the preferred variables are assumed to be available, while frequent estimates of these variables are needed. This dual-rate concept is well studied in the literature for the purpose of standard estimation (SE), that is, estimating all states accurately. However, infrequent measurements of all states are needed in SE. Proving the convergence of an observer structure where not all state variables are measurable is another contribution of this thesis. The advantage of PE is a less stringent assumption on the number of available infrequent measurements.

To simplify the mathematical developments, PE is formulated for linear

time-invariant (LTI) systems. The study of linear systems has already revealed the usefulness of PE, and the ideas extend to more general systems as well, as shown by the application.

Observer design for preferential estimation

Two observer types will be considered:

- *Proportional observer.* This is the classical structure consisting of a single term proportional to the output error obtained from frequent measurements. The information available from the infrequent measurements of preferred variables is used uniquely to choose the observer gains.

  A first contribution is to show that it is possible to eliminate the bias completely in the preferred variables by an appropriate choice of gains. A second contribution is to find these gains via numerical optimization, based on the available infrequent measurements. This is analogous to the concept of calibration used in chemometrics.

  Due to the structure of the observer, for each value of the deterministic disturbances a different set of gains is needed to eliminate the bias. As a consequence, each time a new measurement becomes available, the observer gains have to be retuned.

- *Integral observer.* In addition to the proportional term based on output measurements, an integral term based on the infrequent measurements of the preferred variables is introduced. Hence, a dual-rate estimator structure is obtained.

  The contribution compared to the work existing in the literature is to prove the convergence of an observer structure where not all state variables are measurable infrequently. Also, a tuning procedure that ensures the convergence of the observer is provided. The available degrees of freedom within this tuning procedure are also made via numerical optimization, using the same calibration-type approach as for the proportional observer.

  Due to the presence of the integral term, the stability of the observer implies bias elimination in the preferred variables. Hence, retuning of the integral observer is not needed.

Application to experimental data

The proposed observers are applied to a pilot-scale filamentous fungal fermentation operated at Novozymes A/S, Bagsvaerd, Denmark. The objective is to estimate accurately the biomass and product concentrations, two key quantities that are measurable only infrequently. Both observers are capable of improving the accuracy of these estimates compared to open-loop model prediction. While the proportional observer requires continuous retuning to cope with time-varying deterministic disturbances, a properly tuned integral observer does not. The gains of the observers are succesfully determined by the calibration-based approach. Due to the use of constant gains, the tuning and implementation of these observers is computationally less expensive than that of a Kalman filter.

1.4 Organization of the thesis

This thesis is organized as follows:

Chapter 2: Preliminaries. The notions of stability and observability, as well as several single-rate and dual-rate observer structures are introduced. The objective of this chapter is to recall those well-known concepts available in the literature that will be used in later chapters.

Chapter 3: Proportional observer for preferential estimation. First, the problem of PE is formulated and the proposed observer structures are detailed. Next, the properties of the proportional observer P^y are analyzed. It is shown that for each value of the constant disturbances, a different observer gain is needed to eliminate the bias in the preferred variables.

Chapter 4: Integral observer for preferential estimation. Due to the introduction of the integral term, a time-invariant observer can follow variations in the value of the disturbances. Nevertheless, exact mathematical results can only be obtained for piecewise-constant disturbances.

Chapter 5: Application. PE is applied to an experimental setup. The results obtained on this nonlinear system with time-varying disturbances

confirm the ideas of the previous chapters.

Chapter 6: Conclusions. The results are summarized and possible new research topics discussed.

Chapter 2

Preliminaries

This chapter introduces the notions of stability and observability as well as the common observers found in the literature. The objective is to discuss in detail these observers, since they will be used as benchmarks in later chapters. Single-rate, full-state observers are presented first and illustrated for the following types of uncertainty:

- For the case where only errors in the initial conditions affect the system, a Luenberger observer can be used;
- Compensating for the effect of deterministic disturbances can be done with an integral observer;
- Noise filtering can be achieved with Kalman filtering;
- Simultaneous noise filtering and compensating for the effect of deterministic disturbances can be achieved by extending the Kalman filter with integrators.

Next, the use of dual-rate measurements in the above observers is discussed. Most of the proofs are omitted since they can be easily found in the literature. Bibliographical references are provided each time a result is stated.

2.1 Plant description

Consider a plant described by the following linear time-invariant (LTI) discrete state-space equations:

$$\begin{aligned} x_{k+1} &= Ax_k + Bu_k + d_k + w_k, \quad x_0 = x_o \\ y_k &= Hx_k + v_k \end{aligned} \tag{2.1}$$

where $u_k \in \Re^{n_u}$ is the input vector, $x_k \in \Re^n$ the state vector with unknown initial value x_o, $y_k \in \Re^p$ the measured output vector, $d_k \in \Re^n$ the disturbance vector, w_k the process noise, and v_k the measurement noise. The matrix A is the state propagation matrix, B describes the effect of the inputs on the states and H is the measurement model. The noise sequences w_k and v_k are assumed to be zero-mean, white sequences with covariance matrices Q and R, respectively. In addition, the noise sequences are supposed to be uncorrelated with each other.

The vector d_k corresponds to deterministic disturbances, without stochastic effects. Note that d_k can incorporate a combination of several disturbances usually present in the real world such as [20]:

- *Parametric uncertainty* – The order and the structure of the model are correctly chosen. However, the matrices A and B are erroneous, thus not able to describe the plant behavior accurately. The effect of inaccurate knowledge of these matrices, denoted by ΔA and ΔB, can be represented as a time-varying, deterministic disturbance vector $d_k = \Delta A x_k + \Delta B u_k$.

- *Unmodeled dynamics* – Neither the order of the model nor the mathematical expressions are selected appropriately. For example, a linear representation is used for a nonlinear plant or a time-varying plant is represented as a time-invariant model, thus giving rise to the time-varying disturbance vector d_k. This category also encompasses the disturbances due to model reduction.

- *Exogenous deterministic inputs* – There are unmodeled deterministic disturbances, or unknown inputs, ω_k that affect the plant operation. Their effect can be represented in the model equations as $d_k = D\omega_k$, where $D \in \Re^{n \times n_d}$, $\omega_k \in \Re^{n_d}$. A particular type of this unknown input

appears when non-zero mean stochastic disturbances affect the plant. In this case the mean of the stochastic disturbance can be regarded as the deterministic disturbance d_k, while the stochastic part of the disturbance, after removing the mean, corresponds to the noise sequence w_k.

2.2 Notions of stability and observability

Throughout Section 2.2, deterministic and stochastic disturbances are considered to be zero, i.e. $d_k = 0$, $w_k = 0$ and $v_k = 0$. Hence, the state-space description (2.1) becomes:

$$\begin{aligned} x_{k+1} &= Ax_k + Bu_k, \quad x_0 = x_o \\ y_k &= Hx_k \end{aligned} \tag{2.2}$$

The system (2.2) is only excited by the input and the initial condition. The notions of stability and observability are taken from [19].

2.2.1 Asymptotic stability

Definition 2.1 *Consider* $u_k = 0$. *The state equation* (2.2) *is asymptotically stable if every finite initial state* x_o *generates a bounded response* x_k, *which, in addition, approaches* 0 *as* $k \to \infty$.

Definition 2.1 shows that asymptotic stability is an internal property of the state-space model, that is, it does not refer to the input-output behavior of the system.

Theorem 2.1 *The state equation* (2.2) *is asymptotically stable if and only if all eigenvalues of* A *have magnitudes less than 1.*

Definition 2.2 *A matrix whose eigenvalues have magnitudes less than 1 is said to be Schur stable.*

Steady state

For an asymptotically stable state equation with a non-zero input, $u_k \neq 0$, the state x_k will not converge to zero. For the case of a constant input, $u_k = \bar{u}$, the state converges to a constant value $x_k \to \bar{x}$ as $k \to \infty$, which is called the *steady-state value*, and the system is said to be at a *steady state*. If u_k varies, the state x_k does not converge.

2.2.2 Observability

Definition 2.3 *The model* (2.2)*, or the pair* (A, H)*, is said to be observable if for any unknown initial state* x_0 *there exists a finite integer* $k_1 > 0$ *such that knowledge of the input sequence* u_k *and output sequence* y_k *from* $k = 0, \ldots, k_1$ *suffices to determine uniquely the initial state* x_0*. Otherwise, the state-space model is said to be unobservable.*

Theorem 2.2 *The following statements are equivalent:*

1. *The pair* (A, H) *is observable.*
2. *The* $np \times n$ *observability matrix*

$$\mathcal{O} = \begin{bmatrix} H \\ HA \\ \vdots \\ HA^{n-1} \end{bmatrix} \tag{2.3}$$

   has rank n*, that is, full-column rank.*

3. *The* $(n + p) \times n$ *matrix*

$$\begin{bmatrix} A - \lambda_i I \\ H \end{bmatrix} \tag{2.4}$$

   has full-column rank n *for each eigenvalue,* λ_i*, of* A*, where* $i = 1, 2, \ldots, n$*.*

The property of observability indicates whether all states can be recovered from the available measurements. In other words, it shows whether

all states have a measurable effect on the output. This is reflected most explicitly by Condition 3 in Theorem 2.2. Each direction defined by the eigenvalues of the matrix A has to be projected by the matrix H to the output y. In turn, this means that the unobservable directions simply do not influence the output of the system.

Note that, in the case $\text{rank}(H) = n$ (all state directions are measurable), the pair (A, H) is observable. For this case, both in (2.3) and (2.4) there is a submatrix, H itself, which is of rank n.

2.3 Luenberger observer

2.3.1 Observer structure

Consider the plant model (2.2) for which the only perturbation is the error in the initial condition, i.e. only an estimate of the initial condition is available.

Consider the following linear proportional observer P^y:

$$\begin{aligned} \hat{x}_{k+1} &= A\hat{x}_k + Bu_k + K^y(y_k - \hat{y}_k), \quad \hat{x}_0 = \mathrm{E}\,(x_o) \\ \hat{y}_k &= H\hat{x}_k \end{aligned} \tag{2.5}$$

where the symbol $\hat{(\cdot)}$ denotes the estimate of a variable, $K^y \in \Re^{n\times p}$ is the observer gain matrix and $\mathrm{E}\,(\cdot)$ is the mathematical expectation operator.

Using (2.2) and (2.5), the error dynamics $e_{x,k} = x_k - \hat{x}_k$ can be written as:

$$e_{x,k+1} = A_c e_{x,k}, \qquad e_{x,0} = x_o - \mathrm{E}\,(x_o) \tag{2.6}$$

with

$$A_c = A - K^y H \tag{2.7}$$

Equation (2.6) is a dynamic equation with no input. Its asymptotic stability is guaranteed by the condition $|eig(A_c)| < 1$. The observer guaran-

teeing asymptotic stability of (2.6) is called the *Luenberger observer* (LO). Note that, even though the error dynamics (2.6) converge to zero, the estimated state $\hat{x}_k$ in (2.5) does not necessarily converge, for example if u_k varies.

2.3.2 Pole placement

Theorem 2.3 *All eigenvalues of A_c can be assigned arbitrarily (provided complex conjugate eigenvalues are assigned in pairs) by selecting a real constant gain matrix K^y if and only if (A, H) is observable.*

Assigning the eigenvalues of the matrix A_c by selecting the observer gain matrix K^y is referred to as pole placement [19]. Note that placing the poles of A_c for observer design is the dual of the pole placement of $(A - BK^y)$ for controller design. For multivariable systems, the choice of the gain K^y is not unique.

There are several pole-placement methods available implemented in software packages. The one implemented in both Matlab [42] and Mathematica [43] is the Kautsky-Nichols-Van Dooren algorithm (KNVD) [49]. This algorithm optimizes the available degrees of freedom in K^y in order to avoid numerical ill-conditioning.

Choice of pole locations

The choice of fast poles (close to the origin) yields fast convergence, but also large gains leading to aggressive correction. On the other hand, poles close to the unit circle result in slow convergence, but smaller values of the gains. In a noise-free scenario, fast gains are preferred; however, when measurement noise is present, large gains can amplify the noise considerably. Hence, in practical situations where noise is present, the choice of pole locations has to reflect the best compromise between convergence speed and noise attenuation. For noise-corrupted scenarios, a particular tuning method, labeled Kalman filter, is available. The KF finds the optimal gains, or pole locations, that minimize the estimation error covariance. This tuning procedure is discussed in Section 2.5.

2.4 Integral observer

2.4.1 Need for an integral term

It will be shown next that, in the presence of deterministic disturbances, the proportional observer (2.5) cannot eliminate the estimation error, thus motivating the need for an integral observer.

Consider the plant (2.1) without stochastic disturbances ($w_k = 0$, $v_k = 0$) and a non-zero deterministic disturbance vector d_k:

$$\begin{aligned} x_{k+1} &= Ax_k + Bu_k + d_k, \quad x_0 = x_o \\ y_k &= Hx_k \end{aligned} \tag{2.8}$$

The error dynamics using a proportional observer are:

$$e_{x,k+1} = A_c e_{x,k} + d_k, \qquad e_{x,0} = x_o - \mathrm{E}\,(x_o) \tag{2.9}$$

Depending on the disturbance vector d_k, the following situations might occur:

1. $d_k = 0$ – This is the case for which a Luenberger observer can be applied (Section 2.3). The error dynamics (2.9) converge to zero provided A_c is stable.

2. d_k is constant ($d_k = \bar{d}$, $\forall k$) – The error dynamics (2.9) converge to a non-zero steady state. An additional term that corresponds to the integral of the output error has to be added to the observer structure in order to reach zero steady-state error. This integral observer structure is studied in this section.

3. d_k is time varying – The error dynamics (2.9) do not reach steady state at all. There is no solution to this estimation problem. As a rule of thumb, an integral observer much faster than the dynamics of d_k should be chosen. Through this choice, the disturbances become quasi constant from the point of view of the observer, thereby leading back to Case 2.

Remark - Piecewise-constant disturbances. This is a special case of time-varying disturbances with d_k approximated by a sequence of j disturbances, $\tilde{d}$, each of which is constant for a large number of iterations $k_i \gg 0$, where $i = 1, 2, \ldots, j$ and $j \in \mathcal{N}$.

$$\tilde{d} = \begin{cases} \bar{d}_1 \quad for \quad k \in [0, k_1] \\ \bar{d}_2 \quad for \quad k \in [k_1 + 1, k_1 + k_2] \\ \vdots \\ \bar{d}_j \quad for \quad k \in \left[\sum_{i=1}^{j-1} k_i + 1, \sum_{i=1}^{j} k_i \right] \end{cases} \tag{2.10}$$

This case corresponds to Case 2 above, given that each k_i is large enough for the error dynamics to reach (quasi) steady state.

In order to show the advantage of the integral observer over the proportional observer, consider the error dynamics (2.9) with $d_k = \bar{d}$:

$$e_{x,k+1} = A_c e_{x,k} + \bar{d}, \qquad e_{x,0} = x_o - \mathrm{E}(x_o) \tag{2.11}$$

Due to the constant disturbance vector $\bar{d}$, the above equation reaches steady state:

$$\bar{e}_x = A_c \bar{e}_x + \bar{d} \tag{2.12}$$

that can be rewritten as:

$$\bar{e}_x = (I - A_c)^{-1} \bar{d} \tag{2.13}$$

The objective of estimation is to force this error to zero, that is to estimate accurately all states:

$$\bar{e}_x = (I - A_c)^{-1} \bar{d} \stackrel{!}{=} 0 \tag{2.14}$$

This can be achieved if the disturbances are zero, $\bar{d} = 0$, or the matrix $(I - A_c)^{-1}$ and the vector $\bar{d}$ are orthogonal to each other. However, the matrix $(I - A_c)$ is considered to be invertible, or full rank, and consequently $(I - A_c)^{-1}$ is also full rank, i.e. without a null space. Hence, proportional observers cannot eliminate the bias in the state estimates $\hat{x}_k$ in the presence of non-zero deterministic disturbances.

In contrast, integral observers are able to eliminate bias by introducing an additional term G_k, leading to the following correction term: $K^y(y_k - \hat{y}_k) + G_k$. Thus, the integral observer aims at zero steady-state error using the following structure:

$$\bar{e}_x = (I - A_c)^{-1}(\bar{d} - \bar{G}) \stackrel{!}{=} 0 \tag{2.15}$$

This objective can be satisfied with $\bar{G} = \bar{d}$. The integral observer presented next meets this objective.

2.4.2 Observer structure

Consider the linear proportional-integral observer P^yI^y for the system (2.8):

$$\begin{array}{rcll} \hat{x}_{k+1} & = & A\hat{x}_k + Bu_k + K^y(y_k - \hat{y}_k) + K^\alpha\alpha_k, & \hat{x}_0 = \mathrm{E}\,(x_o) \\ \alpha_{k+1} & = & \alpha_k + (y_k - \hat{y}_k), & \alpha_0 = 0 \\ \hat{y}_k & = & H\hat{x}_k & \end{array} \tag{2.16}$$

where $\alpha \in \Re^p$ is the integral of the output error, $K^y \in \Re^{n\times p}$ is the proportional gain matrix and $K^\alpha \in \Re^{n\times p}$ is the integral gain matrix.

The above system can be rewritten as:

$$\begin{array}{rcll} \hat{x}_{k+1} & = & A\hat{x}_k + Bu_k + K^y(y_k - \hat{y}_k) + \alpha_k^K, & \hat{x}_0 = \mathrm{E}\,(x_o) \\ \alpha_{k+1}^K & = & \alpha_k^K + K^\alpha(y_k - \hat{y}_k), & \alpha_0^K = 0 \\ \hat{y}_k & = & H\hat{x}_k & \end{array} \tag{2.17}$$

with $\alpha_k^K = K^\alpha\alpha_k$. Even though this structure has n integrators compared to the p integrators in (2.16), i.e. it is redundant if $n > p$, it has the advantage of being in the typical observer form $(\mathcal{A} - \mathcal{K}\mathcal{H})$, as shown next.

Considering the case of a constant disturbance vector, i.e. $d_k = \bar{d}$, with the observer (2.17), the estimation error in the $2n$-dimensional augmented state $\begin{bmatrix} x \\ \alpha^K \end{bmatrix}$ is:

$$e_{k+1} = (\mathcal{A} - \mathcal{K}\mathcal{H})\, e_k + U(\bar{d}) \tag{2.18}$$

$$e_k = \begin{bmatrix} e_{x,k} \\ \alpha_k^K \end{bmatrix}, \qquad \mathcal{A} = \begin{bmatrix} A & -I \\ 0 & I \end{bmatrix}$$
$$\mathcal{K} = \begin{bmatrix} K^y \\ -K^\alpha \end{bmatrix}, \qquad \mathcal{H} = \begin{bmatrix} H & 0 \end{bmatrix}, \qquad U(\bar{d}) = \begin{bmatrix} \bar{d} \\ 0 \end{bmatrix}$$

2.4.3 Integral observability

Given a constant input $U(\bar{d})$, the error dynamics (2.18) converge to a steady state if the matrix $(\mathcal{A} - \mathcal{K}\mathcal{H})$ is stable. The condition ensuring arbitrary pole placement for $(\mathcal{A} - \mathcal{K}\mathcal{H})$ is called integral observability [85, 72].

Definition 2.4 *The system* (2.8) *is integral observable if the pair* $(\mathcal{A}, \mathcal{H})$ *in* (2.18) *is observable.*

Theorem 2.4 *The pair* $(\mathcal{A}, \mathcal{H})$ *is observable if and only if* $\text{rank}(H) = n$.

For a constant disturbance $\bar{d}$, the next theorem gives the condition for having a zero steady-state estimation error.

Theorem 2.5 *For the case of a constant disturbance* $\bar{d}$*, the integral observer* (2.18) *leads to zero steady-state error in all state directions if and only if* $\text{rank}(H) = n$.

Proof. At steady-state, (2.18) becomes:

$$\begin{aligned} \bar{e}_x &= A_c \bar{e}_x + \bar{d} - \bar{\alpha}^K \\ \bar{\alpha}^K &= \bar{\alpha}^K + K^\alpha H \bar{e}_x \end{aligned} \tag{2.19}$$

that can be rewritten as:

$$\begin{aligned} \bar{e}_x &= (I - A_c)^{-1} \left(\bar{d} - \bar{\alpha}^K\right) \\ 0 &= K^\alpha H \bar{e}_x \end{aligned} \tag{2.20}$$

The second equation indicates that $\bar{e}_x = 0$ if and only if $\text{rank}(H) = n$. Given $(I - A_c)$ is invertible, therefore from the first equation $\bar{\alpha}^K = \bar{d}$. Note that the rank of $(I - A_c)$ can be influenced through the eigenvalues of A_c if the pair (A, H) is observable. □

The objective of the $P^y I^y$ observer is to force convergence of the error dynamics (2.18) to zero. The first step in achieving this is to ensure asymptotic stability of the error dynamics. As explained in Section 2.3.2, stability can be ensured by placing the poles of $(\mathcal{A} - \mathcal{K}\mathcal{H})$ within the unit circle. These poles can be placed arbitrarily if $\text{rank}(H) = n$.

The same condition, $\text{rank}(H) = n$, ensures zero estimation error. Hence, if all state directions are measurable, the $P^y I^y$ observer is able to cancel the effect of the deterministic disturbance via the $\bar{G} = \bar{\alpha}^K = \bar{d}$ term discussed in (2.15). Note that $\text{rank}(H) = n$ implies observability of the pair (A, H) (Theorem 2.2), but the converse is not true. Obviously, this rank condition is more restrictive than the observability requirement on the pair (A, H) needed by the Luenberger observer. It is intuitively correct to say that coping with deterministic disturbances is more demanding in terms of the amount of information required about the system than just coping with initial errors alone.

2.5 Kalman filter

Consider the plant (2.1) without deterministic disturbances, i.e. $d_k = 0$.

$$\begin{aligned} x_{k+1} &= Ax_k + Bu_k + w_k, \quad x_0 = x_o \\ y_k &= Hx_k + v_k \end{aligned} \tag{2.21}$$

Using the proportional observer P^y (2.5), the error dynamics read:

$$e_{x,k+1} = A_c e_{x,k} + w_k + K^y v_k, \qquad e_{x,0} = x_o - \mathrm{E}\,(x_o) \tag{2.22}$$

Taking the mean of this error gives:

$$\mathrm{E}\,(e_{x,k+1}) = A_c \mathrm{E}\,(e_{x,k})\,, \qquad e_{x,0} = x_o - \mathrm{E}\,(x_o) \tag{2.23}$$

since w_k and v_k are zero-mean.

Observe from (2.22) and (2.23) that any gain matrix giving a stable error dynamics, as in the LO, ensures asymptotic convergence of the error mean to zero. However, since noise is present, the second-order statistics of the estimation error also need to be taken into account. The tuning that minimizes the estimation error covariance, while ensuring asymptotic convergence of the error mean, is the Kalman filter (KF) [32].

2.5.1 Observer structure

The Kalman filter proposes to minimize the estimation error covariance P_k by using a proportional observer with time-varying gain:

$$\begin{array}{ll} \min\limits_{K_k^y} & P_k = \mathrm{E}\left(e_{x,k} e_{x,k}^T\right) \\ s.t. & \hat{x}_{k+1} = A\hat{x}_k + Bu_k + K_k^y(y_k - \hat{y}_k), \quad \hat{x}_0 = \mathrm{E}\,(x_o) \\ & \hat{y}_k = H\hat{x}_k \end{array} \tag{2.24}$$

If the pair (A, H) is observable, the above problem can be solved by the following n-dimensional recursion:

$$\begin{array}{rcll} P_k^- & = & AP_{k-1}A^T + Q & P_0 = E\left(e_{x,0} e_{x,0}^T\right) \\ K_k^y & = & P_k^- H^T \left(HP_k^- H^T + R\right)^{-1} & \\ P_k & = & \left(I_n - K_k^y H\right) P_k^- & \end{array} \tag{2.25}$$

The observer gain K_k^y given by the above recursion converges to the

constant value K^y, which is determined by the 'ratio' of the noise covariance matrices Q and R. P_0 is the initial estimate of the estimation error covariance that influences the number of iterations needed for convergence.

The covariance matrices Q and R have to be determined prior to the implementation of the filter. R can be determined off-line from the available measurements. However, Q cannot be inferred from measured variables. In general, Q is a tuning parameter that expresses the confidence of the user in the model. If the model is good, a low Q can be chosen, whereas if the model is poor, a high Q is more appropriate. As a function of the relative values of Q and R, the filter will give more or less weight to the measurements compared to the model predictions.

In other words, while the Kalman filter uses the same observer structure as the LO, that is a proportional term based on the output error, the pole location is determined by (2.25). The advantage of the KF over the LO is the presence of this analytical expression, which provides the optimal gains, or poles, as a function of the physically interpretable quantities Q and R. However, the Kalman filter can also be difficult to tune, since the choice of these quantities may not always be trivial.

Note that, for the LTI system considered above, the recursive computation of the gain K_k^y is independent of the measurements. Thus, the gain can be computed off-line prior to the filter implementation.

2.5.2 Kalman filter extended with integrators

Consider the plant (2.1) with stochastic disturbances and a constant deterministic disturbance vector, $d_k = \bar{d}$:

$$\begin{aligned} x_{k+1} &= Ax_k + Bu_k + \bar{d} + w_k, \quad x_0 = x_o \\ y_k &= Hx_k + v_k \end{aligned} \tag{2.26}$$

The idea is to use the P^yI^y observer structure (2.17) with the gain $\mathcal{K} = \begin{bmatrix} K^y \\ K^\alpha \end{bmatrix}$ given by a Kalman filter. The equations (2.24)-(2.25) are extended to the augmented state $\begin{bmatrix} x \\ \alpha^K \end{bmatrix}$ from (2.18), leading to:

$$\begin{aligned} \min_{\mathcal{K}_k} \quad & \mathcal{P}_k = \mathrm{E}\left(e_k e_k^T\right) \\ s.t. \quad & \hat{x}_{k+1} = A\hat{x}_k + Bu_k + K_k^y(y_k - \hat{y}_k) + \alpha_k^K, \qquad \hat{x}_0 = \mathrm{E}\left(x_o\right) \\ & \alpha_{k+1}^K = \alpha_k^K + K_k^\alpha(y_k - \hat{y}_k), \qquad \alpha_0^K = 0 \\ & \hat{y}_k = H\hat{x}_k \end{aligned} \tag{2.27}$$

If the integral observability condition of the pair $(\mathcal{A}, \mathcal{H})$ holds, that is $\mathrm{rank}(H) = n$, the solution to the above problem is given by the following $2n$-dimensional recursion:

$$\begin{aligned} \mathcal{P}_k^- &= \mathcal{A}_k \mathcal{P}_{k-1} \mathcal{A}_k^T + \mathcal{Q}, \qquad \mathcal{P}_0 = \begin{bmatrix} \mathrm{E}\left(e_{x,0} e_{x,0}^T\right) & 0 \\ 0 & P_{0,\alpha} \end{bmatrix} \\ \mathcal{K}_k &= \mathcal{P}_k^- \mathcal{H}^T \left(\mathcal{H}\mathcal{P}_k^- \mathcal{H}^T + R\right)^{-1} \\ \mathcal{P}_k &= \left(I_{2n} - \mathcal{K}_k \mathcal{H}\right) \mathcal{P}_k^- \end{aligned} \tag{2.28}$$

In (2.27) and (2.28) $\mathcal{A}$, $\mathcal{H}$, $\mathcal{K}$ and e_k are the same as in (2.18) and $\mathcal{Q} = \begin{bmatrix} Q & 0 \\ 0 & Q_\alpha \end{bmatrix}$. $P_{0,\alpha} > 0$ and $Q_\alpha > 0$ are diagonal matrices of tuning parameters. $P_{0,\alpha}$ influences the rate of convergence of the integral gains to their steady-state values. Q_α determines the steady-state values to which the integral gains converge. These gains determine the dynamics of the integral states.

Using this observer, both elimination of disturbance and optimal noise filtering can be achieved. The price to pay, however, is to require both the condition $\mathrm{rank}(H) = n$ specific to the integral observer, and the knowledge of the noise statistics Q and R specific to the Kalman filter. Additionally, the tuning parameters $P_{0,\alpha}$ and Q_α have to be determined.

Combined state and parameter estimation

The extension of the Kalman filter with integrators is widely used in the literature to compensate for parametric errors [24], which are a particular type of time-varying disturbance d_k as explained in Section 2.1.

Consider the parametric error

$$\Delta A = \begin{bmatrix} 0 & \cdots & 0 & \cdots & 0 \\ \vdots & \ddots & \vdots & \ddots & \vdots \\ 0 & \cdots & \delta a & \cdots & 0 \\ \vdots & \ddots & \vdots & \ddots & \vdots \\ 0 & \cdots & 0 & \cdots & 0 \end{bmatrix} \tag{2.29}$$

that is, only one element of the matrix A is uncertain. $\delta a \in \Re$ is the additive error affecting this parameter.

For this case, the system (2.26) can be rewritten as:

$$\begin{aligned} x_{k+1} &= Ax_k + Bu_k + \Delta A x_k + w_k, \quad x_0 = x_o \\ y_k &= Hx_k + v_k \end{aligned} \tag{2.30}$$

and the observer structure (2.17) as:

$$\begin{aligned} \hat{x}_{k+1} &= A\hat{x}_k + Bu_k + K_k^y(y_k - \hat{y}_k) + \Delta\hat{A}_k\hat{x}_k, & \hat{x}_0 &= \mathrm{E}\,(x_o) \\ \delta\hat{a}_{k+1} &= \delta\hat{a}_k + K_k^{\delta a}(y_k - \hat{y}_k), & \delta\hat{a}_0 &= 0 \\ \hat{y}_k &= H\hat{x}_k \end{aligned} \tag{2.31}$$

where $\Delta\hat{A}_k$ is obtained from ΔA in (2.29) by replacing δa with $\delta\hat{a}$.

In equation (2.30), $\Delta A x_k$ plays the role of the time-varying disturbance vector d_k. However, its structure is known and can be incorporated in the observer (2.31). Using this structure, only one integral state corresponding to the uncertain parameter is needed. In the case where there are several unknown parameters, a separate integrator has to be introduced for each unknown parameter. In order to be able to estimate all unknown parameters accurately, persistence of excitation is needed, a notion defined in the system identification literature [51]. In other words, in this case, the strict condition of integral observability is not required. However, the available measurements must be sufficiently rich in information to reveal the true values of the parameters.

Note that (2.31) is nonlinear due to the term $\Delta\hat{A}\hat{x}_k$ which involves the terms $\delta\hat{a}_k$ and $\hat{x}_k$. Thus, the linear Kalman filter has to be extended (EKF)

to nonlinear systems by using a linear time-varying (LTV) approximation of nonlinear systems that is based on Taylor series expansion [32]. The word *extended* here refers to extending a linear filter to the nonlinear case, not extending the filter with integrators. Note also that the observability measures defined in Section 2.2.2 are not valid for nonlinear systems.

The idea of the EKF is to use:

- The nonlinear model from observer structure (2.31) for prediction:

$$\hat{\xi}_{k+1} = f(\hat{\xi}_k) + \mathcal{B}u_k + \mathcal{K}_k\mathcal{H}(\xi_k - \hat{\xi}_k) \tag{2.32}$$

  where

$$\hat{\xi}_k = \begin{bmatrix} \hat{x}_k \\ \delta\hat{a}_k \end{bmatrix}, \qquad f(\hat{\xi}_k) = \begin{bmatrix} A\hat{x}_k + \Delta\hat{A}_k\hat{x}_k \\ \delta\hat{a}_k \end{bmatrix}$$
$$\mathcal{H} = \begin{bmatrix} H & 0 \end{bmatrix}, \qquad \mathcal{K}_k = \begin{bmatrix} K_k^y \\ -K_k^{\delta a} \end{bmatrix} \qquad \mathcal{B} = \begin{bmatrix} B \\ 0 \end{bmatrix}$$

- A linear time-varying approximation (Taylor series) of the model in the recursion (2.28), leading to a $(n+1)$-dimensional recursion in this specific case:

$$\begin{aligned} \mathcal{P}_k^- &= \mathcal{A}_k\mathcal{P}_{k-1}\mathcal{A}_k^T + \mathcal{Q}, \qquad \mathcal{P}_0 = \begin{bmatrix} \mathrm{E}\left(e_{x,0}e_{x,0}^T\right) & 0 \\ 0 & P_{0,\alpha} \end{bmatrix} \\ \mathcal{K}_k &= \mathcal{P}_k^-\mathcal{H}^T\left(\mathcal{H}\mathcal{P}_k^-\mathcal{H}^T + R\right)^{-1} \\ \mathcal{P}_k &= \left(I_{n+1} - \mathcal{K}_k\mathcal{H}\right)\mathcal{P}_k^- \end{aligned} \tag{2.33}$$

  with

$$\mathcal{A}_k = \left.\frac{\partial f}{\partial \hat{\xi}}\right|_{\hat{\xi}_k} = \begin{bmatrix} A + \Delta\hat{A}_k & \mathcal{I}\hat{x}_k \\ 0 & 1 \end{bmatrix}$$

$$\mathcal{I} = \begin{bmatrix} 0 & \cdots & 0 & \cdots & 0 \\ \vdots & \ddots & \vdots & \ddots & \vdots \\ 0 & \cdots & 1 & \cdots & 0 \\ \vdots & \ddots & \vdots & \ddots & \vdots \\ 0 & \cdots & 0 & \cdots & 0 \end{bmatrix} \qquad \mathcal{Q} = \begin{bmatrix} Q & 0 \\ 0 & Q_\alpha \end{bmatrix}$$

2.6 Dual-rate observers

In addition to measurements of the output variables considered in (2.1), measurements of other less frequently available variables are considered in this section. Hence, (2.1) can be rewritten as:

$$\begin{aligned} x_{k+1} &= Ax_k + Bu_k + d_k + w_k, \quad x_0 = x_o \\ y_k &= Hx_k + v_k \\ z_l &= Lx_{lr} + \nu_l \end{aligned} \tag{2.34}$$

where $L \in \Re^{m\times n}$ is the measurement model and ν_l is the measurement noise, with zero mean covariance Z, associated with the infrequent measurements z_l. The subscripts $(\cdot)_k$ and $(\cdot)_l$ indicate that the corresponding quantities are considered at the small sampling time t_k and the large sampling time t_l, respectively. The sampling time t_l is considered to be an integer multiple of t_k, i.e. $t_l = t_k r$ with $r \geq 1$. Thus, the relationship between the indices k and l at the time of the z measurements is $k = lr$. In addition, a delay of θ small sampling periods is considered in the availability of the infrequent measurements, θ being an integer with $0 \leq \theta < r$ (Figure 2.1).

The sampling frequency must be adapted to the frequency of the signal to be sampled. Usually, it is recommended to choose a sampling period between one-fifth and one-tenth of the dominant time constant of the system [64, 70]. This is the requirement that the fast sampling of the output y_k must satisfy. However, the sampling of the variables z_l is (much) less

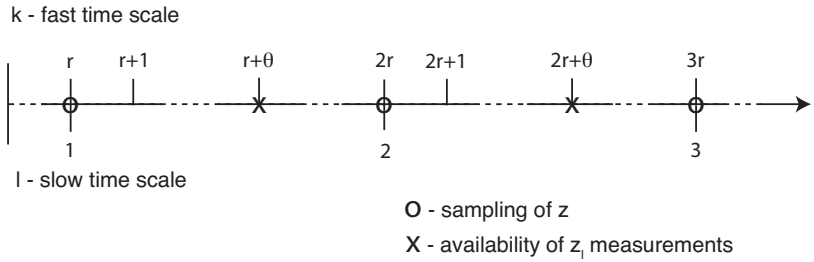

Figure 2.1: Multirate estimation scheme. The y_k measurements are available at the discrete time instants k, $k = 0, \ldots, r, r+1, \ldots$. The z_l measurements are taken at the time instants l, $l = 0, 1, 2, \ldots$ for which $k = lr$. The z_l measurements are indicated by circles and become available at the time instants marked by crosses, i.e. with a delay of θ small sampling periods.

frequent. Thus, it cannot be assumed that the slow sampling captures the main dynamics of the system. However, the role of the additional infrequent measurements is rather to compensate for the deterministic disturbances d_k affecting the system. Hence, the sampling of z_l must capture the dynamics of this disturbance. This can be easily met for constant $\bar{d}$ or piecewise-constant $\tilde{d}$ disturbances. For arbitrary time-varying deterministic disturbances d_k, this cannot be guaranteed. As a rule of thumb, the use of z_l measurements for estimation purposes is beneficial only when slow sampling is appropriate for the disturbance to be eliminated.

The above system is of dual-rate nature, since measurements at two time scales are available. For estimation purposes, the infrequent measurements can be used for correction at two scales:

- at the fast time scale, by extrapolating the infrequent measurements to this scale, thereby leading to the single-rate estimation scheme discussed in previous sections, or

- at the slow time scale, that is using a hierarchical observer structure, where at the lower level an estimator based on the frequent measurements is used, while at the higher level the frequent estimates provided by the lower level estimator are corrected based on the infrequent measurements only when these become available.

These two possibilities are discussed next.

2.6.1 Fast-time-scale correction

Extrapolation of the infrequent measurements to the fast time scale can be done via poly-nomial approximations [85]. For example, by using a zero-order hold (ZOH) approximation and taking into account the measurement delay, (2.34) can be rewritten as:

$$\begin{aligned} x_{k+1} &= Ax_k + Bu_k + d_k + w_k, \quad x_0 = x_o \\ y_k &= Hx_k + v_k \\ z_k &= \begin{cases} Lx_{lr} + \nu_l & if \quad \frac{k+r-\theta}{r} \in \mathcal{N} \\ z_{k-1} & otherwise \end{cases} \end{aligned} \tag{2.35}$$

The single-rate observers presented before can be applied to the above system by considering the augmented measurement vector $\zeta_k = \begin{bmatrix} y_k \\ z_k \end{bmatrix}$, model $\mathcal{H} = \begin{bmatrix} H \\ L \end{bmatrix}$ and covariance $\mathcal{R} = \begin{bmatrix} R & 0 \\ 0 & Z \end{bmatrix}$. The disadvantage, however, is the error induced by the polynomial extrapolations, as well as by assuming that the noise properties of the extrapolated measurements do not change upon applying the polynomial approximations.

2.6.2 Slow-time-scale correction

The gains corresponding to the terms based on infrequent measurements are set to zero between two slow sampling instants. However, at the slow sampling instants, these gains are nonzero. The advantage of this method is to avoid polynomial extrapolations. The disadvantage is that the correction is made infrequently, and thus higher gains might be needed, leading to a possibly more aggressive behavior.

When using a Kalman filter for either frequent or infrequent corrections, the augmented measurement vector, model and covariance have to be used. However, the gains can be set to zero by choosing a very large Z ($Z = \infty$)

between two slow sampling instants. Since the inverse of $\mathcal{R}$ is used for gain computation, the elements of the resulting gain matrix that correspond to Z become zero. Additionally, the measurement model corresponding to the infrequent measurements is set to zero, $L = 0$, between two slow sampling instants. Hence, the measurement model and the measurement noise covariance become periodic, and the filter will converge to a periodic solution [67]:

$$\begin{aligned} \mathcal{H} &= \begin{bmatrix} H \\ c_k L \end{bmatrix} \\ \mathcal{R} &= \begin{bmatrix} R & 0 \\ 0 & \frac{1}{c_k} Z \end{bmatrix} \\ c_k &= \begin{cases} 1 & if \quad \frac{k+r-\theta}{r} \in \mathcal{N} \\ 0 & otherwise \end{cases} \end{aligned} \tag{2.36}$$

2.7 Illustration

A 4th-order discrete-time linear system is considered as an illustrative example throughout the thesis. All the results are obtained by computer simulation using the MATLAB software. Both single-rate and dual-rate systems are considered.

Single-rate system

Consider the plant (2.1) with deterministic and stochastic disturbances:

$$\begin{aligned} x_{k+1} &= Ax_k + Bu_k + d_k + w_k, \quad x_0 = x_o \\ y_k &= Hx_k + v_k \end{aligned}$$

with:

$$A = \begin{bmatrix} 0.91 & 0 & 0.11 & 0 \\ 0 & 0.66 & 0.13 & -0.06 \\ 0 & -0.06 & 0.75 & 0.02 \\ 0.10 & 0.05 & 0 & 0.80 \end{bmatrix}$$

Table 2.1: Simulation scenarios considered for illustrating the single-rate observers.

Simulation	1 - no disturb.	2 - determ. disturb.	3 - stoch. disturb.	4 - determ. & stoch. disturb.	5 - param. error & stoch. disturb.
d_k	0	d	0	d	$\Delta A x_k$
w_k	0	0	$N(0,Q)$	$N(0,Q)$	$N(0,Q)$
v_k	0	0	$N(0,R)$	$N(0,R)$	$N(0,R)$
$\hat{x}_0$	$x_{o,e}$	$x_{o,e}$	$x_{o,e}$	$x_{o,e}$	$x_{o,e}$
H	H_1	H_2	H_1	H_2	H_1
Appropriate observer	LO (2.5)	Integral (2.17)	KF (2.24)-(2.25)	KF-Integral (2.27) - (2.28)	KF with param. est. (2.32) - (2.33)
Observer for comparison	-	LO	LO	Integral; KF	KF

$$
\begin{aligned}
B &= \begin{bmatrix} -0.05 & 0.05 & 0.1 & -0.1 \end{bmatrix}^T \\
x_o &= \begin{bmatrix} 40 & -60 & 100 & -60 \end{bmatrix}^T \\
u_k &= -0.005k - 16\sin 0.1k + 200
\end{aligned}
$$

and $k = 0, 1, \ldots, 200$. The disturbance vector and the measurement model are given in Table 2.1 for various simulation scenarios. Each of these scenarios corresponds to a single-rate observer presented in previous sections. Additionally, the performances of these observers are compared to each other, as indicated by the last row in this table. Note that different measurement models are used for different scenarios, depending on the observer requirements.

The values of some quantities in Table 2.1 are:

$$
x_{o,e} = \begin{bmatrix} -20 & 30 & -50 & 30 \end{bmatrix}^T, \qquad \bar{d} = \begin{bmatrix} 3 & 6 & 4.5 & 0.6 \end{bmatrix}^T
$$

$$
\Delta A = \begin{bmatrix} 0 & 0 & 0 & 0 \\ 0 & 0 & 0 & 0 \\ 0 & 0.3 & 0 & 0 \\ 0 & 0 & 0 & 0 \end{bmatrix}, \qquad Q = \begin{bmatrix} 2 & 0 & 0 & 0 \\ 0 & 3 & 0 & 0 \\ 0 & 0 & 5 & 0 \\ 0 & 0 & 0 & 3 \end{bmatrix}
$$

Table 2.2: Measurement model and noise covariance used in the dual-rate observers for Simu-lation 4 in Table 2.1.

Observer	KF-Integral-ZOH Section 2.6.1 using (2.27) - (2.28)	KF-Integral-Switch Section 2.6.2 using (2.27) - (2.28)
H	$\begin{bmatrix} H_1 \\ L \end{bmatrix}$	$\begin{bmatrix} H_1 \\ c_k L \end{bmatrix}$
$\mathcal{R}$	$\begin{bmatrix} R & 0 \\ 0 & Z \end{bmatrix}$	$\begin{bmatrix} R & 0 \\ 0 & \frac{1}{c_k} Z \end{bmatrix}$

$$R = \begin{cases} 2 & for \quad H_1 \\ Q & for \quad H_2 \end{cases}$$
$$H_1 = \begin{bmatrix} 1 & 0 & 0 & 0 \end{bmatrix}, \qquad H_2 = I_4$$

Note that the pair (A, H) is observable and the matrix A is stable with eigenvalues:

$$\lambda = \begin{bmatrix} 9.2387 \cdot 10^{-1} & 7.6346 \cdot 10^{-1} & 7.1634 \cdot 10^{-1} \pm 9.5074 \cdot 10^{-2} i \end{bmatrix}^T$$

Dual-rate system

The single-rate system above is considered with the infrequent measurements:

$$z_l \;=\; L x_{lr} + \nu_l$$

For this system the disturbances in Simulation 4 from Table 2.1 are considered. The two dual-rate observers from Section 2.6 are applied with the measurement models and noise covariance given in Table 2.2. The values of the quantities in Table 2.2 are the same as in Table 2.1 except for:

$$L = \begin{bmatrix} 0 & 1 & 0 & 0 \\ 0 & 0 & 1 & 0 \end{bmatrix}, \qquad Z = \begin{bmatrix} 3 & 0 \\ 0 & 5 \end{bmatrix}$$
$$c_k = \begin{cases} 1 & if \quad \frac{k+r-\theta}{r} \in \mathcal{N} \\ 0 & otherwise \end{cases}$$
$$r = 10, \qquad \theta = 9$$

Performance measures

In order to compare the performance of the various estimation methods in the sequel, Monte-Carlo simulations are carried out. 10 realizations[1] that use different noise sequences w_k and v_k are considered. The following quantities are computed from the estimation error at the k^{th} sampling instant, $e_k = x_k - \hat{x}_k$:

- $\bar{e}_k = \mathrm{E}\,(e_k)$ - the bias, n-dimensional. This is the mean of the estimation error for each state over the realizations.
- $\mathcal{V}_{e_k} = \mathrm{diag}\left(\mathrm{E}\left((e_k - \mathrm{E}\,(e_k))(e_k - \mathrm{E}\,(e_k))^T\right)\right)$ - the error variance, n-dimensional. This results from the process and measurement noises considered in the simulation.
- $\Pi_{e_k} = \mathrm{diag}\left(\mathrm{E}\left(e_k e_k^T\right)\right)$ - the mean square error (MSE), n-dimensional.
- $\Sigma_{\Pi_{e_k}} = \sum_{i=1}^{n} \Pi_{e_{i,k}}$ - the total MSE, a scalar. This represents the sum of the MSE over its n states.

Additionally, to have a global indication of the performance of the observer for the entire time interval considered, the above quantities are simply summed up over the index k to give:

$$\bar{e} = \sum_k |\bar{e}_k|, \quad \mathcal{V}_e = \sum_k \mathcal{V}_{e_k}, \quad \Pi_e = \sum_k \Pi_{e_k}, \quad \Sigma_{\Pi_e} = \sum_k \Sigma_{\Pi_{e_k}}$$

Simulation 1 - Luenberger observer

Consider the observer (2.5), the single-rate system and Simulation 1 in Table 2.1. Since the matrix A is stable and only the initial conditions are unknown, the open-loop model prediction converges to the true values. By closing the loop, i.e. using the observer (2.5), the rate of convergence can be increased by choosing poles closer to the origin, e.g. $\lambda_{LO} = \begin{bmatrix} 0.55 & 0.40 & 0.50 & 0.80 \end{bmatrix}^T$, as illustrated in Figure 2.2. Since this a noise-free scenario, no Monte-Carlo simulations are required.

[1] Such a small number of realizations does not allow accurate statistical properties to be computed. However, sufficiently good approximations of these properties can be obtained for comparing the performance of different observers, with minimal computational effort.

Table 2.3: Performance of Luenberger and integral observers in Simulation 2 for $k \in [60, 200]$.

	Open loop	LO	Integral
$\bar{e}$	$\begin{bmatrix} 5.3480 \cdot 10^{1} \\ 1.7893 \cdot 10^{1} \\ 1.6446 \cdot 10^{1} \\ 3.4229 \cdot 10^{1} \end{bmatrix}$	$\begin{bmatrix} 6.6667 \\ 1.0000 \cdot 10^{1} \\ 9.0000 \\ 3.0000 \end{bmatrix}$	$\begin{bmatrix} 1.1259 \cdot 10^{-16} \\ -2.5019 \cdot 10^{-16} \\ -2.5019 \cdot 10^{-17} \\ 1.5574 \cdot 10^{-15} \end{bmatrix}$

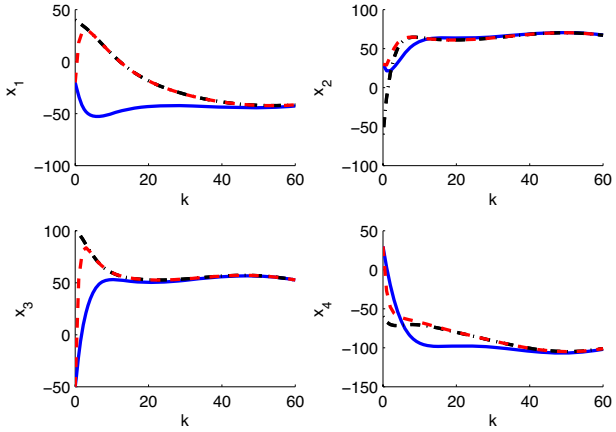

Figure 2.2: Comparison of open-loop model prediction and Luenberger observer in Simulation 1. Plant – dash-dotted line (black); open-loop model – solid line (blue); Luenberger observer – dashed line (red).

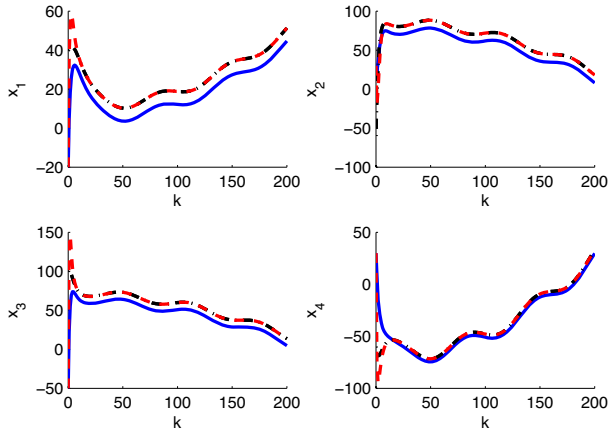

Figure 2.3: Comparison of Luenberger and integral observers in Simulation 2. Plant – dash-dotted line (black); Luenberger observer – solid line (blue); Integral observer – dashed line (red).

Simulation 2 - Integral observer

Consider the observer (2.17), the single-rate system and Simulation 2 in Table 2.1. In order to ensure zero-mean estimation error for a non-zero disturbance $\bar{d}$, it is required that $\text{rank}(H) = n$. Thus, H_2 is used for all observers discussed here. As can be seen in Figure 2.3, the LO does not ensure zero-mean estimation error, while the integral observer (2.17) is able to eliminate the bias upon convergence. However, the LO is able to reduce this bias compared to the open-loop prediction, as shown in Table 2.3. Since a noise-free scenario is considered, no Monte-Carlo simulations are carried out and only the error mean is compared in Table 2.3. As shown in Figure 2.3, the integral observer overshoots due to the choice of a rather aggressive (close to the origin) set of poles:

$\lambda_I = \begin{bmatrix} 0.55 & 0.40 & 0.50 & 0.30 & 0.35 & 0.45 & 0.20 & 0.10 \end{bmatrix}^T$.

Simulation 3 - Kalman filter

Consider the observer (2.24)-(2.25), the single-rate system and Simulation 3 in Table 2.1. The observer given by (2.24)-(2.25) is used with $P_0 = I_n$.

Table 2.4: Performance of Luenberger observer and Kalman filter in Simulation 3 for $k \in [60, 200]$ over 10 realizations.

	Open loop	LO	KF
$\bar{e}$	$\begin{bmatrix} 7.9598 \cdot 10^{1} \\ 9.0758 \cdot 10^{1} \\ 8.9710 \cdot 10^{1} \\ 1.1328 \cdot 10^{2} \end{bmatrix}$	$\begin{bmatrix} 6.2913 \cdot 10^{1} \\ 8.7658 \cdot 10^{1} \\ 1.3858 \cdot 10^{2} \\ 1.2103 \cdot 10^{2} \end{bmatrix}$	$\begin{bmatrix} 7.5059 \cdot 10^{1} \\ 9.0100 \cdot 10^{1} \\ 9.0625 \cdot 10^{1} \\ 1.1418 \cdot 10^{2} \end{bmatrix}$
$\mathcal{V}_e$	$\begin{bmatrix} 2.0689 \cdot 10^{3} \\ 9.5495 \cdot 10^{2} \\ 1.3916 \cdot 10^{3} \\ 1.3133 \cdot 10^{3} \end{bmatrix}$	$\begin{bmatrix} 5.6633 \cdot 10^{2} \\ 1.0337 \cdot 10^{3} \\ 2.3933 \cdot 10^{3} \\ 1.4215 \cdot 10^{3} \end{bmatrix}$	$\begin{bmatrix} 1.2541 \cdot 10^{3} \\ 9.5457 \cdot 10^{2} \\ 1.3686 \cdot 10^{3} \\ 1.1622 \cdot 10^{3} \end{bmatrix}$
Π_e	$\begin{bmatrix} 2.1393 \cdot 10^{3} \\ 1.0422 \cdot 10^{3} \\ 1.4847 \cdot 10^{3} \\ 1.4572 \cdot 10^{3} \end{bmatrix}$	$\begin{bmatrix} 6.1213 \cdot 10^{2} \\ 1.1177 \cdot 10^{3} \\ 2.6113 \cdot 10^{3} \\ 1.5786 \cdot 10^{3} \end{bmatrix}$	$\begin{bmatrix} 1.3153 \cdot 10^{3} \\ 1.0405 \cdot 10^{3} \\ 1.4631 \cdot 10^{3} \\ 1.3111 \cdot 10^{3} \end{bmatrix}$
Σ_{Π_e}	$6.1233 \cdot 10^{3}$	$5.9197 \cdot 10^{3}$	$5.1300 \cdot 10^{3}$

Upon convergence, the gains of the Kalman filter are optimal for balancing the uncertain predictions given by the model and the noisy measurements. In other words, the Kalman filter does not only ensure convergence of the estimator to the true values, as the Luenberger observer does, but it also finds the most appropriate set of poles in order to ensure measurement noise attenuation. These poles are determined by the recursion (2.25) using the prior knowledge of the noise covariances Q and R.

The results upon convergence, presented in Table 2.4, show that the total MSE is smaller for KF than for LO (compare the blue numbers). This performance is achieved through variance reduction, by having closed-loop poles (after convergence) in between those of the open-loop system (λ) and LO (λ_{LO}):

$$\lambda_{KF} = \begin{bmatrix} 8.7143 \cdot 10^{-1} & 7.5349 \cdot 10^{-1} & 7.1919 \cdot 10^{-1} \pm 9.9263 \cdot 10^{-2} i \end{bmatrix}^T.$$

Due to slower poles, the KF gives less weight to the measurement in comparison to the LO. Since x_1 is the measured variable, the MSE in x_1 is larger for KF than for LO (compare the green numbers). However, by relying more on the model predictions, the KF gives a smoother estimate, as shown by the reduced variance in x_2, x_3 and x_4 (compare the red numbers). This is also confirmed by Figure 2.4, which is an enlargement of a specific region for better visibility of the curves.

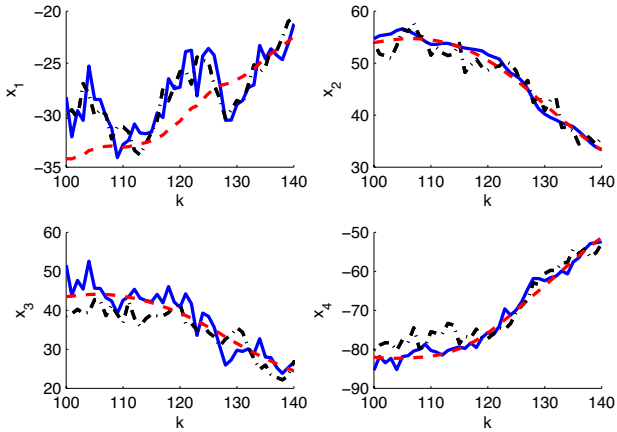

Figure 2.4: Comparison of Luenberger observer and Kalman filter in Simulation 3 for one realization of the noises. Plant – dash-dotted line (black); Luenberger observer – solid line (blue); Kalman filter – dashed line (red).

Simulation 4 - Kalman filter extended with integrators

Consider the observer (2.27) - (2.28), the single-rate system and Simulation 4 in Table 2.1. The measurement model H_2 is used for all observers discussed here. The observer structure (2.17) is used with the gain $\mathcal{K}$ given by the recursion (2.28). This recursion is extended to the augmented state $\begin{bmatrix} x \\ \alpha^K \end{bmatrix}$ from (2.18) by using:

$$\mathcal{H} = \begin{bmatrix} I_n & 0 \end{bmatrix}, \qquad \mathcal{A} = \begin{bmatrix} A & -I_n \\ 0 & I_n \end{bmatrix}$$

$$\mathcal{Q} = \begin{bmatrix} Q & 0 \\ 0 & 0_{n\times n} \end{bmatrix}, \qquad R = Q, \qquad \mathcal{P}_0 = 20\, I_{2n}$$

The results in Table 2.5 show that the total MSE is smallest with the Kalman filter extended with integrators (compare the blue numbers). This performance is achieved through both variance reduction compared to the integral observer (red numbers) and bias reduction compared to the stan-

Table 2.5: Performance of KF, integral observer and KF extended with integrators in Simulation 4 for $k \in [60, 200]$ over 10 realizations.

	Open loop	KF	Integral observer	KF-Integral
$\bar{e}$	$7.5796 \cdot 10^3$ $2.5412 \cdot 10^3$ $2.3623 \cdot 10^3$ $4.8597 \cdot 10^3$	$3.9896 \cdot 10^3$ $2.5507 \cdot 10^3$ $1.7667 \cdot 10^3$ $2.3927 \cdot 10^3$	$1.1613 \cdot 10^2$ $7.5411 \cdot 10^1$ $1.1707 \cdot 10^2$ $9.9926 \cdot 10^1$	$1.5730 \cdot 10^2$ $8.2630 \cdot 10^1$ $1.1444 \cdot 10^2$ $1.2280 \cdot 10^2$
$\mathcal{V}_e$	$1.7698 \cdot 10^3$ $8.1284 \cdot 10^2$ $1.5136 \cdot 10^3$ $1.5003 \cdot 10^3$	$1.0764 \cdot 10^3$ $7.6566 \cdot 10^2$ $1.4048 \cdot 10^3$ $1.1335 \cdot 10^3$	$1.4277 \cdot 10^3$ $7.9516 \cdot 10^2$ $1.6707 \cdot 10^3$ $8.4536 \cdot 10^2$	$1.1047 \cdot 10^3$ $7.8692 \cdot 10^2$ $1.4038 \cdot 10^3$ $1.1289 \cdot 10^3$
Π_e	$4.0661 \cdot 10^5$ $4.6373 \cdot 10^4$ $4.0960 \cdot 10^4$ $1.6793 \cdot 10^5$	$1.1333 \cdot 10^5$ $4.6658 \cdot 10^4$ $2.3527 \cdot 10^4$ $4.1552 \cdot 10^4$	$1.5818 \cdot 10^3$ $8.6530 \cdot 10^2$ $1.8183 \cdot 10^3$ $9.4637 \cdot 10^2$	$1.3498 \cdot 10^3$ $8.6393 \cdot 10^2$ $1.5484 \cdot 10^3$ $1.2938 \cdot 10^3$
Σ_{Π_e}	$6.6187 \cdot 10^5$	$2.2507 \cdot 10^5$	$5.2118 \cdot 10^3$	$5.0559 \cdot 10^3$

dard Kalman filter (magenta numbers). Note that, in this case as well, the estimation error of the measured state x_4 is smallest in the observer with the fastest poles, i.e. the integral observer (compare the green numbers).

The poles upon convergence are:

$$\lambda_{KF-I} = \begin{bmatrix} 6.9761 \cdot 10^{-1} \pm 1.0036 \cdot 10^{-1} i & 7.3953 \cdot 10^{-1} & 8.5944 \cdot 10^{-1} \\ 9.9477 \cdot 10^{-1} & 9.9494 \cdot 10^{-1} & 9.9501 \cdot 10^{-1} & 9.9498 \cdot 10^{-1} \end{bmatrix}^T$$

The moduli of the first 4 poles are close to those of the standard Kalman filter, while the remaining poles, corresponding to the integral states, are near the unit circle since $Q_\alpha = 0_{n \times n}$ is used. Nevertheless, the resulting dynamics of the integral states are fast enough to compensate for the effect of $\bar{d}$.

Simulation 5 - Kalman filter with parameter estimation

In order to illustrate the extension of the Kalman filter with integrators for parameter estimation, consider the observer (2.32) - (2.33), the single-rate system and Simulation 5 in Table 2.1 with:

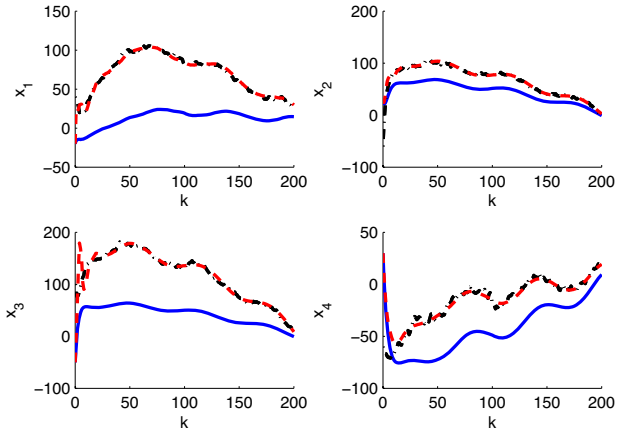

Figure 2.5: Comparison of KF and combined state and parameter estimation using a KF extended with integrators in Simulation 5 for one realization. Plant – dash-dotted line (black); Kalman filter – solid line (blue); Parameter estimation using the KF – dashed line (red).

$$\Delta\hat{A}_k = \begin{bmatrix} 0 & 0 & 0 & 0 \\ 0 & 0 & 0 & 0 \\ 0 & \delta\hat{a}_k & 0 & 0 \\ 0 & 0 & 0 & 0 \end{bmatrix}$$

$$\mathcal{I} = \begin{bmatrix} 0 & 0 & 0 & 0 \\ 0 & 0 & 0 & 0 \\ 0 & 1 & 0 & 0 \\ 0 & 0 & 0 & 0 \end{bmatrix}, \qquad \mathcal{Q} = \begin{bmatrix} Q & 0 \\ 0 & 0 \end{bmatrix}$$

$$\mathcal{P}_0 = \begin{bmatrix} 100 & 0 & 0 & 0 & 0 \\ 0 & 20 & 0 & 0 & 0 \\ 0 & 0 & 300 & 0 & 0 \\ 0 & 0 & 0 & 100 & 0 \\ 0 & 0 & 0 & 0 & 0.05 \end{bmatrix}$$

Figure 2.5 compares the performance of the combined state and parameter estimation with that of the standard Kalman filter. P_0 is chosen to ensure smooth convergence. Note that, due to the LTV approximation used in the EKF, the recursion (2.33) does not converge. Hence, the gains of the filter will continue to vary with time.

Dual-rate Kalman filters

The dual-rate system with the disturbances as in Simulation 4 from Table 2.1 are considered. The observer (2.27) - (2.28) using infrequent measurements as described in Section 2.6.1 (KF-Integral-ZOH) and in Section 2.6.2 (KF-Integral-Switch) is used.

The measurement model and noise covariances are taken from Table 2.2 with:

$$\mathcal{H} = \begin{bmatrix} H & 0 \end{bmatrix}, \qquad \mathcal{A} = \begin{bmatrix} A & -I_n \\ 0 & I_n \end{bmatrix}$$
$$\mathcal{Q} = \begin{bmatrix} Q & 0 \\ 0 & I_n \end{bmatrix}, \qquad \mathcal{P}_0 = 20\, I_{2n}$$

Note that $\text{rank}(\mathcal{H}) < n$. This means that, since the condition of integral observability is not satisfied, arbitrary pole placement is not possible. The KF-Integral-ZOH observer has one pole on the unit circle. This is due to the redundant structure of the observer, that is, having more integrators (4) than 'augmented' measurements (3). The pole on the unit circle corresponds to that extra integrator:

$$\begin{aligned} \lambda_{KF-I-ZOH} \;=\; & \begin{bmatrix} 7.1867 \cdot 10^{-1} \pm 3.0584 \cdot 10^{-1} i & 6.7028 \cdot 10^{-1} \pm 2.5251 \cdot 10^{-1} i \\ 7.3073 \cdot 10^{-1} \pm 1.6536 \cdot 10^{-1} i & 7.9466 \cdot 10^{-1} \quad 1.0000 \end{bmatrix}^T \end{aligned}$$

Note that the same also holds for the KF-Integral-Switch, with the difference that, between two slow sampling instants, there is only one measurement for 4 integrators. Hence, 3 poles are on the unit circle. Note also that, due to the varying noise covariance matrix, the gains of the KF-Integral-Switch are periodic. In this case, $Q_\alpha = I_n$ is used to ensure fast reaction of the observer to the infrequent measurements.

Table 2.6: Performance of KF extended with integrators, based on infrequent measurements in Simulation 4 for $k \in [60, 200]$ over 10 realizations.

	Open loop	KF-Integral	KF-Integral-ZOH	KF-Integral-Switch
Rate	-	single	dual	dual
H	-	H_2	$\begin{bmatrix} H_1 \\ L \end{bmatrix}$	$\begin{bmatrix} H_1 \\ c_k L \end{bmatrix}$
$\bar{e}$	$7.5796 \cdot 10^3$ $2.5412 \cdot 10^3$ $2.3623 \cdot 10^3$ $4.8597 \cdot 10^3$	$1.5730 \cdot 10^2$ $8.2630 \cdot 10^1$ $1.1444 \cdot 10^2$ $1.2280 \cdot 10^2$	$9.3012 \cdot 10^1$ $7.9252 \cdot 10^2$ $7.3814 \cdot 10^2$ $3.3016 \cdot 10^4$	$8.7249 \cdot 10^1$ $4.8556 \cdot 10^2$ $4.7936 \cdot 10^2$ $2.7168 \cdot 10^3$
$\mathcal{V}_e$	$1.7698 \cdot 10^3$ $8.1284 \cdot 10^2$ $1.5136 \cdot 10^3$ $1.5003 \cdot 10^3$	$1.1047 \cdot 10^3$ $7.8692 \cdot 10^2$ $1.4038 \cdot 10^3$ $1.1289 \cdot 10^3$	$6.2552 \cdot 10^2$ $2.0565 \cdot 10^3$ $3.0443 \cdot 10^3$ $1.6723 \cdot 10^3$	$6.1558 \cdot 10^2$ $1.7710 \cdot 10^3$ $2.6791 \cdot 10^3$ $2.6712 \cdot 10^3$
Π_e	$4.0661 \cdot 10^5$ $4.6373 \cdot 10^4$ $4.0960 \cdot 10^4$ $1.6793 \cdot 10^5$	$1.3498 \cdot 10^3$ $8.6393 \cdot 10^2$ $1.5484 \cdot 10^3$ $1.2938 \cdot 10^3$	$7.2473 \cdot 10^2$ $8.9704 \cdot 10^3$ $8.7794 \cdot 10^3$ $7.6784 \cdot 10^6$	$7.0313 \cdot 10^2$ $4.2693 \cdot 10^3$ $4.9842 \cdot 10^3$ $5.4790 \cdot 10^4$
Σ_{Π_e}	$6.6187 \cdot 10^5$	$5.0559 \cdot 10^3$	$7.6969 \cdot 10^6$	$6.4747 \cdot 10^4$

As can be seen in Figure 2.6, by using both dual-rate observer structures the bias can be eliminated in the three measured states. The error in the 4th direction, however, is out of control since, as shown in Theorem 2.5, only the bias in the measured directions can be eliminated with integral observers. The large initial overshoot is due to the rather aggressive tuning ($Q_\alpha = I_n$).

As expected, the performance of these observers is worse than that of the Kalman filter extended with integrators using H_2, that is, frequent measurements of all states (Table 2.6 - compare the blue numbers). This performance is especially worse in x_4, the state whose measurement is not available at all for the dual-rate observers (compare the red numbers). What is interesting to note, however, is the somewhat better performance of the KF-Integral-Switch compared to that of the KF-Integral-ZOH (green numbers). This is due to the absence of approximations in the KF-Integral-Switch.

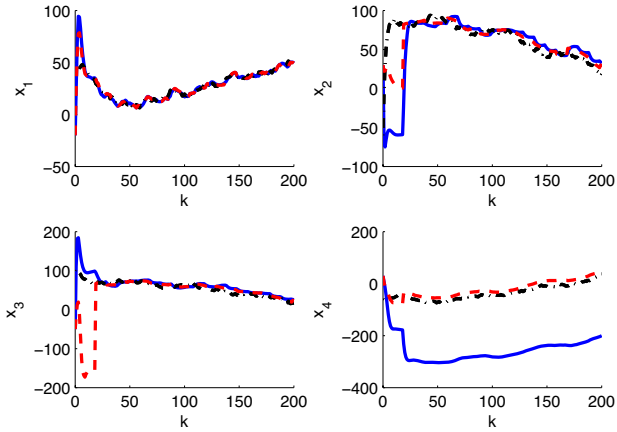

Figure 2.6: Comparison of KF extended with integrators based on infrequent measurements in Simulation 4 for one realization. Plant – dash-dotted line (black); KF-Integral-ZOH observer – solid line (blue); KF-Integral-Switch observer – dashed line (red).

Chapter 3

Proportional observer for preferential estimation

The problem of preferential estimation is formulated in Section 3.1.1, while two observer structures are proposed in Section 3.1.2. The first structure, a proportional observer based on the output measurements, is discussed in Section 3.2. The second structure, which in addition has a proportional and an integral term based on measurements of the preferred variables, will be the subject of Chapter 4.

3.1 Preferential estimation

3.1.1 Problem formulation

Consider the plant described by (2.34):

$$\begin{aligned} x_{k+1} &= Ax_k + Bu_k + d_k + w_k, \quad x_0 = x_o \\ y_k &= Hx_k + v_k \\ z_l &= Lx_{lr} + \nu_l \end{aligned} \tag{3.1}$$

The concept of PE consists in restricting attention to certain linear combinations of states, termed preferred variables, while using a full-order model to avoid errors related to order reduction. The preferred variables are denoted by $z \in \Re^m$, with L being an $m \times n$ projection matrix, $m < n$ and $\text{rank}(L) = m$. The preferred variables z are typically defined by the problem at hand and thus given a priori. The same also holds for L. Note that

a different index l is used for the preferred variables, that is their measurements are available less frequently than that of the outputs y_k, as detailed in Section 2.6.

Preferential estimation is formulated as the minimization of the mean-square estimation error J of the preferred variables z_l:

$$\begin{aligned} \min_{K} \quad & J = \sum_{l} \mathrm{E}\left((z_l - \hat{z}_l)^T (z_l - \hat{z}_l)\right) \\ s.t. \quad & \hat{x}_{k+1} = A\hat{x}_k + Bu_k + \Phi(K, e_{y,k}, e_{z,l}), \quad \hat{x}_0 = \mathrm{E}\left(x_o\right) \\ & \hat{y}_k = H\hat{x}_k \\ & \hat{z}_l = L\hat{x}_{lr} \end{aligned} \tag{3.2}$$

where Φ comprises the correction terms, $e_{y,k} = y_k - \hat{y}_k$, the estimation error in y at the sampling instant k and $e_{z,l} = z_l - \hat{z}_l$, the estimation error in z at the sampling instant $k = lr$. Constant gains K are considered to simplify the optimization problem.

Note that the objective function in (3.2) is the mean-square error (a scalar) and not the covariance matrix that is typically used in estimation problems [32]. The reason for choosing a scalar objective function rather than a matrix is that, except for the special case of linear systems without deterministic disturbance, there exists no unique estimator gain that minimizes every element of the matrix. Thus, a weighted sum of the various elements of the matrix is necessary to define the solution. The mean-square estimation error $\mathrm{E}\left((z_l - \hat{z}_l)^T (z_l - \hat{z}_l)\right)$, which is the trace of the matrix $\mathrm{E}\left((z_l - \hat{z}_l)(z_l - \hat{z}_l)^T\right)$, represents one such possible weighting. Additionally, these MSEs are added up over all the data points available, $l = 0, 1, \ldots, N$.

3.1.2 Observers for preferential estimation

In Section 2.4, the effect of a constant deterministic disturbance $d_k = \bar{d}$ is discussed. It is shown that the bias introduced by $\bar{d} \neq 0$ cannot be eliminated by a P^y observer. However, a $P^y I^y$ observer with $\Phi = K^y(y_k - \hat{y}_k) + G_k$ is able to eliminate the bias thanks to the integral term $G_k = \alpha_k^K$

based on y_k measurements, which at steady state gives:

$$\bar{e}_x = (I - A_c)^{-1}(\bar{d} - \bar{G})$$

However, the condition of integral observability has to be satisfied to ensure $\bar{G} = \bar{d}$. This condition implies that it is possible to measure all state variables, $\text{rank}(H) = n$.

Since the objective of PE is accurate estimation of the preferred variables z_l, the error $\bar{e}_z$ is forced to zero:

$$\bar{e}_z = L(I - A_c)^{-1}(\bar{d} - \bar{G}) \stackrel{!}{=} 0 \tag{3.3}$$

Note that, while the matrix $(I - A_c)^{-1}$ has full rank, the matrix $L(I - A_c)^{-1}$ does not due to the rank condition imposed on L in PE. This makes it possible to have $\bar{e}_z = 0$ by having the matrix $L(I - A_c)^{-1}$ and the vector $\bar{d} - \bar{G}$ orthogonal to each other, without all state variables being measurable or, in other words, without satisfying the condition of integral observability. Candidate observers to satisfy (3.3) include:

1. *Proportional observer - P^y*

   Consider (3.2) with $\Phi = K^y(y_k - \hat{y}_k)$, that is, only a correction term proportional to the error in e_y is used, with $G_k = 0$. The observer dynamics at the fast time scale can be written as:

   $$\begin{aligned} \hat{x}_{k+1} &= A\hat{x}_k + Bu_k + K^y(y_k - \hat{y}_k), \quad \hat{x}_0 = \mathrm{E}\,(x_o) \\ \hat{y}_k &= H\hat{x}_k \end{aligned} \tag{3.4}$$

   The steady-state error is:

   $$\bar{e}_z = L(I - A_c)^{-1}\bar{d} \tag{3.5}$$

   The main idea is to choose K^y such that the matrix $L(I - A_c)^{-1}$, which has a null space, is orthogonal to the disturbance vector $\bar{d}$. However, the information contained in the y_k measurements does not allow determination of the value of K^y satisfying (3.5). This information has to come from the z_l measurements themselves. Hence, K^y is found by

solving Optimization problem (3.2) with the objective function J being evaluated based on these z_l measurements.

2. *Integral observer based on z_l measurements - $P^yP^zI^z$*

The idea is to determine the observer gains such that the resulting term $(\bar{d}-\bar{G})$ is orthogonal to the matrix $L(I-A_c)^{-1}$. The term G_k is based on the integral states β_k driven by the infrequent measurements of the preferred variables. The $P^yP^zI^z$ observer has proportional terms based on both y_k and z_l measurements and an integral term based on the z_l measurements. Hence, $\Phi = K^y(y_k-\hat{y}_k)+G_k+c_kK^{z,x}(z_l-\hat{z}_l)$, with $G_k = K^\beta\beta_k$ where β_k is the integral state driven by the infrequent measurements of the preferred variables. The observer is:

$$\begin{aligned}
\hat{x}_{k+1} &= A\hat{x}_k + Bu_k + K^y(y_k-\hat{y}_k) + K^\beta\beta_k + c_kK^{z,x}(z_l-\hat{z}_l), && \hat{x}_0 = \mathrm{E}\,(x_o)\\
\beta_{k+1} &= \beta_k + c_kK^{z,\beta}(z_l-\hat{z}_l), && \beta_0 = 0\\
\hat{y}_k &= H\hat{x}_k, && (3.6)\\
\hat{z}_l &= L\hat{x}_{lr}\\
c_k &= \begin{cases} 1 & if \quad \frac{k+r-\theta}{r} \in \mathcal{N} \\ 0 & otherwise \end{cases}
\end{aligned}$$

Considering this observer structure at the slow time scale, (3.3) becomes:

$$\bar{e}_z = L(I-A_c+K^{z,x}L)^{-1}(\bar{d}-K^\beta\bar{\beta}) \stackrel{!}{=} 0 \qquad (3.7)$$

$\mathrm{rank}\left(L(I-A_c+K^{z,x}L)^{-1}\right) < n$ and it is possible to have $\bar{e}_z = 0$ without satisfying the condition of integral observability.

In this observer structure, there are only m integrators, in contrast to the P^yI^y observer (2.17) with n integrators. That is, the form (2.16) is used, with an $n\times m$ dimensional gain matrix K^β in the state equation. In addition to this, the gain matrix $K^{z,\beta}$ is considered in the integral state equation. The advantage of using such a structure is that, under some Assumptions, the error dynamics can be transformed into the

typical linear form $\mathcal{A} - \mathcal{K}\mathcal{H}$ with $\mathcal{K} = \begin{bmatrix} K^{z,x} \\ -K^{z,\beta} \end{bmatrix}$. In order to stabilize this structure, only the observability of the pair (A, H) is required, as will be shown in Section 4.3. This is a less restrictive condition than that of integral observability ($\text{rank}(H) = n$), discussed in Section 2.4.3.

Note that the integral states β_k are updated only when the z_l measurements, delayed by θ small sampling periods, become available (Figure 2.1). This update law is implemented via the switching coefficient c_k, as explained in Section 2.6.

3.2 Proportional observer P^y

Observers containing a term proportional to the output error e_y are frequently used in the field of estimation, e.g. the Kalman filter and Luenberger observer [47]. In this section, their use for preferential estimation purposes is studied.

In Section 3.1.2, a P^y observer is proposed to cancel the effect of the constant deterministic disturbance $\bar{d}$, by exploiting the fact that only a subspace of the states has to be estimated in PE. P^y observers are mainly used in the literature for noise filtering [73]. Hence, with the same proportional term, two objectives have to be met simultaneously: bias elimination and noise filtering. Additionally, stable observer dynamics are required, thus constraining the choice of the gain K^y.

This section aims at designing a P^y observer that tries to minimize both the bias and the variance of the estimates, while ensuring a stable behavior. This is achieved by tuning the P^y observer based on the z_l measurements that are available up to date, either off-line or on-line, through solving an optimization problem numerically. Once the observer gains have been determined, they are used for estimation purposes, thus leading to a calibration-like two-step approach.

In order to adapt the P^y observer to time-varying disturbances, the tuning step would have to be repeated for each value of d_k or, since d_k is not measurable, each time a new z_l measurement becomes available. However, solving the proposed optimization problem repeatedly may not be feasible in practice, due to the high computational load.

In Section 3.2.1, the structure of the observer and some necessary Assumptions are presented. Section 3.2.2 discusses the convergence of this observer. The possibility of eliminating bias is studied in Section 3.2.3, while the tradeoff between bias and variance is analyzed in Section 3.2.4. Section 3.2.5 presents the tuning procedure for the P^y observer, while Section 3.2.6 illustrates the performance of the observer. The results are discussed in Section 3.2.7.

3.2.1 Observer structure

Considering a P^y observer, the optimization problem (3.2) specialized to the plant (3.1) reads:

$$\begin{aligned} \min_{K^y} \quad & J = \sum_l \mathrm{E}\left((z_l - \hat{z}_l)^T (z_l - \hat{z}_l)\right) \\ s.t. \quad & \hat{x}_{k+1} = A\hat{x}_k + Bu_k + K^y(y_k - \hat{y}_k), \quad \hat{x}_0 = \mathrm{E}\,(x_o) \\ & \hat{y}_k = H\hat{x}_k, \\ & \hat{z}_l = L\hat{x}_{lr} \end{aligned} \tag{3.8}$$

Note that the P^y observer does not contain any terms based on z_l measurements.

In order to ease analysis of PE using the P^y observer, the following is assumed:

A.1 *Constant, non-zero deterministic disturbance* $d_k = \bar{d} \neq 0$*;*

A.2 *The pair* (A, H) *is observable, that is, the state* x *is observable from the output* y*.*

3.2.2 Convergence of the error dynamics

From (3.1) and (3.8) and with Assumption A.1, the dynamics of the state estimation error $e_{x,k} = x_k - \hat{x}_k$ and of its mean over the noise, $\mathrm{E}\,(e_{x,k})$, can

be written as:

$$\begin{aligned} e_{x,k+1} = x_{k+1} - \hat{x}_{k+1} &= A(x_k - \hat{x}_k) - K^y(y_k - \hat{y}_k) + \bar{d} + w_k \\ &= A_c e_{x,k} + \bar{d} + w_k - K^y v_k \end{aligned} \tag{3.9}$$

$$\mathrm{E}\left(e_{x,k+1}\right) = A_c \mathrm{E}\left(e_{x,k}\right) + \bar{d} \tag{3.10}$$

With Assumption A.2, the poles of the observers can be placed arbitrarily. There are several numerically efficient algorithms suitable for this task [19, 49] (Section 2.3).

By having a constant disturbance and stable observer dynamics, the mean estimation error reaches a steady-state value, $\mathrm{E}\left(e_{x,k}\right) \to \bar{e}_x$. Note that the estimate $\hat{x}_k$ does not reach steady state, only the error dynamics converge to a constant value. The expression (3.5) is obtained for the estimation error in the preferred variables. Section 3.2.3 considers whether it is possible to eliminate the bias $\bar{e}_z$. The effect of the noise terms in (3.9) is discussed in Section 3.2.4.

3.2.3 Estimation bias

The impossibility to eliminating bias in all states

This subsection addresses the question of whether using the P^y observer in the presence of constant deterministic disturbances it is possible to eliminate the bias in all states ($\mathrm{rank}(L) = n$), that is for the case of standard estimation (SE) discussed in Section 2.4.1.

Theorem 3.1 *Consider the plant* (3.1) *and the observer* (3.8)*. Assume* A.1 *and* A.2*. If* $\mathrm{rank}(L) = n$*, then there exists no finite* K^y *that leads to* $\bar{e}_z = 0$*.*

Proof. A possible solution to $\bar{e}_z = 0$ from (3.5) is $(I - A_c)^{-1} = 0$, which is equivalent to $K^y \to \infty$. However, if a finite value of K^y is sought, $\bar{e}_z$ cannot be pushed to zero since $(I - A_c)^{-1}$ and L are both of rank n. □

This theorem, though simple, illustrates important features of estimation with deterministic disturbances. Firstly, the bias can never be eliminated

in all states with a finite-gain P^y observer. Secondly, high-gain observers can be used to reduce the bias [17, 30, 26].

In the above theorem, $d_k = \bar{d} \neq 0$ from Assumption A.1, which is required to avoid the trivial case of no deterministic disturbance, for which the theorem is falsified. Assumption A.2 is needed to ensure that the poles of the observers can be placed arbitrarily and, thus, the observer is stable and a steady state is reached (see Section 3.2.2).

The possibility of eliminating bias in preferred states

This subsection investigates the conditions under which the P^y observer, for the case of non-zero constant deterministic disturbances, can eliminate the bias in given preferred variables.

Theorem 3.2 *Consider the plant* (3.1) *and the observer* (3.8). *Assume* A.1 *and* A.2. *If* $\text{rank}(L) < n$ *and rank* $\begin{bmatrix} H \\ L \end{bmatrix} > \text{rank}(L)$, *then, for each value of* $\bar{d}$, *there exists infinitely many values of* K^y *that lead to* $\bar{e}_z = 0$. *Additionally, for each value of* $\bar{d}$, *a different set of* K^y *values leads to* $\bar{e}_z = 0$.

Proof.

If $\text{rank}(L) < n$, the matrix L has a null space. If, in addition, $rank \begin{bmatrix} H \\ L \end{bmatrix} > rank(L)$, then there exists a $(n \times 1)$ dimensional vector q in the null space of L such that $Lq = 0_{m\times 1}$ and $Hq \neq 0_{p\times 1}$. This implies that there exists at least one row in H, denoted by h, for which $hq \neq 0$.

Equation (3.5) can be rewritten as:

$$\bar{e}_z = LM^{-1}\bar{d} = 0$$

with $M = (I - A + K^y H)$. Therefore $M^{-1}\bar{d}$ should be in the null space of L to satisfy $\bar{e}_z = 0$. For example, $M^{-1}\bar{d} = \frac{1}{\gamma}q$, where $\gamma \in \Re$, will do. Multiplying $M^{-1}\bar{d} = \frac{1}{\gamma}q$ by γM on the left gives:

$$K^y Hq = \gamma\bar{d} - (I - A)q$$

One of the solutions of the above equation is:

$$K^y = \left[\begin{array}{cc} \frac{1}{hq}(\gamma\bar{d} - (I - A)q) & 0 \end{array} \right] \tag{3.11}$$

and infinitely many solutions can be obtained by changing γ. Besides, the solution K^y depends on $\bar{d}$, that is, for each $\bar{d}$ a different set of K^y values solves (3.5). □

Theorem 3.2 shows that, for an observable system, the effect of a constant deterministic disturbance can be eliminated in the preferred variables through an appropriate choice of the gains of a P^y observer. However, to eliminate the bias, it is not sufficient to have the classical observability condition from the measured outputs. The effect of the deterministic disturbances cannot be eliminated in the traditional way by ensuring the stability of the error dynamics by placing the poles of $A_c = A - K^y H$ within the unit circle. In addition to this condition, $rank \left[\begin{array}{c} H \\ L \end{array} \right] > \text{rank}(L)$ has to be satisfied. An intuitive interpretation of this condition is that, to influence the null space ($M^{-1}d$) of the matrix L, it is necessary that the handles ($K^y H$) lie outside its range space.

3.2.4 Bias - variance tradeoff

This section analyzes in more detail the bias and the variance of the estimation error in relation to the optimization problem (3.8). J can be rewritten as:

$$\begin{aligned} J &= \sum_l \text{E}\left((z_l - \hat{z}_l)^T (z_l - \hat{z}_l)\right) = \sum_l \text{tr E}\left(L(x_{lr} - \hat{x}_{lr})(x_{lr} - \hat{x}_{lr})^T L^T\right) \\ &= \sum_l \text{tr}\ (L P_{lr} L^T) \end{aligned} \tag{3.12}$$

where $P_{lr} = \text{E}\left((x_{lr} - \hat{x}_{lr})(x_{lr} - \hat{x}_{lr})^T\right)$ is the matrix of the mean-square error and not the covariance of the estimation error:

$$\begin{aligned} P_{lr} &= \mathrm{E}\left(e_{x,lr}^T e_{x,lr}\right) = \mathrm{tr}\ \mathrm{E}\left(e_{x,lr} e_{x,lr}^T\right) = \\ &= \mathrm{tr}\ \mathrm{E}\left(\bar{e}_{x,lr}\bar{e}_{x,lr}^T\right) + \mathrm{tr}\ \mathrm{E}\left((e_{x,lr}-\bar{e}_{x,lr})(e_{x,lr}-\bar{e}_{x,lr})^T\right) \end{aligned} \tag{3.13}$$

where $e_{x,lr} = x_{lr} - \hat{x}_{lr}$, $\bar{e}_{x,lr}$ is the error mean (or bias) that is non-zero in the presence of deterministic disturbances, $\mathrm{tr}\ \mathrm{E}\left(\bar{e}_{x,lr}\bar{e}_{x,lr}^T\right)$ is the bias term, and $\mathrm{E}\left((e_{x,lr}-\bar{e}_{x,lr})(e_{x,lr}-\bar{e}_{x,lr})^T\right)$ is the covariance caused by the stochastic disturbance. Thus, the objective function (3.12) contains both a bias term, due to the deterministic disturbances, and a covariance term, caused by the stochastic noises.

A recursive equation for P_k will be derived. From (3.9), one can write:

$$\begin{aligned} \mathrm{E}\left(e_{x,k+1}e_{x,k+1}^T\right) &= A_c\mathrm{E}\left(e_{x,k}e_{x,k}^T\right)A_c{}^T + K^y\mathrm{E}\left(v_k v_k^T\right)K^{yT} + \mathrm{E}\left(w_k w_k^T\right) \\ &\quad + \bar{d}\bar{d}^T + \mathrm{E}\left(\bar{d}e_{x,k}^T\right)A_c{}^T + A_c\mathrm{E}\left(e_{x,k}\bar{d}^T\right) \end{aligned} \tag{3.14}$$

Since $\bar{d}$ is a deterministic variable, $\mathrm{E}\left(\bar{d}e_{x,k}^T\right) = \bar{d}\mathrm{E}\left(e_{x,k}^T\right)$. Moreover, considering that the time interval for which the objective function J is evaluated is much larger than the dominant time constant of the observer, $\mathrm{E}\left(e_{x,k}^T\right)$ can be approximated by its steady-state value $\mathrm{E}\left(e_{x,k}^T\right) \approx \bar{e}_x^T$.

Using the following notations:

$$\begin{aligned} &R = \mathrm{E}\left(v_k v_k^T\right), \quad Q = \mathrm{E}\left(w_k w_k^T\right), \quad M = I - A_c \\ &\bar{Q} = Q + K^y R K^{yT} + A_c M^{-1}\bar{d}\bar{d}^T + \bar{d}\bar{d}^T M^{-T}A_c{}^T + \bar{d}\bar{d}^T \end{aligned}$$

(3.14) can be written in the following recursive form:

$$P_{k+1} = A_c P_k A_c{}^T + \bar{Q} \tag{3.15}$$

Note that, due to Assumptions A.1 and A.2, P_k converges to $\bar{P}$, and (3.15) becomes a discrete Lyapunov equation.

In (3.15), $\bar{Q}$ contains the variance terms Q and $K^y R K^{yT}$ along with several bias terms (the terms containing $\bar{d}$). The estimator gain K^y has to be chosen so as to minimize not only the bias but also the variance in order

to minimize $\mathrm{tr}(LP_{lr}L^T)$. Thus, (3.15) expresses a bias-variance tradeoff that is due to the fact that the same estimator gains are used for both bias elimination and noise filtering.

3.2.5 Calibration-based tuning

Sections 3.2.2 - 3.2.4 presented different objectives to be met by adjusting the gain K^y:

1. The eigenvalues of the matrix $A_c = A - K^y H$ have to be within the unit circle in order to ensure stability. Due to Assumption A.2, efficient numerical algorithms, e.g. the KNVD algorithm (see Section 2.3.2), can be used to achieve this objective. However, the optimal pole location remains an open question.

2. The proportional gain $K^y = \begin{bmatrix} \frac{1}{hq}(\gamma\bar{d} - (I - A)q) & 0 \end{bmatrix}$ ensures zero bias in the preferred direction. This equation, however, involves the unknown disturbance vector $\bar{d}$. Additionally, the variance due to stochastic noise is ignored. As a consequence, (3.11) cannot be used to compute the gain K^y. This equation is just a mathematical guarantee that, given the conditions of Theorem 3.2, the observer structure is appropriate for the purpose of PE.

3. The scalar $\mathrm{tr}(LP_{lr}L^T)$ has to be minimized in order to achieve good noise filtering in addition to bias reduction. This can be done by solving the recursion (3.15), which again contains the unknown $\bar{d}$. However, the mathematical equivalent of $\mathrm{tr}(LP_{lr}L^T)$, $\mathrm{E}\left((z_l - \hat{z}_l)^T(z_l - \hat{z}_l)\right)$, can be evaluated from experimental data, i.e. from the measurements of z_l.

Hence, only objectives 1 and 3 can be evaluated from the available information. In order to meet these objectives, the following optimization problem is proposed:

$$\begin{aligned} \min_{\lambda_1^*,\ldots,\lambda_n^*} \quad & J = \sum_l \mathrm{E}\left((z_l - \hat{z}_l)^T (z_l - \hat{z}_l)\right) \\ s.t. \quad & \hat{x}_{k+1} = A\hat{x}_k + Bu_k + K^y(y_k - \hat{y}_k), \quad \hat{x}_0 = \mathrm{E}\,(x_o) \\ & \hat{y}_k = H\hat{x}_k, \\ & \hat{z}_l = L\hat{x}_{lr} \\ & KNVD \text{ algorithm to compute } K^y \\ & |\lambda_i^*| < 1 \end{aligned} \tag{3.16}$$

where $\lambda_i^*,\ i = 1, \cdots, n$ are the desired eigenvalues of the matrix $A - K^y H$. The gains K^y are computed from λ^* via the KNVD algorithm [49] (Section 2.3).

The above optimization problem does not guarantee bias elimination, since it does not contain the condition $K^y = \left[\ \frac{1}{hq}(\gamma\bar{d} - (I - A)q) \quad 0\ \right]$ that cannot be evaluated in practice. But, even if this condition could be evaluated, there would be no guarantee that it could be satisfied simultaneously with the constraint $|eig(A - K^y H)| < 1$. There are systems where actually it is impossible to satisfy the two conditions simultaneously. Hence, for arbitrary systems, complete bias elimination and stability cannot be ensured at the same time. However, there are exceptions as shown in the illustration considered in the next section.

The resulting gains minimize the objective function J, which is the sum of bias and variance terms and, consequently, express the compromise between bias elimination and variance minimization in the preferred directions. Stability is guaranteed by imposing the constraint $|\lambda_i^*| < 1$.

Note that the optimization problem (3.8) could have been extended with the constraint $|eig(A - K^y H)| < 1$ without changing the decision variable from K^y to λ^*. However, the feasibility of the solution, i.e. a value of K^y that satisfies the constraint $|eig(A - K^y H)| < 1$, would not have been guaranteed by the KNVD algorithm, as this is the case in optimization problem (3.16). Nevertheless, using K^y as the decision variable is computationally less expensive, and could be preferred to (3.16) in some situations, as shown in the next section.

In order to determine the observer gains, a numerical optimization is performed based on the available infrequent measurements of z_l. Thus, preferential estimation consists of two steps: (a) the tuning step, where (3.16) is solved; and (b) the estimation step, where the gains obtained from step (a) are used for estimating $\hat{z}$. The tuning step can be carried out off-line, based on measurements available prior to the implementation of the estimator. This approach is analogous to calibration that is used extensively in the field of chemometrics [55].

Unfortunately, the P^y observer is not able to follow time-varying deterministic disturbances. Optimization problem (3.16) has a different solution for each disturbance $\bar{d}$, as was indicated in Theorem 3.2. Thus, for the P^y observer to work properly, the disturbance $\bar{d}$ is required to be the same in both the tuning and estimation steps.

3.2.6 Illustration

The aim of this section is to illustrate the performance of the P^y observer for several types of deterministic disturbances: constant, piecewise-constant and continuously varying. Several tuning procedures are compared. The most effective one consists of solving Optimization problem (3.8) extended with the constraint $|eig(A - K^y H)| < 1$. For time-varying disturbances, retuning is required for each newly available measurement of z. However, there is no guarantee that retuning is able to cope with any time-varying disturbance. Several simulation scenarios are considered, as detailed in the example below.

In order to quantify the performance of the observer, the same performance measures as in Section 2.7 are computed based on Monte-Carlo simulations. Consider the LTI discrete-time plant (3.1) specialized to a 4-dimensional system with A, B, x_o, $H = H_1$, the number of iterations, L, r and θ as in the dual-rate system in Section 2.7, and with:

Table 3.1: Simulation scenarios considered for the P^y observer.

Simulation	6 - tuning, constant disturb.	7 - test, constant disturb.	8 - test, piecewise-constant disturb.	9 -test, time-varying disturb.
d_k	$\bar{d}$	$\bar{d}$	$\tilde{d}$	$\Delta A x_k + u_{exo,k}$
$\hat{x}_0$	$x_{tune,o}$	$x_{test,o}$	$x_{test,o}$	$x_{test,o}$
u_k	$u_{tune,k}$	$u_{test,k}$	$u_{test,k}$	$u_{test,k}$

$$
\begin{aligned}
w_k \;&\rightarrow\; N(0,Q), \qquad v_k \rightarrow N(0,R), \qquad \nu_l \rightarrow N(0,Z) \\
Q \;&=\; \begin{bmatrix} 2 & 0 & 0 & 0 \\ 0 & 3 & 0 & 0 \\ 0 & 0 & 5 & 0 \\ 0 & 0 & 0 & 3 \end{bmatrix}, \qquad R = 2, \qquad Z = \begin{bmatrix} 3 & 0 \\ 0 & 5 \end{bmatrix}
\end{aligned}
$$

The simulation scenarios presented in Table 3.1 are considered, with:

$$
\begin{aligned}
\bar{d} \;&=\; \begin{bmatrix} 3 & 6 & 4.5 & 0.6 \end{bmatrix}^T \\
\tilde{d} \;&=\; \begin{cases} \bar{d}_1 = \begin{bmatrix} 3 & 6 & 4.5 & 0.6 \end{bmatrix}^T & for \quad k \in [0, 99] \\ \bar{d}_2 = \begin{bmatrix} 3.9 & -6 & -6 & -2.4 \end{bmatrix}^T & for \quad k \in [100, 200] \end{cases} \\
\Delta A \;&=\; \begin{bmatrix} -0.0150 & 0.0450 & -0.0150 & 0.0150 \\ 0.0300 & 0.2100 & -0.0450 & 0.0300 \\ -0.0150 & -0.0300 & 0.1500 & -0.0750 \\ 0.0075 & 0 & -0.0750 & 0.1500 \end{bmatrix} \\
x_{tune,o} \;&=\; \begin{bmatrix} 20 & -30 & 50 & -30 \end{bmatrix}^T, \qquad x_{test,o} = -x_{tune,o}
\end{aligned}
$$

$$
\begin{aligned}
u_{exo,k} \;&=\; \begin{bmatrix} -0.13 & 0.2 & 0.5 & 0.08 \end{bmatrix}^T (-30 + 2.5(0.1k)^{1.7}) \\
u_{tune,k} \;&=\; \frac{0.5(0.1k)^{2.2} + 20 \sin 0.05k - 20}{e^{0.005k}} - 100 \\
u_{test,k} \;&=\; -0.005k^2 - 16 \sin 0.1k + 200
\end{aligned}
$$

Note that the input sequence and the initial conditions are different for observer tuning and performance testing. Note also that the pairs (A, H) and (A, L) are both observable.

Simulation 6 – Observer tuning

Several tuning methods are available for determining the gains of a P^y observer, resulting in the following observers:

- $P^y - \lambda$

  Optimization problem (3.16) is solved based on data generated by the first simulation in Table 3.1. To have the minimal number of decision variables, only real eigenvalues are allowed. In this way, there are 4 decision variables instead of 8. Additionally, the KNVD algorithm requires that the multiplicity of an eigenvalue be at most the rank of H, which is 1. Hence, the constraint $|\lambda_i^*| < |\lambda_{i+1}^*|$ is added, in order to ensure 4 different eigenvalues. The following optimal solution is obtained:

$$\lambda_\lambda^* = \left[\begin{array}{cccc} 2.8486 \cdot 10^{-1} & 3.3486 \cdot 10^{-1} & 6.1666 \cdot 10^{-1} & 8.3709 \cdot 10^{-1} \end{array} \right]^T$$

- $P^y - K^y$

  As mentioned in Section 3.2.5, an alternative to (3.16) is to extend the optimization problem (3.8) with the constraint $|eig(A - K^y H)| < 1$:

$$\begin{aligned} \min_{K^y} \quad & J = \sum_l \mathrm{E}\left((z_l - \hat{z}_l)^T (z_l - \hat{z}_l)\right) \\ s.t. \quad & \hat{x}_{k+1} = A\hat{x}_k + Bu_k + K^y(y_k - \hat{y}_k), \quad \hat{x}_0 = \mathrm{E}\,(x_o) \\ & \hat{y}_k = H\hat{x}_k, \\ & \hat{z}_l = L\hat{x}_{lr} \\ & |eig(A - K^y H)| < 1 \end{aligned} \tag{3.17}$$

  without the guarantee of feasibility. In the above problem, complex eigenvalues can also be reached by using the same number of decision variables as for the $P^y - \lambda$ tuning. For the example considered here, Optimization problem (3.17) is feasible, and the solution found leads to the closed-loop eigenvalues:

$$\lambda^*_{K^y} = \left[\begin{array}{ccc} 7.3540 \cdot 10^{-1} \pm 1.1501 \cdot 10^{-1} i & 8.7789 \cdot 10^{-1} & 7.8570 \cdot 10^{-1} \end{array}\right]^T$$

- $P^y - Th$

  The disturbance $\bar{d}$ is known in simulation. Thus, the observer gains can be determined from the theoretical result (3.11), as discussed in Section 3.2.5. Since the parameter γ in (3.11) can be assigned freely, the following optimization problem is proposed to achieve both stable behavior and minimum variance while ensuring bias elimination:

$$\begin{aligned} \min_{\gamma} \quad & J = \sum_{l} \mathrm{E}\left((z_l - \hat{z}_l)^T (z_l - \hat{z}_l)\right) \\ s.t. \quad & \hat{x}_{k+1} = A\hat{x}_k + Bu_k + K^y(y_k - \hat{y}_k), \quad \hat{x}_0 = \mathrm{E}\,(x_o) \\ & \hat{y}_k = H\hat{x}_k, \\ & \hat{z}_l = L\hat{x}_{lr} \\ & K^y = \frac{1}{hq}(\gamma\bar{d} - (I - A)q) \\ & |eig(A - K^y H)| < 1 \end{aligned} \tag{3.18}$$

  where $q = \left[\begin{array}{cccc} 1 & 0 & 0 & 0 \end{array}\right]^T$ and $h = H$.

  This optimization problem is feasible and the optimal γ value yields the closed-loop eigenvalues:

$$\lambda^*_{Th} = \left[\begin{array}{cc} 7.1760 \cdot 10^{-1} \pm 1.1295 \cdot 10^{-1} i & 8.5049 \cdot 10^{-1} \pm 2.3541 \cdot 10^{-2} i \end{array}\right]^T$$

  In this particular example, both bias elimination and satisfactory noise filtering can be ensured through assigning γ, that is, through assigning the observer gains.

The performance of the observers tuned above are compared to a benchmark proportional observer, the Kalman filter. To ensure a fair comparison, both the frequent y and the infrequent z measurements are used in the Kalman filter. Two structures are tested, which differ in the use of

Table 3.2: Performance of various P^y observers for Simulation 6 in Table 3.1 for $k \in [60, 200]$ over 10 realizations.

	KF-ZOH (2.24) - (2.25)	$P^y - Th$ (3.18)	$P^y - \lambda$ (3.16)	$P^y - K^y$ (3.17)
$\bar{e}$	$7.4563 \cdot 10^2$ $1.3001 \cdot 10^3$ $9.7782 \cdot 10^2$ $1.2417 \cdot 10^3$	$5.6903 \cdot 10^3$ $1.2572 \cdot 10^2$ $1.1682 \cdot 10^2$ $1.0863 \cdot 10^2$	$4.0701 \cdot 10^2$ $2.5592 \cdot 10^2$ $4.2214 \cdot 10^2$ $7.1399 \cdot 10^3$	$5.5361 \cdot 10^3$ $1.2151 \cdot 10^2$ $1.1336 \cdot 10^2$ $3.2733 \cdot 10^3$
$\mathcal{V}_e$	$5.1690 \cdot 10^2$ $1.3956 \cdot 10^3$ $2.7285 \cdot 10^3$ $1.2685 \cdot 10^3$	$1.9485 \cdot 10^3$ $1.1337 \cdot 10^3$ $1.6430 \cdot 10^3$ $1.2741 \cdot 10^3$	$6.7555 \cdot 10^2$ $1.7447 \cdot 10^3$ $3.2990 \cdot 10^3$ $1.0800 \cdot 10^4$	$1.8687 \cdot 10^3$ $1.1321 \cdot 10^3$ $1.6401 \cdot 10^3$ $1.5917 \cdot 10^3$
Π_e	$4.4723 \cdot 10^3$ $1.4024 \cdot 10^4$ $9.8097 \cdot 10^3$ $1.2266 \cdot 10^4$	$2.3009 \cdot 10^5$ $1.3052 \cdot 10^3$ $1.7880 \cdot 10^3$ $1.4111 \cdot 10^3$	$1.9031 \cdot 10^3$ $2.3862 \cdot 10^3$ $4.8105 \cdot 10^3$ $3.7069 \cdot 10^5$	$2.1782 \cdot 10^5$ $1.2919 \cdot 10^3$ $1.7803 \cdot 10^3$ $7.7169 \cdot 10^4$
Σ_{Π_e}	$4.0572 \cdot 10^4$	$2.3459 \cdot 10^5$	$3.7979 \cdot 10^5$	$2.9806 \cdot 10^5$

the infrequent measurements. In the first filter, the measurements are used for fast time-scale correction using a ZOH extrapolation (Section 2.6.1), while in the second filter the measurements are used for slow time-scale correction via a switching structure (Section 2.6.2). The performance of the KF-ZOH and KF-Switch are presented in Figure 3.1. As can be observed, the KF-ZOH is performing better, which is clearly seen in x_2. Note that the observers give similar estimates for the time instants when the z measurements become available. However, at the fast time scale, the prediction of the KF-ZOH is much smoother. In order to account for the presence of the deterministic disturbance, the KF-ZOH uses a frequent correction based on the ZOH extrapolations of the z measurements, i.e. frequent but small corrections. In contrast, the infrequent corrections in the KF-Switch result in important deviations in-between the z measurements that, in turn, require more aggressive correction when the z measurements become available. It is interesting to note that, when using the KF-Integral-Switch observer in Section 2.7, these aggressive corrections were not present at the time instants when the z measurements became available. This can be explained by the use of the integral term α_k that actually ensures frequent correction of the states, even if this term is updated only infrequently.

The simulation results are presented in Table 3.2. The best performance

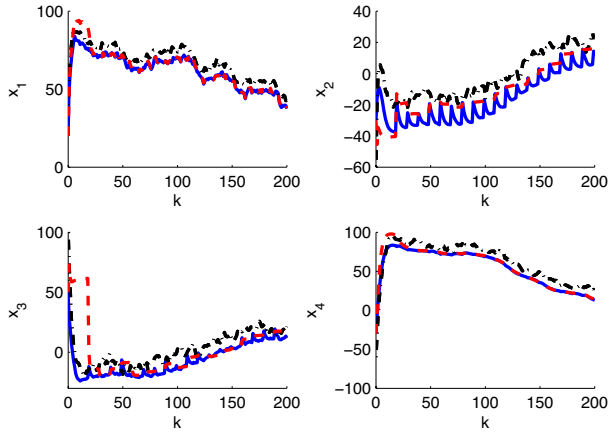

Figure 3.1: Comparison of the KF-ZOH and KF-Switch observers in Simulation 6 for one realization. Plant – dash-dotted line (black); KF-Switch observer – solid line (blue); KF-ZOH observer – dashed line (red).

in the preferred variables x_2 and x_3 is given by the observer $P^y - K^y$ (compare the green numbers). In this particular case, the $P^y - Th$ observer also performs well, being able to eliminate bias, reduce variance and ensure stable dynamics (compare the blue and red numbers). The observer $P^y - \lambda$ suffers from the restricted choice of poles, that is from the fact that only real eigenvalues are allowed (compare the green numbers). The benchmark observer, the Kalman filter with zero-order hold extrapolation (KF-ZOH), does not properly take into account the deterministic disturbances. Even though the KF-ZOH observer uses the z measurements, which provide information on the deterministic disturbances, the observer is not tuned for eliminating the effect of these disturbances. As a result, the KF-ZOH observer yields a higher bias (compare the blue numbers). Figure 3.2 shows the better performance in the preferred variables of the $P^y - K^y$ observer compared to the KF-ZOH. The accuracy of the other states, however, is much worse in the case of the $P^y - K^y$, since it is not considered at all.

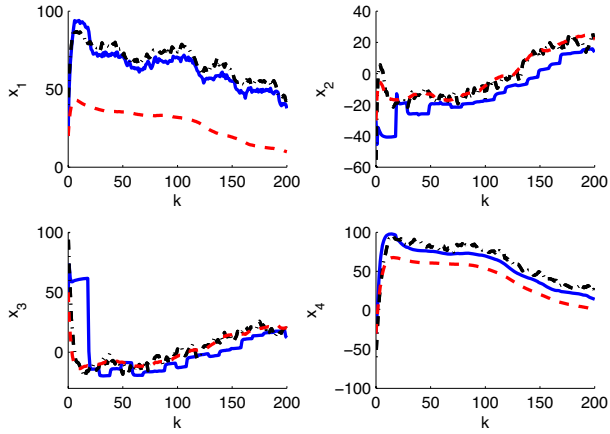

Figure 3.2: Illustration of the best P^y observer on Simulation 6 for $k \in [0, 200]$ for one realization (x_2 and x_3 are the preferred variables). Plant – dash-dotted line (black); KF-ZOH observer – solid line (blue); $P^y - K^y$ observer – dashed line (red).

Simulation 7 – Test with the same disturbances as for tuning

The second simulation is carried out using the previously tuned $P^y - K^y$ observer. The bias is reduced compared to the KF-ZOH in this case as well, as illustrated in Table 3.3 with blue numbers. In spite of different operating conditions, the P^y observer performs the same way as in Simulation 6, since the same value of the deterministic disturbance is used in Simulations 6 and 7.

Simulation 8 – Test with piecewise-constant disturbances

The same $P^y - K^y$ observer as in Simulation 7 is used for piecewise-constant disturbances (Figure 3.3). The observer is able to eliminate the bias when the value of the disturbance is the same as in the tuning data set. However, the observer is not able to compensate for bias caused by another disturbance value.

Hence, retuning of the observer is required. Once the disturbance changes at $k = 100$, Optimization (3.17) is repeated each time a new measurement of z becomes available, using all the z measurements available from iteration

Table 3.3: Performance of the KF-ZOH and $P^y - K^y$ observers in Simulation 7 for $k \in [60, 200]$ over 10 realizations.

	KF-ZOH (2.24) - (2.25)	$P^y - K^y$ (3.17)
$\bar{e}$	$6.1937 \cdot 10^2$	$5.4865 \cdot 10^3$
	$4.9663 \cdot 10^2$	$9.0314 \cdot 10$
	$3.7551 \cdot 10^2$	$1.0859 \cdot 10^2$
	$1.0734 \cdot 10^3$	$3.2442 \cdot 10^3$
$\mathcal{V}_e$	$4.9065 \cdot 10^2$	$1.7960 \cdot 10^3$
	$1.5630 \cdot 10^3$	$1.1450 \cdot 10^3$
	$2.7567 \cdot 10^3$	$1.6440 \cdot 10^3$
	$1.2163 \cdot 10^3$	$1.3582 \cdot 10^3$
Π_e	$3.2550 \cdot 10^3$	$2.1386 \cdot 10^5$
	$4.1234 \cdot 10^3$	$1.2322 \cdot 10^3$
	$4.4919 \cdot 10^3$	$1.7886 \cdot 10^3$
	$9.4639 \cdot 10^3$	$7.5598 \cdot 10^4$
Σ_{Π_e}	$2.1334 \cdot 10^4$	$2.9248 \cdot 10^5$

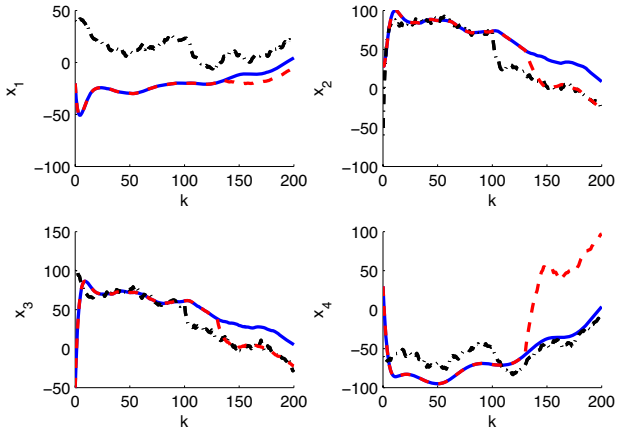

Figure 3.3: Comparison of $P^y - K^y$ and the retuned $P^y - K^y$ observer in Simulation 8 for one realization. Plant – dash-dotted line (black); $P^y - K^y$ observer – solid line (blue); $P^y - K^y$ – *retuned* observer – dashed line (red).

Table 3.4: Performance of the KF-ZOH, $P^y - K^y$ and retuned $P^y - K^y$ observers in Simulation 8 for $k \in [0, 200]$ over 10 realizations.

	KF-ZOH (2.24) - (2.25)	$P^y - K^y$ (3.17)	$P^y - K^y - retuned$ (3.17)
$\bar{e}$	$8.6036 \cdot 10^2$ $3.5769 \cdot 10^3$ $2.1308 \cdot 10^3$ $2.6927 \cdot 10^3$	$6.5314 \cdot 10^3$ $3.5975 \cdot 10^3$ $3.2439 \cdot 10^3$ $3.6073 \cdot 10^3$	$6.9539 \cdot 10^3$ $1.7577 \cdot 10^3$ $1.7405 \cdot 10^3$ $8.4165 \cdot 10^3$
$\mathcal{V}_e$	$6.9706 \cdot 10^2$ $1.9667 \cdot 10^3$ $3.2669 \cdot 10^3$ $1.7147 \cdot 10^3$	$3.1519 \cdot 10^3$ $1.7907 \cdot 10^3$ $2.1899 \cdot 10^3$ $2.0380 \cdot 10^3$	$3.6689 \cdot 10^3$ $2.6298 \cdot 10^3$ $3.1938 \cdot 10^3$ $1.5733 \cdot 10^4$
Π_e	$7.9933 \cdot 10^3$ $1.8146 \cdot 10^5$ $5.6580 \cdot 10^4$ $6.1420 \cdot 10^4$	$2.7828 \cdot 10^5$ $1.1608 \cdot 10^5$ $1.1626 \cdot 10^5$ $8.6851 \cdot 10^4$	$2.9531 \cdot 10^5$ $5.4422 \cdot 10^4$ $7.4100 \cdot 10^4$ $5.5980 \cdot 10^5$
Σ_{Π_e}	$3.0745 \cdot 10^5$	$5.9747 \cdot 10^5$	$9.8363 \cdot 10^5$

$k = 100$ onwards (Figure 3.3). In this way, the estimator is able to adapt to the new disturbance and perform comparably to the KF-ZOH (Table 3.4 - compare the blue numbers). Note that here the performance over the entire time interval is compared, since both the disturbance and the observer gain vary with time. The disadvantage of retuning is that it might not be feasible in real-time applications due to the high computational load.

Simulation 9 – Test with time-varying disturbances caused by parametric errors and an exogenous input

Figure 3.4 shows that the retuned $P^y - K^y$ observer does not improve the accuracy in x_3 compared to the KF-ZOH. Hence, retuning cannot cope with arbitrary varying disturbances, even when it is feasible to repeat the optimization. Nevertheless, it can improve the estimation error, which in this case is visible in the accuracy of x_2. Note that the peak around iteration 50 is due to the optimization being caught in a local minimum.

3.2.7 Discussion

An analysis of the bias and variance properties of the P^y observer for PE has been performed. However, the resulting expressions cannot be used for observer tuning since they involve the disturbance vector $\bar{d}$, which is

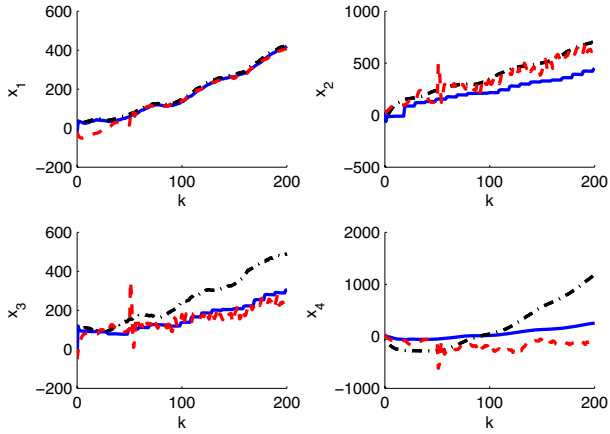

Figure 3.4: Comparison of KF-ZOH and retuned $P^y - K^y$ observer in Simulation 9 for one realization. Plant – dash-dotted line (black); KF-ZOH observer – solid line (blue); $P^y - K^y - retuned$ observer – dashed line (red).

unknown. Nevertheless, these equations give considerable insight into the problem of PE using the P^y observer. It has been shown that, in principle, it is possible to eliminate bias in the preferred variables by taking into account only the mean of the error, i.e. neglecting the stochastic disturbances (Section 3.2.3). However, when such disturbances are present, the gains K^y have to cope with both bias elimination and noise filtering simultaneously. Since there is no theoretical guarantee that these two objectives can be satisfied simultaneously, in general, there is a bias-variance compromise, as explained in Section 3.2.4. To solve this compromise while respecting the stability constraint of the observer, optimization problem (3.16) has been proposed. It is shown in Section 3.2.6 that, from an implementation point of view, optimization problem (3.17) is more appropriate.

To derive the aforementioned analytical results, several Assumptions were introduced in Section 3.2.1. Assumption A.2 on system observability is the standard Assumption for implementing a proportional observer. However, Assumption A.1 that considers constant deterministic disturbances is a restrictive one. Hence, for the chosen observer structure P^y, the tuning pro-

cedure proposed in Section 3.2.5 would have to be repeated for each value of d_k. Since numerical optimization is time consuming, continuous retuning of the observer might not be feasible in practice. Convergence of the continuously retuned P^y observer is not guaranteed either. Moreover, for arbitrary disturbances, the performance of a retuned P^y observer is not significantly better than that of a Kalman filter using the same amount of information, as shown in Section 3.2.6 (see the accuracy of x_3 given by the retuned $P^y - K^y$ observer in Simulation 9). Therefore, the applicability of the P^y observer tuned in the preferential way is limited to constant disturbance $\bar{d}$ or to piecewise-constant disturbance $\tilde{d}$ at best. This motivates the use of an observer structure with an integral term that can follow the changes in the deterministic disturbances. Such an observer will be discussed in the next chapter.

Chapter 4

Integral observer for preferential estimation

Integral observers are proposed in the literature to eliminate the effect of deterministic disturbances [72, 85]. This chapter studies the conditions under which they can be used successfully for PE purposes.

The main result of this chapter is to show that integral observers can eliminate bias in the preferred variables for any value of a piecewise-constant disturbance vector without having to be retuned. Due to the integral term based on the z_l measurements, the estimation error in the preferred variables converges to zero. The role of the observer gains is to ensure convergence. This makes these observers suitable for practical implementation and represents a clear advantage over the P^y observer discussed in Section 3.

However, the price to pay for this capability is a more sophisticated structure. The integral observer proposed in this section is a dual-rate observer with a P^y observer based on the frequent y_k measurements, and a proportional and an integral term ($P^z I^z$) based on the infrequent z_l measurements. The dynamics of this structure are studied at the slow time scale corresponding to the availability of the z_l measurements.

In the proposed structure, the condition of bias elimination is the asymptotic stability of the observer structure. Stability can be guaranteed by an appropriate tuning procedure, given the model is observable from the fast measurements. The tuning parameters can be chosen to reduce the variance. Therefore, there is no bias-variance compromise in the integral observer.

Section 4.1 presents the structure of the $P^y P^z I^z$ observer. Section 4.3 discusses its convergence. The possibility of eliminating bias is studied

in Section 4.4. Section 4.5 presents the tuning procedure for the $P^yP^zI^z$ observer. Section 4.6 illustrates the performance of the observer, while a final discussion is included in Section 4.7.

4.1 Observer structure $P^yP^zI^z$

Consider the plant (3.1) with $d_k = \tilde{d}$:

$$\begin{aligned} x_{k+1} &= Ax_k + Bu_k + \tilde{d} + w_k, \quad x_0 = x_o \\ y_k &= Hx_k + v_k \\ z_l &= Lx_{lr} + \nu_l \end{aligned} \tag{4.1}$$

with $k = lr$ used to indicate the time of the infrequent z measurements.

Consider a $P^yP^zI^z$ observer based on the y_k and z_l measurements, respectively (see Section 3.1.2). The optimization problem (3.2) specialized to the plant (4.1) gives:

$$\begin{aligned} \min_{K^y,K^\beta,K^{z,x},K^{z,\beta}} \quad & J = \sum_l \mathrm{E}\left((z_l - \hat{z}_l)^T(z_l - \hat{z}_l)\right) \\ s.t. \quad & \hat{x}_{k+1} = A\hat{x}_k + Bu_k + K^y(y_k - \hat{y}_k) + K^\beta\beta_k + c_kK^{z,x}(z_l - \hat{z}_l), \quad \hat{x}_0 = \mathrm{E}(x_o) \\ & \beta_{k+1} = \beta_k + c_kK^{z,\beta}(z_l - \hat{z}_l), \quad \beta_0 = 0 \\ & \hat{y}_k = H\hat{x}_k, \\ & \hat{z}_l = L\hat{x}_{lr} \\ & c_k = \begin{cases} 1 & if \quad \frac{k+r-\theta}{r} \in \mathcal{N} \\ 0 & otherwise \end{cases} \end{aligned} \tag{4.2}$$

The role of the integral states β is to ensure asymptotic convergence of $\hat{z}$ to z, i.e. bias elimination in the vector of preferred variables. Note that the integral states β_k are updated only when the z_l measurement, delayed by θ small sampling periods (Figure 2.1), is available. This update scheme is implemented via the switching coefficient c_k.

Since measurements are available at two time scales, the problem (4.2) represents a dual-rate estimation scheme. The dynamic behavior of the

system formed by the plant (4.1) and the $P^yP^zI^z$ observer from (4.2) is studied at the slow time scale corresponding to the index l, i.e. the quantities available at the fast sampling are only considered at the instants $k = lr$, $l = 0, 1, 2, \ldots$.

For the study of the $P^yP^zI^z$ observer the following Assumptions are introduced:

A.2 *The pair* (A, H) *is observable, that is, the state* x *is observable from the output* y*;*

A.3 *Piecewise-constant, deterministic disturbance*

$$d_k = \tilde{d} = \left\{\bar{d}_1, \bar{d}_2, \ldots, \bar{d}_j\right\}$$

as defined in (2.10)*, where each constant piece lasts for a time interval* $k_jt_k \gg 0$*;*

A.4 k_jt_k *is much larger than the dominant time constant of the observer.*

The above Assumptions are needed in order to prove the stability of the observer in Theorem 4.1 and to ensure bias elimination for each constant piece of $\tilde{d}$ in Theorem 4.2.

4.2 Observability from the z measurements

Before discussing the convergence conditions of the error dynamics using the $P^yP^zI^z$ observer, the observability from z measurements of both a single-rate and a dual-rate system using a P^y observer is discussed. This will be needed in the proof of Theorem 4.1.

4.2.1 Observability of a single-rate system ($r = 1$) from z

Consider the single-rate system with a proportional observer based on y measurements:

$$\begin{aligned} \mathrm{E}\left(e_{x,k+1}\right) &= A_c \mathrm{E}\left(e_{x,k}\right) + \tilde{d} \\ \mathrm{E}\left(e_{z,k}\right) &= L\mathrm{E}\left(e_{x,k}\right) \end{aligned} \tag{4.3}$$

where $A_c = A - K^y H$. This is the 'open-loop' system on which observers based on z measurements can be applied. In order to ease the mathematical transformations, it is first considered that the z and y measurements are available at the same rate, i.e. $r = 1$. Consider the 'closed-loop' system with a P^z term:

$$\mathrm{E}\left(e_{x,k+1}\right) = A_c \mathrm{E}\left(e_{x,k}\right) - K^{z,x} L\mathrm{E}\left(e_{x,k}\right) + \tilde{d} \tag{4.4}$$

where $K^{z,x}$ is the gain of the term proportional to the z error.

Stabilization of (4.4) requires that the pair (A_c, L) be observable. According to Assumption A.2, the eigenvalues of the matrix A_c can be chosen arbitrarily. This implies that in the $(nm \times n)$-dimensional observability matrix of the pair (A_c, L):

$$\mathcal{O} = \begin{bmatrix} L \\ LA_c \\ LA_c^2 \\ \vdots \\ LA_c^{n-1} \end{bmatrix} \tag{4.5}$$

it is possible to find an $(n \times n)$-dimensional submatrix $\mathcal{O}_S$, whose determinant is a finite-order polynomial in K^y. Hence, by choosing K^y it is possible to have $\det(\mathcal{O}_S) \neq 0$ for any non-zero L.

4.2.2 Observability of a dual-rate system ($r > 1$) from z

Consider the system (4.3) in a dual-rate scenario by considering infrequent z measurements. The dynamics of the system are studied at the slow time scale, without considering measurement delays. In order to find the general expression, first (4.3) is rewritten at the $l = 1$ and $l = 2$ time instants. For

this, consider the corresponding iterations at the fast time scale $k \in [r, 2r-1]$ (see Figure 2.1):

- $k = r$

$$\mathrm{E}\left(e_{x,r+1}\right) = A_c \mathrm{E}\left(e_{x,r}\right) + \tilde{d} \tag{4.6}$$

- $k = r+1$

$$\mathrm{E}\left(e_{x,r+2}\right) = A_c \mathrm{E}\left(e_{x,r+1}\right) + \tilde{d}$$

Substituting $\mathrm{E}\left(e_{x,r+1}\right)$ from (4.6), results in:

$$\mathrm{E}\left(e_{x,r+2}\right) = A_c^2 \mathrm{E}\left(e_{x,r}\right) + A_c\tilde{d} + \tilde{d} \tag{4.7}$$

- $k = 2r-1$

$$\mathrm{E}\left(e_{x,2r}\right) = A_c \mathrm{E}\left(e_{x,2r-1}\right) + \tilde{d}$$

which can be rewritten as a function of $\mathrm{E}\left(e_{x,r}\right)$

$$\begin{aligned} \mathrm{E}\left(e_{x,2r}\right) &= A_c^r \mathrm{E}\left(e_{x,r}\right) + A_c^{r-1}\tilde{d} + \cdots + \tilde{d} \\ &= A_c^r \mathrm{E}\left(e_{x,r}\right) + \sum_{i=0}^{r-1} A_c^i \tilde{d} \end{aligned} \tag{4.8}$$

Thus, from (4.8), the dynamics of the system (4.3) at the slow time scale can be written as:

$$\begin{aligned} \mathrm{E}\left(e_{x,(l+1)r}\right) &= A_c^r \mathrm{E}\left(e_{x,lr}\right) + \sum_{i=0}^{r-1} A_c^i \tilde{d} \\ \mathrm{E}\left(e_{z,lr}\right) &= L\mathrm{E}\left(e_{x,lr}\right) \end{aligned} \tag{4.9}$$

By using a P^z observer, the following error dynamics are obtained:

$$\mathrm{E}\left(e_{x,(l+1)r}\right) = A_c^r \mathrm{E}\left(e_{x,lr}\right) - K^{z,x} L\mathrm{E}\left(e_{x,lr}\right) + \sum_{i=0}^{r-1} A_c^i \tilde{d} \tag{4.10}$$

In order to guarantee the convergence of these error dynamics, the pair (A_c^r, L) must be observable. Following the same reasoning as for the single-rate system, the observability matrix of the pair (A_c^r, L),

$$\mathcal{O}^r = \begin{bmatrix} L \\ LA_c^r \\ LA_c^{2r} \\ \vdots \\ LA_c^{(n-1)r} \end{bmatrix} \tag{4.11}$$

can be made full rank by an appropriate choice of the K^y matrix.

In other words, both $\mathcal{O}$ and $\mathcal{O}^r$ have an $(n \times n)$-dimensional submatrix whose determinant is a finite-order polynomial in K^y. These polynomials have a finite number of real roots. Since the elements of K^y are free decision variables in the infinite set $\Re$, it is always possible to find a value of K^y that is not a solution of either $\det(\mathcal{O}_S) = 0$ or $\det(\mathcal{O}_S^r) = 0$. Hence, the observability of both the single-rate system and its dual-rate counterpart can be ensured simultaneously.

4.3 Convergence of the error dynamics

Using Assumption A.3, the dynamics of the error $e_{x,lr} = x_{lr} - \hat{x}_{lr}$ and of the integral state β_{lr}, $l = 1, 2, \cdots$, at the slow time scale, can be obtained from (4.1) and (4.2) as:

$$\begin{aligned} e_{x,(l+1)r} &= \left(A_c^r - A_c^{r-1-\theta} K^{z,x} L - \sum_{i=0}^{r-2-\theta} A_c^i K^\beta K^{z,\beta} L \right) e_{x,lr} \\ &\quad - \sum_{i=0}^{r-1} A_c^i K^\beta \beta_{lr} + \sum_{i=0}^{r-1} A_c^i \left(\tilde{d} + w_{(l+1)r-(i+1)} - K^y v_{(l+1)r-(i+1)} \right) \\ &\quad - \sum_{i=0}^{r-2-\theta} A_c^i K^\beta L \nu_l \end{aligned} \tag{4.12}$$

$$\beta_{(l+1)r} = \beta_{lr} + K^{z,\beta} L e_{x,lr} + \nu_l \tag{4.13}$$

Considering the fact that w, v and ν are zero-mean, the mean of the error over the noise is:

$$\begin{aligned} \mathrm{E}\left(e_{x,(l+1)r}\right) &= \left(A_c^r - A_c^{r-1-\theta}K^{z,x}L - \sum_{i=0}^{r-2-\theta} A_c^i K^\beta K^{z,\beta} L\right)\mathrm{E}\left(e_{x,lr}\right) \\ &\quad -\sum_{i=0}^{r-1} A_c^i K^\beta \mathrm{E}\left(\beta_{lr}\right) + \sum_{i=0}^{r-1} A_c^i \tilde{d} \qquad (4.14) \\ \mathrm{E}\left(\beta_{(l+1)r}\right) &= \mathrm{E}\left(\beta_{lr}\right) + K^{z,\beta} L \mathrm{E}\left(e_{x,lr}\right) \qquad (4.15) \end{aligned}$$

In matrix form, (4.14) reads:

$$\mathrm{E}\left(e_{(l+1)r}\right) = (\mathcal{A} - \mathcal{K}\mathcal{H})\mathrm{E}\left(e_{lr}\right) + U(\tilde{d}) \qquad (4.16)$$

with

$$\mathrm{E}\left(e_{lr}\right) = \begin{bmatrix} \mathrm{E}\left(e_{x,lr}\right) \\ \mathrm{E}\left(\beta_{lr}\right) \end{bmatrix}, \qquad \mathcal{A} = \begin{bmatrix} A_c^r & -\sum_{i=0}^{r-1} A_c^i K^\beta \\ 0_{m\times n} & I_m \end{bmatrix}$$

$$\mathcal{K} = \begin{bmatrix} -A_c^{r-1-\theta}K^{z,x} - \sum_{i=0}^{r-2-\theta} A_c^i K^\beta K^{z,\beta} \\ -K^{z,\beta} \end{bmatrix}$$

$$\mathcal{H} = \begin{bmatrix} L & 0_{m\times m} \end{bmatrix}, \qquad U = \begin{bmatrix} \sum_{i=0}^{r-1} A_c^i \tilde{d} \\ 0_{m\times 1} \end{bmatrix}$$

Note that in the above expression the measurement delay is taken into account explicitly, i.e. no Assumption is made in this respect. By using the notation:

$$P = \begin{bmatrix} -A_c^{r-1-\theta} & -\sum_{i=0}^{r-2-\theta} A_c^i K^\beta \\ 0 & -I_m \end{bmatrix}$$
$$K^z = \begin{bmatrix} K^{z,x} \\ K^{z,\beta} \end{bmatrix}$$

$\mathcal{K}$ simplifies to:

$$\mathcal{K} = PK^z \tag{4.17}$$

The error dynamics (4.16) are in the usual form of a linear estimator, since choosing $\mathcal{K}$ is equivalent to choosing K^z, due to the fact that P is a full-rank matrix by construction. The condition for these error dynamics to converge is the observability of the pair $(\mathcal{A}, \mathcal{H})$. Note that this condition is the dual-rate equivalent of the integral observability condition in Section 2.4.3. Since the condition $\text{rank}(\mathcal{H}) = n$ cannot be satisfied due to the definition of the problem PE ($m < n$), a different condition for guaranteeing the observability of this pair is given in Theorem 4.1. This condition is based on the dual-rate observability discussed in Section 4.2.

Theorem 4.1 *Assumptions* A.2 *to* A.4 *hold. The eigenvalues of* $(\mathcal{A} - \mathcal{K}\mathcal{H})$ *in* (4.16) *can be placed anywhere within the unit circle if and only if the pair* (A_c^r, L) *is observable.*

Proof. The eigenvalues of $(\mathcal{A} - \mathcal{K}\mathcal{H})$ can be placed arbitrarily if and only if the pair $(\mathcal{A}, \mathcal{H})$ is observable. The observability matrix reads:

$$\mathcal{O} = \begin{bmatrix} \mathcal{H} \\ \mathcal{H}\mathcal{A} \\ \mathcal{H}\mathcal{A}^2 \\ \vdots \\ \mathcal{H}\mathcal{A}^{n+m-1} \end{bmatrix} =$$

$$= \begin{bmatrix} L & 0 \\ LA_c^r & -L\sum_{i=0}^{r-1} A_c^i K^\beta \\ LA_c^{2r} & -L\left(A_c^r + I\right)\sum_{i=0}^{r-1} A_c^i K^\beta \\ LA_c^{3r} & -L\left(A_c^{2r} + A_c^r + I\right)\sum_{i=0}^{r-1} A_c^i K^\beta \\ \vdots & \vdots \\ LA_c^{(n+m-1)r} & -L\left(A_c^{(n+m-2)r} + \cdots + A_c^r + I\right)\sum_{i=0}^{r-1} A_c^i K^\beta \end{bmatrix}$$

The rank of $\mathcal{O}$ must be $n+m$ for the pair $(\mathcal{A}, \mathcal{H})$ to be observable. The $(n+m)m \times n+m$ matrix $\mathcal{O}$ can be rewritten as the product of two matrices of dimensions $(n+m)m \times n+2m$ and $n+2m \times n+m$, respectively:

$$\mathcal{O} = \tag{4.18}$$

$$\begin{bmatrix} 0 & I_m & 0 \\ L & 0 & -L\sum_{i=0}^{r-1} A_c^i K^\beta \\ LA_c^r & 0 & -L\left(A_c^r + I\right)\sum_{i=0}^{r-1} A_c^i K^\beta \\ LA_c^{2r} & 0 & -L\left(A_c^{2r} + A_c^r + I\right)\sum_{i=0}^{r-1} A_c^i K^\beta \\ \vdots & \vdots & \vdots \\ LA_c^{(n+m-2)r} & 0 & -L\left(A_c^{(n+m-2)r} + \cdots + A_c^r + I\right)\sum_{i=0}^{r-1} A_c^i K^\beta \end{bmatrix} \begin{bmatrix} A_c^r & 0 \\ L & 0 \\ 0 & I_m \end{bmatrix}$$

It can be observed that the second matrix is of rank $(n+m)$ since the rank of A_c^r is n. Note that $\text{rank}(A_c^r) = n$ can be guaranteed from Assump-

tion A.2, which ensures that arbitrary eigenvalues for the matrix A_c (and consequently A_c^r) can be chosen. For the product of the two matrices from (4.18) to be of rank $(n+m)$, it is sufficient to show that the intersection of the null space of the first matrix and the range space of the second matrix is the empty set. In other words, it has to be shown that linear combinations of the columns of the second matrix cannot be null vectors of the first matrix.

To show that a given vector is not a null vector of the first matrix in (4.18):

$$M = \begin{bmatrix} 0 & I_m & 0 \\ L & 0 & -L\sum_{i=0}^{r-1} A_c^i K^\beta \\ LA_c^r & 0 & -L\left(A_c^r + I\right)\sum_{i=0}^{r-1} A_c^i K^\beta \\ LA_c^{2r} & 0 & -L\left(A_c^{2r} + A_c^r + I\right)\sum_{i=0}^{r-1} A_c^i K^\beta \\ \vdots & \vdots & \vdots \\ LA_c^{(n+m-2)r} & 0 & -L\left(A_c^{(n+m-2)r} + \cdots + A_c^r + I\right)\sum_{i=0}^{r-1} A_c^i K^\beta \end{bmatrix}$$

it is sufficient to find one row in M whose product with that vector is non-zero.

Combining linearly the columns of the $n+2m \times m$ matrix $\begin{bmatrix} 0 \\ 0 \\ I_m \end{bmatrix}$ with an $n+2m \times m$ dimensional subset $\begin{bmatrix} A_{c,S} \\ L_S \\ 0 \end{bmatrix}$ of $\begin{bmatrix} A_c^r \\ L \\ 0 \end{bmatrix}$ leads to

$$V = \begin{bmatrix} \gamma_1 A_{c,S} \\ \gamma_1 L_S \\ \gamma_2 I_m \end{bmatrix}$$

where $\gamma_1, \gamma_2 \in \Re$ are arbitrary constants.

- For $\gamma_2 \neq 0$, it is possible to choose K^β such that this matrix is nonsingular for any γ_1.

  Given Assumption A.2, it is possible to have $\text{rank}(A_c) = rank\left(\sum_{i=0}^{r-1} A_c^i\right) = n$ and $\text{rank}(A_{c,S}) = rank(LA_{c,S}) = m$.

  Let $K^\beta = \left(\sum_{i=0}^{r-1} A_c^i\right)^{-1} A_{c,S}$.

  Multiplying the second row of M with V gives:

$$\gamma_1 LA_{c,S} - \gamma_2 L \sum_{i=0}^{r-1} A_c^i K^\beta = \gamma_1 LA_{c,S} - \gamma_2 LA_{c,S} = (\gamma_1 - \gamma_2) LA_{c,S}$$

  Observe that for $\forall\, \gamma_1 \neq \gamma_2$ the above product is full rank: $\text{rank}((\gamma_1 - \gamma_2) LA_{c,S}) = m$.

  Multiplying the third row of M with V gives:

$$\gamma_1 LA_c^r A_{c,S} - \gamma_2 L \left(A_c^r + I\right) \sum_{i=0}^{r-1} A_c^i K^\beta = \gamma_1 LA_c^r A_{c,S} - \gamma_2 L \left(A_c^r + I\right) A_{c,S}$$

  In the case $\gamma_1 = \gamma_2 = \gamma$, the above expression becomes:

$$-\gamma LA_{c,S}$$

  which is also of rank m. Hence, for $\forall\, \gamma_1,\, \gamma_2 \in \Re$ there is a row in M that multiplied by V yields a rank m matrix, given that the same $A_{c,S}$ is used both in V and K^β.

  If a different subset of A_c^r is considered:

$$V' = \begin{bmatrix} \gamma_1 A'_{c,S} \\ \gamma_1 L'_S \\ \gamma_2 I_m \end{bmatrix}$$

multiplication with the second row of M gives:

$$\gamma_1 LA'_{c,S} - \gamma_2 L\sum_{i=0}^{r-1} A_c^i K^\beta = \gamma_1 LA'_{c,S} - \gamma_2 LA_{c,S} = \gamma_2 \left(\frac{\gamma_1}{\gamma_2} LA'_{c,S} - LA_{c,S}\right)$$

By using the notation $\gamma_3 = \frac{\gamma_1}{\gamma_2}$ and since $\gamma_2 \neq 0$ ($\gamma_2 = 0$ is a different case, which is discussed below), the determinant of the above expression becomes an m-order polynomial in γ_3.

Similarly, multiplying the third row of M with V' will lead to another expression whose determinant is an m-order polynomial in γ_3. Since, A_c^r and $LA_{c,S}$ are full rank, this polynomial will be different from that resulting from the multiplication of the second row of M with V'. Besides, the other rows of the matrix M can also be used to show that V' is not a null vector. Overall, there are $(n+m-2)$ different polynomials of order m in γ_3, which certainly cannot be made simultaneously zero.

Hence, neither V nor V' are null vectors of M with the choice of $K^\beta = \left(\sum_{i=0}^{r-1} A_c^i\right)^{-1} A_{c,S}$. Note that the choice of K^β is not unique. The above choice simplifies the proof considerably. However, other choices might also lead to an observable pair $(\mathcal{A}, \mathcal{H})$.

- For $\gamma_2 = 0$, K^β will no longer be a handle. In this case, however, it is sufficient to show that the column $\begin{bmatrix} A_c^r \\ L \\ 0 \end{bmatrix}$ is not a null vector of the first matrix in (4.18). For this, multiply the first matrix with the column $\begin{bmatrix} A_c^r \\ L \\ 0 \end{bmatrix}$. The result is:

$\begin{bmatrix} L \\ LA_c^r \\ LA_c^{2r} \\ LA_c^{3r} \\ \vdots \\ LA_c^{(m+n-1)r} \end{bmatrix}$ which contains the observability matrix of the pair (A_c^r, L). Hence, this matrix is of full-column rank if the pair (A_c^r, L) is observable, which is assumed to be the case. So, $\begin{bmatrix} A_c^r \\ L \\ 0 \end{bmatrix}$ does not belong to the null space of the first matrix.

□

The following observations can be made:

- The condition $\text{rank}(\mathcal{H}) = n$ is not required, in contrast to the condition for integral observability in Section 2.4. This can be explained by the non-redundant structure of the integral observer proposed in this chapter. In the $P^y P^z I^z$ observer, only as many integrators are used as there are preferred variables, in contrast to the integral observer discussed in Section 2.4, where n integrators are used even if less variables are measured.
- The $P^y P^z I^z$ observer contains additional degrees of freedom compared to the integral observer of Section 2.4. These are the gains K^β and K^y that are both used to ensure observability of the pair $(\mathcal{A}, \mathcal{H})$: the gain K^β must be chosen as $K^\beta = \left(\sum_{i=0}^{r-1} A_c^i \right)^{-1} A_{c,S}$, while the gain K^y has to ensure observability of the pair (A_c^r, L), for the case where K^β cannot be used as a handle.

4.4 Estimation bias

The objective of this section is to show that, for constant or piecewise-constant non-zero deterministic disturbances, the mean of the estimation error for the preferred variables converges asymptotically to zero.

Theorem 4.2 *Consider the error dynamics* (4.16) *and the Assumptions* A.2 *to* A.4. *The mean of the steady-state error in z vanishes for any value of the piecewise-constant disturbances $\tilde{d}$ within the interval Δt_j if and only if $(\mathcal{A} - \mathcal{KH})$ is Schur stable.*

Proof.

For piecewise-constant deterministic disturbances considered (Assumption A.4), the term $U(\tilde{d})$ in (4.16) is constant in an interval $k_j t_k$, and plays the role of a constant exogenous input. Since $k_j t_k$ is sufficiently long (Assumption A.4), steady state is reached if and only if the system is stable, i.e. the matrix $(\mathcal{A} - \mathcal{KH})$ has all eigenvalues within the unit circle.

At steady state, (4.16) gives:

$$0 = K^{z,\beta} L \bar{e}_x \tag{4.19}$$

The fact that the matrix $(\mathcal{A} - \mathcal{KH})$ is Schur stable guarantees that $K^{z,\beta}$ is full rank (otherwise there would be at least one eigenvalue at 1). This means that the proposed observer leads to $L\bar{e}_x = 0$, i.e. to a zero-mean steady-state error in z, for any value of $\tilde{d}$. □

Remark. From Theorem 4.1, $(\mathcal{A} - \mathcal{KH})$ can be made Schur stable if the pair (A_c^r, L) is observable. This observability condition can always be satisfied by an appropriate choice of the gain matrix K^y, given Assumption A.2 (see Section 4.2).

4.5 Calibration-based tuning

Theorem 4.2 shows that, for any value of $\tilde{d}$, bias in z can be eliminated provided the matrix $(\mathcal{A} - \mathcal{KH})$ is stable. A procedure for constructing a stable matrix $(\mathcal{A} - \mathcal{KH})$ can be inferred from the proof of Theorem 4.1. The procedure involves the following steps:

1. Choose K^y.

2. Check the observability of the pair (A_c^r, L). If it is not observable, go back to Step 1.

3. Choose $K^{\beta} = \left(\sum_{i=0}^{r-1} A_c^i\right)^{-1} A_{c,S}$, which guarantees the observability of the pair $(\mathcal{A}, \mathcal{H})$. Note that this choice is not unique, since other K^{β} values could also lead to an observable pair $(\mathcal{A}, \mathcal{H})$.

4. Choose the desired poles λ_i^*, $i = 1, \cdots, n+m$, to lie within the unit circle.

5. Choose K^z by the KNVD algorithm such that $(\mathcal{A} - \mathcal{K}\mathcal{H})$ has the desired poles λ_i^*.

The above procedure does not give information regarding the choice of either the coefficients in Steps 1 and 3 or the desired poles in Step 4, except that the poles have to be within the unit circle. This is because only the mean of the estimation error is used in (4.16), while its variance related to the process and measurement noises is not considered. However, the degrees of freedom available in Steps 1, 3 and 4 can be used to shape this variance and express the compromise between convergence speed and noise-filtering capabilities, while still respecting the stability condition, which is equivalent to bias elimination. Note that zero bias is guaranteed even when the available degrees of freedom are chosen to reduce the variance. Thus, a bias-variance compromise does not exist in the sense that was discussed in the case of the P^y observer in Section 3.2.4.

Although there are available degrees of freedom in Steps 1 and 3, Steps 4-5 alone ensure arbitrary pole placement. Thus, it is not necessary to consider the gains K^y in Step 1 as decision variables.

Consequently, it is proposed to leave out Steps 1-3 from the optimization problem used for observer tuning. They could be carried out manually. Only the degrees of freedom available in Step 4, which are sufficient for arbitrary pole placement, are used for variance reduction in the numerical optimization problem:

$$
\begin{aligned}
\min_{\lambda_1^*,\cdots,\lambda_{n+m}^*} \quad & J = \sum_l \mathrm{E}\left((z_l - \hat{z}_l)^T (z_l - \hat{z}_l)\right) && (4.20)\\
s.t. \quad & \hat{x}_{k+1} = A\hat{x}_k + Bu_k + K^y(y_k - \hat{y}_k) + K^\beta \beta_k + c_k K^{z,x}(z_l - \hat{z}_l), \\
& \qquad\qquad \hat{x}_0 = \mathrm{E}\,(x_o) \\
& \beta_{k+1} = \beta_k + c_k K^{z,\beta}(z_l - \hat{z}_l), \qquad \beta_0 = 0 \\
& \hat{y}_k = H\hat{x}_k \\
& \hat{z}_l = L\hat{x}_{lr} \\
& c_k = \begin{cases} 1 & if \quad \frac{k+r-\theta}{r} \in \mathcal{N} \\ 0 & otherwise \end{cases} \\
& KNVD\ algorithm\ to\ compute\ K^{z,x}\ and\ K^{z,\beta} \\
& |\lambda_i^*| < 1
\end{aligned}
$$

This optimization problem is similar to that in (4.2) except for the decision variables and for the stability constraint $|\lambda_i^*| < 1$ that is considered explicitly here. Note that the optimization problem (4.2) could also have been extended with the stability constraint $|eig(\mathcal{A} - \mathcal{K}\mathcal{H})| < 1$; however, there would not have been any guarantee of the existence of a feasible solution, that is, of a set of gains $\{K^y, K^\beta, K^{z,x}, K^{z,\beta}\}$ satisfying this constraint. In contrast, in the optimization problem (4.20), feasibility is guaranteed by the tuning procedure resulting from Theorem 4.1.

Optimization problem (4.20) can be solved numerically based on historical data, thereby leading to a calibration-based tuning as discussed in Section 3.2.5. This optimization problem yields a stable estimator. Since convergence is the only condition for bias elimination, the $P^yP^zI^z$ observer does not have to be retuned when $\tilde{d}$ changes. Thus, the repeatability condition, needed in Section 3.2.5 for the P^y observer to work, is not required here.

4.6 Illustration

The aim of this section is to illustrate the performance of the integral observer $P^yP^zI^z$ on the same dual-rate system and for the same simulation scenarios as in Section 3.2.6. Here again, several tuning procedures are

compared. These yield observers of similar efficiency, which can only be explained by the presence of the integral term. Hence, tuning of integral observers is much easier than that of P^y observers. Additionally, integral observers can better follow variations in deterministic disturbances, even without retuning.

Simulation 6 – Observer tuning

The tuning procedure in Section 4.5 is applied. Steps 1-3 are carried out manually. K^y in Step 1 is chosen to be the gain after convergence of a Kalman filter using the y measurements:

$$K^y = \left[\begin{array}{cccc} 5.6693 \cdot 10^{-2} & 3.9472 \cdot 10^{-3} & 1.2375 \cdot 10^{-2} & 1.7781 \cdot 10^{-2} \end{array} \right]^T \quad (4.21)$$

With this choice, the pair (A_c, L) is observable. The pair (A_c^r, L) is also observable, satisfying the requirement of Step 2. In Step 3, the gain K^β is chosen to be:

$$K^\beta = \left[\begin{array}{cc} 0 & 0 \\ 0.1 & 0 \\ 0 & 0.1 \\ 0 & 0 \end{array} \right] \quad (4.22)$$

leading to an observable pair $(\mathcal{A}, \mathcal{H})$.

The gain K^z is tuned in three different ways:

- $P^y P^z I^z - man.$

  The gain $\mathcal{K} = K^z$ in (4.17) is fixed manually to:

$$K^z = \left[\begin{array}{cc} 0 & 0 \\ 0 & 0 \\ 0 & 0 \\ 0 & 0 \\ -1 & 0 \\ 0 & -1 \end{array} \right] \quad (4.23)$$

  The eigenvalues of the matrix $(\mathcal{A} - K^z \mathcal{H})$ in (4.16) are:

$$\lambda_{P^y I^z} = \begin{bmatrix} 6.1493 \cdot 10^{-1} \pm 2.9943 \cdot 10^{-1} i & 1.1245 \cdot 10^{-1} \\ 2.0018 \cdot 10^{-1} & 3.9257 \cdot 10^{-1} \pm 2.4355 \cdot 10^{-1} i \end{bmatrix}^T$$

Thus, without any theoretical considerations supporting this choice of gains, a stable closed-loop system is obtained.

- $P^y P^z I^z - \lambda$

  The optimal pole location can be found by solving Optimization problem (4.20) using K^y from (4.21) and K^β from (4.22). Since the above observer is expected to deal with time-varying disturbances as well, its dynamics need to be rather fast. Thus, eigenvalues $|\lambda_i^*| < 0.6$ are required. Only real eigenvalues are allowed, just as in Section 4.6. The result is:

$$\lambda_{P^y P^z I^z - \lambda} = \begin{bmatrix} 1.5019 \cdot 10^{-1} & 2.0019 \cdot 10^{-1} & 2.5019 \cdot 10^{-1} \\ 3.3296 \cdot 10^{-1} & 3.8296 \cdot 10^{-1} & 5.4000 \cdot 10^{-1} \end{bmatrix}^T$$

- $P^y P^z I^z - K^z$

  Similar to the P^y observer in Section 4.6, Optimization problem (4.2) can be modified by including a constraint on the eigenvalues, however, without any guarantee of feasibility. K^y and K^β from (4.21) and (4.22) are used. This leads to the optimization problem:

$$
\begin{aligned}
\min_{K^z} \quad & J = \sum_l \mathrm{E}\left((z_l - \hat{z}_l)^T (z_l - \hat{z}_l)\right) && (4.24)\\
s.t. \quad & \hat{x}_{k+1} = A\hat{x}_k + Bu_k + K^y(y_k - \hat{y}_k) + K^\beta \beta_k + c_k K^{z,x}(z_l - \hat{z}_l), \\
& \qquad\qquad \hat{x}_0 = \mathrm{E}\left(x_o\right) \\
& \beta_{k+1} = \beta_k + c_k K^{z,\beta}(z_l - \hat{z}_l), \qquad \beta_0 = 0 \\
& \hat{y}_k = H\hat{x}_k, \\
& \hat{z}_l = L\hat{x}_{lr} \\
& c_k = \begin{cases} 1 & if \quad \frac{k+r-\theta}{r} \in \mathcal{N} \\ 0 & otherwise \end{cases} \\
& |eig(\mathcal{A} - K^z\mathcal{H})| < 0.6
\end{aligned}
$$

The resulting observer gains and eigenvalues are:

$$
\begin{aligned}
K^z &= \begin{bmatrix} 6.2754 \cdot 10^{-1} & -1.1196 \\ 4.5425 \cdot 10^{-1} & 1.1111 \cdot 10^{-2} \\ 2.1053 \cdot 10^{-1} & -1.3300 \cdot 10^{-2} \\ 1.5204 & 2.8329 \cdot 10^{-1} \\ -1.8068 & 4.1838 \cdot 10^{-1} \\ -9.4115 \cdot 10^{-1} & -3.4140 \cdot 10^{-1} \end{bmatrix} && (4.25)\\
\lambda_{P^y P^z I^z - K^z} &= \begin{bmatrix} -1.1100 \cdot 10^{-1} & 1.7406 \cdot 10^{-1} \pm 1.9807 \cdot 10^{-1} i \\ 5.5138 \cdot 10^{-1} \pm 3.1489 \cdot 10^{-3} i & 5.4680 \cdot 10^{-1} \end{bmatrix}^T
\end{aligned}
$$

The performance of the three observers is compared in Table 4.1 to the performance of the KF-Integral-Switch from Section 2.6.2, tuned as in Section 2.7. It can be observed that the accuracy in the preferred variables is similar for the three $P^y P^z I^z$ observers (compare the blue numbers), which is better than that of the KF-Integral-Switch observer. Additionally, the performance of these three observers is comparable to, though not as good as, the one given by the $P^y - K^y$ observer tuned in the preferential way (Table 4.1 - green numbers). This shows that a simple manual tuning of the $P^y P^z I^z$ observer can provide results similar to the P^y observer tuned in the preferential way.

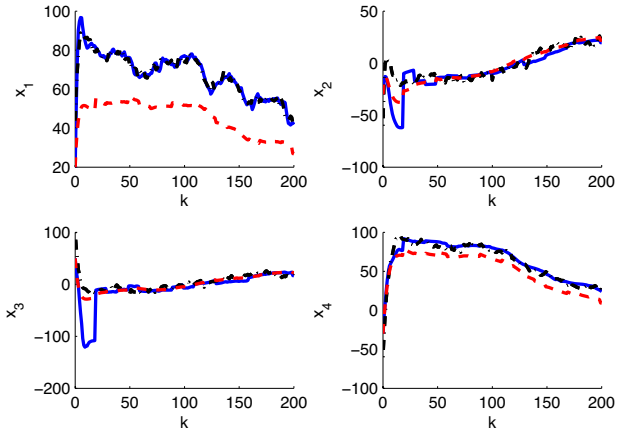

Figure 4.1: Comparison of the KF-Integral-Switch and the $P^yP^zI^z-\lambda$ observers in Simulation 6 (observer tuning) for one realization. Plant – dash-dotted line (black); KF - Integral - Switch observer – solid line (blue); $P^yP^zI^z-\lambda$ observer – dashed line (red).

In the sequel, the $P^yP^zI^z-\lambda$ observer is chosen for illustration purposes to parallel the theoretical developments of this chapter. The $P^yP^zI^z-\lambda$ observer is compared to the KF-Integral-Switch observer in Figure 4.1. The KF-Integral-Switch observer results in a large initial overshoot, which is due to the aggressive tuning used in Section 2.7. But, just as in the case of the $P^yP^zI^z-\lambda$ observer, fast dynamics are required for coping with time-varying deterministic disturbances.

Simulation 7 – Test with the constant disturbances used for tuning

Table 4.2 shows that the P^y-K^y observer provides the best performance (compare the blue numbers). A possible explanation is that the performance of the integral observers is affected more by the change in the initial conditions compared to those used in the tuning step (the disturbances are the same for tuning and test).

Simulation 8 – Test with piecewise-constant disturbances

The KF-Integral-Switch still yields a large initial overshoot (Figure 4.2 -

Table 4.1: Performance of the KF-Integral-Switch observer and the integral observers $P^yP^zI^z - man.$, $P^yP^zI^z - \lambda$ and $P^yP^zI^z - K^z$ in Simulation 6 for $k \in [60, 200]$ over 10 realizations.

	KF-Integral-Switch Section 2.6.2	$P^yP^zI^z - man.$ (4.23)	$P^yP^zI^z - \lambda$ (4.20)	$P^yP^zI^z - K^z$ (4.24)
$\bar{e}$	$7.1331 \cdot 10^1$ $3.5845 \cdot 10^2$ $2.9064 \cdot 10^2$ $1.1793 \cdot 10^2$	$2.8284 \cdot 10^3$ $1.3900 \cdot 10^2$ $1.0631 \cdot 10^2$ $1.6072 \cdot 10^3$	$2.8398 \cdot 10^3$ $1.2184 \cdot 10^2$ $1.1589 \cdot 10^2$ $1.6166 \cdot 10^3$	$2.8086 \cdot 10^3$ $1.2431 \cdot 10^2$ $1.0441 \cdot 10^2$ $1.6060 \cdot 10^3$
$\mathcal{V}_e$	$7.3079 \cdot 10^2$ $1.8278 \cdot 10^3$ $3.2153 \cdot 10^3$ $2.4691 \cdot 10^3$	$1.7469 \cdot 10^3$ $1.4806 \cdot 10^3$ $2.5764 \cdot 10^3$ $1.5494 \cdot 10^3$	$1.6351 \cdot 10^3$ $1.3699 \cdot 10^3$ $2.2036 \cdot 10^3$ $1.5442 \cdot 10^3$	$3.4454 \cdot 10^3$ $1.4464 \cdot 10^3$ $2.0947 \cdot 10^3$ $2.5354 \cdot 10^3$
Π_e	$7.8148 \cdot 10^2$ $3.2349 \cdot 10^3$ $4.0889 \cdot 10^3$ $2.6259 \cdot 10^3$	$5.8209 \cdot 10^4$ $1.6826 \cdot 10^3$ $2.7032 \cdot 10^3$ $1.9860 \cdot 10^4$	$5.8547 \cdot 10^4$ $1.5235 \cdot 10^3$ $2.3425 \cdot 10^3$ $2.0080 \cdot 10^4$	$5.9089 \cdot 10^4$ $1.6031 \cdot 10^3$ $2.2171 \cdot 10^3$ $2.0860 \cdot 10^4$
Σ_{Π_e}	$1.0731 \cdot 10^4$	$8.2454 \cdot 10^4$	$8.2493 \cdot 10^4$	$8.3770 \cdot 10^4$

Table 4.2: Performance of the KF-Integral-Switch, $P^y - K^y$ and $P^yP^zI^z - \lambda$ observers in Simulation 7 for $k \in [60, 200]$ over 10 realizations.

	KF-Integral-Switch Section 2.6.2	$P^y - K^y$ (3.17)	$P^yP^zI^z - \lambda$ (4.20)
$\bar{e}$	$5.9228 \cdot 10^1$ $5.2925 \cdot 10^2$ $5.3962 \cdot 10^2$ $2.5859 \cdot 10^3$	$5.4865 \cdot 10^3$ $9.0314 \cdot 10$ $1.0859 \cdot 10^2$ $3.2442 \cdot 10^3$	$2.8343 \cdot 10^3$ $9.6257 \cdot 10$ $1.3143 \cdot 10^2$ $1.6173 \cdot 10^3$
$\mathcal{V}_e$	$6.4687 \cdot 10^2$ $1.9742 \cdot 10^3$ $3.1168 \cdot 10^3$ $3.0996 \cdot 10^3$	$1.7960 \cdot 10^3$ $1.1450 \cdot 10^3$ $1.6440 \cdot 10^3$ $1.3582 \cdot 10^3$	$1.3357 \cdot 10^3$ $1.4638 \cdot 10^3$ $1.9684 \cdot 10^3$ $1.3171 \cdot 10^3$
Π_e	$6.8566 \cdot 10^2$ $4.9244 \cdot 10^3$ $5.7475 \cdot 10^3$ $5.0277 \cdot 10^4$	$2.1386 \cdot 10^5$ $1.2322 \cdot 10^3$ $1.7886 \cdot 10^3$ $7.5598 \cdot 10^4$	$5.7977 \cdot 10^4$ $1.5671 \cdot 10^3$ $2.1673 \cdot 10^3$ $1.9857 \cdot 10^4$
Σ_{Π_e}	$6.1635 \cdot 10^4$	$2.9248 \cdot 10^5$	$8.1568 \cdot 10^4$

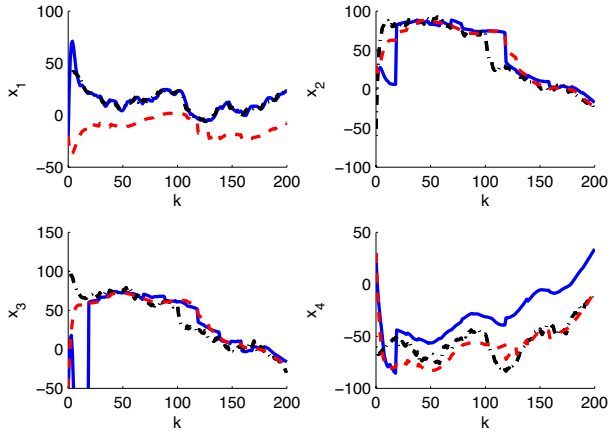

Figure 4.2: Comparison of the KF-Integral-Switch and $P^yP^zI^z-\lambda$ observers in Simulation 8 for one realization. Plant – dash-dotted line (black); KF-Integral-Switch observer – solid line (blue); $P^yP^zI^z-\lambda$ observer – dashed line (red).

compare the blue numbers), but for the rest its performance is comparable to that of the $P^yP^zI^z-\lambda$ observer. The performance of the retuned P^y-K^y observer is still better than that of the integral observers (Table 4.3), but the latter do not require retuning.

Simulation 9 – Test with time-varying disturbances caused by parametric errors and an exogenous input

For this scenario, the performance of the two integral observers are rather close when looking at the sum of the MSEs in x_2 and x_3 (Figure 4.3 and Table 4.4 - compare the blue numbers). The error is slightly smaller for the KF-Integral-Switch, which is due to its faster dynamics that, in this case, not only result in an initial overshoot but also in a better tracking later on.

Both integral observers provide better results than the retuned P^y-K^y observer. Hence, although the disturbances are varying continuously, integral observers are able to compensate their effect to a certain extent, given that their dynamics are sufficiently fast with respect to the dynamics of the disturbances. In this case, this is ensured for the $P^yP^zI^z-\lambda$ observer

Table 4.3: Performance of the KF-Integral-Switch, $P^y - K^y - retuned$ and $P^yP^zI^z - \lambda$ observers in Simulation 8 for $k \in [0, 200]$ over 10 realizations.

	KF-Integral-Switch Section 2.6.2	$P^y - K^y - retuned$ (3.17)	$P^yP^zI^z - \lambda$ (4.20)
$\bar{e}$	$3.4945 \cdot 10^2$ $2.6001 \cdot 10^3$ $4.9228 \cdot 10^3$ $6.4624 \cdot 10^3$	$6.9539 \cdot 10^3$ $1.7577 \cdot 10^3$ $1.7405 \cdot 10^3$ $8.4165 \cdot 10^3$	$5.0242 \cdot 10^3$ $1.7248 \cdot 10^3$ $1.8942 \cdot 10^3$ $1.9398 \cdot 10^3$
$\mathcal{V}_e$	$9.9673 \cdot 10^2$ $2.5536 \cdot 10^3$ $5.1615 \cdot 10^3$ $3.2605 \cdot 10^3$	$3.6689 \cdot 10^3$ $2.6298 \cdot 10^3$ $3.1938 \cdot 10^3$ $1.5733 \cdot 10^4$	$2.3224 \cdot 10^3$ $1.7179 \cdot 10^3$ $2.7239 \cdot 10^3$ $2.1019 \cdot 10^3$
Π_e	$8.5061 \cdot 10^3$ $1.2269 \cdot 10^5$ $8.1204 \cdot 10^5$ $2.4927 \cdot 10^5$	$2.9531 \cdot 10^5$ $5.4422 \cdot 10^4$ $7.4100 \cdot 10^4$ $5.5980 \cdot 10^5$	$1.6075 \cdot 10^5$ $5.5370 \cdot 10^4$ $8.5644 \cdot 10^4$ $4.2885 \cdot 10^4$
Σ_{Π_e}	$1.1925 \cdot 10^6$	$9.8363 \cdot 10^5$	$3.4465 \cdot 10^5$

by the constraint $|\lambda_i^*| < 0.6$, and for the KF-Integral-Switch by the choice of $Q_\alpha = I_n$.

4.7 Discussion

The observer structure $P^yP^zI^z$ has been studied in this chapter. The analytical results show that it is possible to eliminate bias in the preferred directions for piecewise-constant deterministic disturbances $\tilde{d}$. This is due to the presence of the integral states based on the infrequent z measurements. The condition for bias elimination is stability of the observer structure, which can be guaranteed by an appropriate choice of the observer gains. However, since not all the degrees of freedom associated with these gains are needed for ensuring stability, the remaining ones can be used to reduce the variance of the estimation error. The tuning of the observers can be carried out via numerical optimization, which, in addition to leading to a stable observer structure, also minimizes the estimation variance.

Several Assumptions are needed to show the above results. Assumption A.2 is needed to ensure the observability of the pair (A_c^r, L) in Section 4.2. This is the Assumption commonly seen in the estimation literature. Assumptions A.3 and A.4 ensure that, given the observer is stable, steady

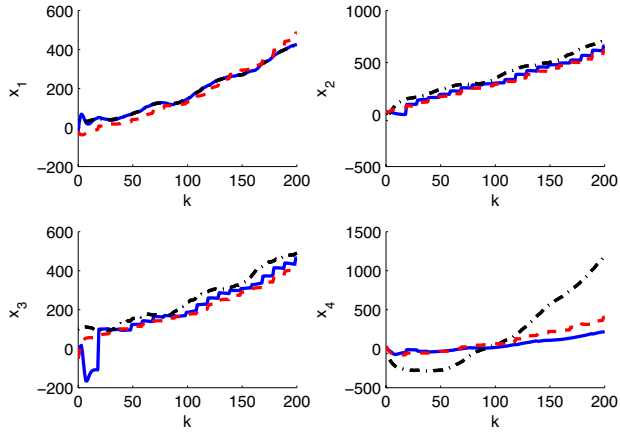

Figure 4.3: Comparison of the $P^yP^zI^z - \lambda$ and retuned $P^y - K^y$ observers in Simulation 9 for one realization. Plant – dash-dotted line (black); $P^y - K^y - retuned$ observer – solid line (blue); $P^yP^zI^z - \lambda$ observer – dashed line (red).

Table 4.4: Performance of the KF-Integral-Switch, $P^y - K^y - retuned$ and $P^yP^zI^z - \lambda$ observers in Simulation 9 for $k \in [0, 200]$ over 10 realizations.

	KF-Integral-Switch Section 2.6.2	$P^y - retuned$ (3.17)	$P^yP^zI^z - \lambda$ (4.20)
$\bar{e}$	$4.2403 \cdot 10^2$ $1.1335 \cdot 10^4$ $1.0175 \cdot 10^4$ $6.2409 \cdot 10^4$	$4.4166 \cdot 10^3$ $7.9304 \cdot 10^3$ $2.1324 \cdot 10^4$ $8.7400 \cdot 10^4$	$5.2816 \cdot 10^3$ $1.5574 \cdot 10^4$ $1.1416 \cdot 10^4$ $5.1692 \cdot 10^4$
$\mathcal{V}_e$	$1.0890 \cdot 10^3$ $9.2861 \cdot 10^3$ $1.5138 \cdot 10^4$ $1.5516 \cdot 10^4$	$1.9169 \cdot 10^3$ $1.2337 \cdot 10^5$ $4.7513 \cdot 10^4$ $6.9576 \cdot 10^4$	$3.3804 \cdot 10^3$ $7.0344 \cdot 10^3$ $9.9937 \cdot 10^3$ $1.0059 \cdot 10^4$
Π_e	$8.3908 \cdot 10^3$ $7.6199 \cdot 10^5$ $1.0035 \cdot 10^6$ $3.2195 \cdot 10^7$	$1.8639 \cdot 10^5$ $6.0565 \cdot 10^5$ $3.4001 \cdot 10^6$ $6.3908 \cdot 10^7$	$1.8927 \cdot 10^5$ $1.3297 \cdot 10^6$ $7.9789 \cdot 10^5$ $2.1332 \cdot 10^7$
Σ_{Π_e}	$3.3969 \cdot 10^7$	$6.8100 \cdot 10^7$	$2.3649 \cdot 10^7$

state is reached for each value of the piecewise-constant disturbances $\tilde{d}$. In this way, the steady-state performance of the observers is studied for various constant input values.

Note that the mathematical proof of observer performance in Theorem 4.2 requires Assumptions A.3 and A.4, that is, to have the integrator converge to steady state. However, since in a more general framework the disturbance d_k might be varying continuously, these two Assumptions might not be satisfied. Nevertheless, by choosing the observer dynamics significantly faster than the disturbance dynamics, integral observers will help to reduce the estimation bias. This rule of thumb has been illustrated in Section 4.6, where eigenvalues with absolute values smaller than 0.6 were imposed in the optimization problems (4.20) and (4.24). As a result, the integral observer is able to track the continuously varying disturbance relatively well (Simulation 9). The next chapter will also illustrate the effectiveness of this rule of thumb.

Performance similar to that of the $P^yP^zI^z$ observer is obtained with a Kalman filter extended with integrators. Since not all state directions can be measured in the illustration example ($\text{rank}(H) < n$), there are redundant integrators in the KF-Integral-Switch observer. The eigenvalues corresponding to these integrators cannot be influenced and are on the unit circle. As a consequence, the poles of the Kalman filter extended with integrators cannot be chosen arbitrarily and there is no theoretical guarantee that the dynamics of this observer can be made arbitrarily fast. The contribution of this chapter is to provide an observer structure ($P^yP^zI^z$) for which arbitrary pole placement can be guaranteed. This is ensured by the use of only as many integrators as there are preferred variables, which eliminates the redundancy and the poles that are on the unit circle.

However, in practice, ensuring arbitrary pole placement in the $P^yP^zI^z$ observer does not lead to a better estimation performance compared to the Kalman filter extended with integrators, which is already available in the literature. From an implementation point of view, the advantage of the $P^yP^zI^z$ observer is its simpler structure compared to the KF-Integral-Switch observer. In preferential estimation, the error caused by deterministic disturbances is more important than the error caused by stochastic ones. Hence, the Kalman recursion designed for noise filtering can be omit-

ted. In this way, the performance loss in the estimates is minimal. Additionally, there are no redundant integrators in the $P^yP^zI^z$ observer. As a consequence, significantly less computation is needed for both tuning and implementation, due to the constant gains and non-redundant structure of the $P^yP^zI^z$ observer. This advantage is illustrated in the next chapter.

Chapter 5

Experimental study of a fed-batch filamentous fungal fermentation

Filamentous fungi are among the most frequently used cell factories in the fermentation industry. Their success is due to the relatively well-established fermentation technology and the versatility of strains available, thus allowing the production of a wide variety of products: primary metabolites, antibiotics, enzymes, and proteins [57].

Traditionally, filamentous fungal fermentations are operated in fed-batch mode. As a result of the filamentous structure of the biomass, its concentration is considerably higher than in other biological processes. High biomass concentration induces high viscosity, which makes oxygen transfer difficult [50]. Insufficient concentrations of dissolved oxygen, however, can lower the performance of the microorganisms and, thus, production. Hence, it is important to monitor and control the biomass and product concentrations as accurately as possible. In general, these quantities are measurable only at low frequency, due to the complex operations involved in the measurement process [59, 61]. One possibility to extrapolate these measurements to a time scale appropriate for control is to estimate these quantities based on a process model.

The filamentous fungal considered here is an α-amylase producing strain of *Aspergillus oryzae* used in the pilot plant of Novozymes A/S, Bagsvaerd, Denmark. A first-principles model of this filamentous fungal fermentation process is proposed in [1, 14], while a data-driven model is described in [68]. Here, the first-principles model from [14] is used, which provides a description of biomass, glucose and enzyme concentrations, as well as the

influence on these concentrations of limiting dissolved oxygen. However, although the model was fitted on experimental data, its extrapolative power for operating conditions different from those used for fitting remains poor. The accuracy of the model is especially sensitive to variations in the initial substrate concentration.

This bioprocess is considered to be a case study for preferential estimation. The objective is to estimate accurately the biomass and enzyme concentrations (preferred variables) on the basis of a first-principles model with an important model-plant mismatch under certain operating conditions (deterministic disturbances) and infrequent measurements of the preferred variables.

Section 5.1 describes the process under consideration and its operation in industry. Section 5.2 details a first-principles model of filamentous fungal fermentation. Section 5.3 presents the observer structures used for preferential estimation. Results based on experimental data from the pilot plant at Novozymes are shown in Section 5.4. A discussion closes the chapter in Section 5.5

5.1 Process description and industrial practice

Fungal fermentation

The process studied in this paper is the α-amylase production by *Aspergillus oryzae*. The same substrate is consumed for both biomass growth and enzyme production. The main difficulty with this process is oxygen limitation in the liquid phase. This depletion is usually caused by high biomass concentration, which, due to its filamentous structure, increases the viscosity and makes oxygen transfer difficult.

5.1.1 Current operation

The fermentation at Novozymes Pilot Plant, (Bagsvaerd, Denmark) is carried out in a 2500 L stirred vessel. pH is controlled through dosing ammonia (gas) and phosphoric acid. The fermenter is aerated at the constant rate

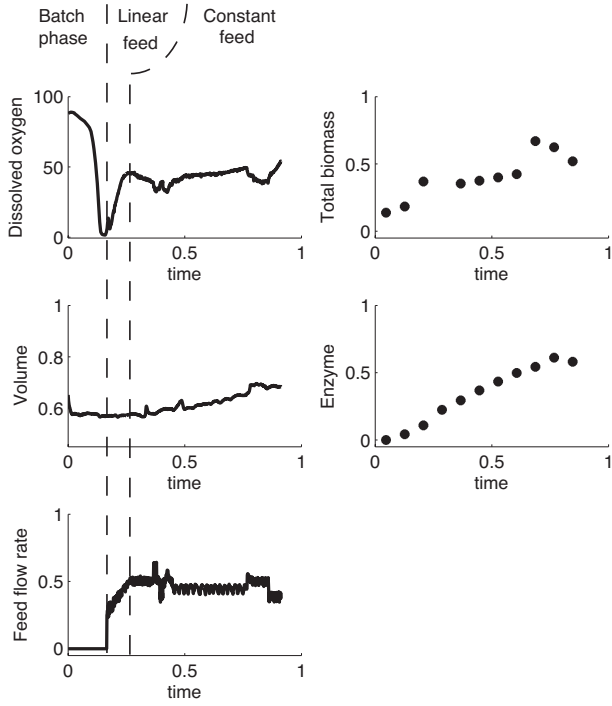

Figure 5.1: Experiment I - Current operation with three phases: Batch operation - biomass growth; Linearly-increasing feed - avoiding oxygen limitation; Constant feed - enzyme production.

of 1 vvm and agitation speed of 275 rpm. Temperature and pressure are kept at a constant level by the process control system DeltaV from Fisher Rosemount.

The typical way of operating the fermentation process is presented in Figure 5.1. For the sake of confidentiality, the experimental results have been normalized and thus no measurement units are presented. The substrate feeding policy consists of:

1. A batch phase, during which the substrate concentration is reduced from a high initial value, favorable to biomass growth, to its operational range,

2. A linearly-increasing feed rate whose role is to avoid oxygen limitation in the early phase of the fed-batch, and

3. A 'constant' feed rate that is chosen in order to keep the substrate concentration at a low level, favorable to product formation, and keep the dissolved oxygen above the limiting region ($< 25\%$).

Note that, in the third phase of the batch, the feed rate deviates from the constant value of 0.5. This is done on purpose to excite the oxygen dynamics and provide a data set rich in information for parameter identification.

As can be seen in Figure 5.1, the measurements of the total biomass and enzyme are available infrequently. Additionally, the biomass measurements are not always reliable, as can be seen at time instant 0.3. Hence, frequent estimates of total biomass and enzyme are required in order to be able to implement a control law maximizing production while avoiding oxygen limitation.

5.1.2 Measurements

The measurements available on-line are the volume V, the viscosity η, the dissolved oxygen concentration DO, the aeration rate Q_g, the amount of oxygen consumed $\Delta[O_2]$, and the amount of carbon dioxide produced $\Delta[CO_2]$.

The volume is calculated from mass measurements, assuming constant density throughout the fermentation. The viscosity is determined by a

viscosimeter from Hydramotion, York, England. DO is determined by an Ingold electrode from Mettler Toledo. The oxygen and carbon dioxide concentrations in the exhaust gases are determined by a mass spectrometer (VG Prima dB) from Thermo.

The oxygen uptake rate OUR and the carbon dioxide evolution rate CER are determined from gas analysis. The inlet flow rate is measured, as are the mass fractions of oxygen and carbon dioxide in the inlet and the outlet flows. By using these quantities and a nitrogen (inert) balance, the volumetric output gas flow rate G_{out} can be determined as follows:

$$G_{out}\, y_{N_2,out} = G_{in}\, y_{N_2,in} \tag{5.1}$$

$$G_{out} = G_{in} \frac{1 - y_{O_2,in} - y_{CO_2,in}}{1 - y_{O_2,out} - y_{CO_2,out} - y_{W,out}} \tag{5.2}$$

where

G_{out} – volumetric flow rate of the output gas (nL/h)

$y_{N_2,out}$ – mass fraction of nitrogen in output

G_{in} – volumetric flow rate of the input gas (nL/h)

$y_{N_2,in}$ – mass fraction of nitrogen in input

$y_{O_2,in}$ – mass fraction of oxygen in input

$y_{O_2,out}$ – mass fraction of oxygen in output

$y_{CO_2,out}$ – mass fraction of carbon dioxide in output

$y_{W,out}$ – mass fraction of water in output

The mass fraction of water in the output can be calculated from measurement of the dilution of oxygen by purging the reactor without any reaction [37]:

$$y_{W,out} = y_{O_2,in} - y_{O_2,out} \tag{5.3}$$

Once the output gas flow rate has been computed, OUR and CER can be determined from balance equations without accumulation terms:

$$OUR = \frac{G_{in}\, y_{O_2,in} - G_{out}\, y_{O_2,out}}{V} \frac{\rho}{M_{O_2}} \tag{5.4}$$

$$CER = \frac{G_{out}\, y_{CO_2,out} - G_{in}\, y_{CO_2,in}}{V} \frac{\rho}{M_{CO_2}} \tag{5.5}$$

where ρ is the average density of the gas flow, while M_{O_2} and M_{CO_2} are the molecular weights for oxygen and carbon dioxide, respectively.

Note that, in general, an acceptable approximation is to simply consider OUR $\approx$ OTR, since the solubility of oxygen is very low [66]. Typically, the same does not hold for CER and CTR as the solubility of carbon dioxide depends on the physical and chemical properties of the medium, such as temperature and pH. However, since here the fermentor is operated at constant temperature, pressure and pH in the fed-batch phase, it can be assumed that the rate at which CO_2 is formed by microbial metabolism corresponds to the carbon dioxide transfer rate and thus CER $\approx$ CTR.

The infrequent measurements available are the biomass dry weight and the enzyme activity. In order to determine the biomass dry weight, a separation step using centrifugation is needed first. Then, the wet biomass is dried and its mass measured. The enzyme activity is measured by the amount of starch it hydrolyzes within a given time interval. The methods used for measuring biomass and enzyme are described in [1]. All these operations are time consuming, resulting in a large ratio of slow to fast sampling times $r = 72$. Additionally, a delay of $\theta = r - 1 = 71$ fast sampling periods is considered in the availability of the infrequent measurements. This value of the delay is the maximum possible, corresponding to the worst case scenario the observer has to face.

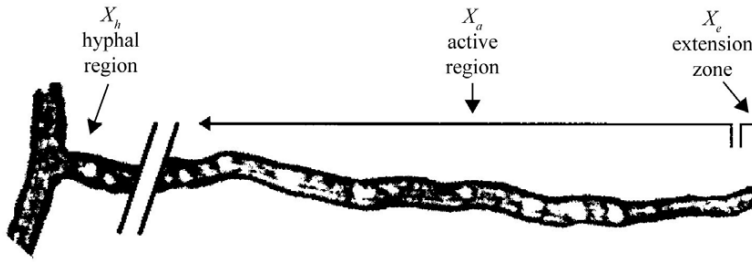

Figure 5.2: Morphological division of the biomass [1].

5.2 Filamentous fungal fermentation model

5.2.1 Morphology and rate expressions

Growth kinetics. The morphologically structured model is based on the division of the biomass into three different compartments (Figure 5.2) [1]:

- *Active region (X_a)* - responsible for the uptake of substrate and growth of the hyphal elements. It is assumed that only the active region is responsible for enzyme production.
- *Extension region (X_e)* - responsible for new cell wall generation and extension.
- *Hyphal region (X_h)* - the degenerated part of the hyphal elements that is inactive.

The macroscopic reactions for growth and production can be expressed as:

$$S + O_2 \xrightarrow{X_a} X_e \tag{5.6}$$

$$S + O_2 \xrightarrow{X_e} X_a \tag{5.7}$$

$$X_a \rightarrow X_h \tag{5.8}$$

$$S + O_2 \xrightarrow{X_a} P \tag{5.9}$$

where S stands for the substrate (glucose), O_2 for the dissolved oxygen and P for the product (α-amylase).

The corresponding kinetic expressions read:
Branching (Equation (5.6)):

$$q_1 = x_a \frac{DO}{DO + K_{DO}} \frac{k_1 s}{a_t (s + K_{s1})} \tag{5.10}$$

Growth of the active region (Equation (5.7)):

$$q_2 = a_t x_e \frac{DO}{DO + K_{DO}} \frac{k_2 s}{s + K_{s2}} \tag{5.11}$$

Differentiation (Equation (5.8)):

$$q_3 = k_3 x_a \tag{5.12}$$

The specific growth rate of total biomass is:

$$\mu = \frac{q_2}{x_t} \tag{5.13}$$

where $x_t = x_e + x_a + x_h$ represents the total biomass concentration, x_e, x_a and x_h are the concentrations of the extension, active and hyphal zones, respectively, s and DO are the substrate and dissolved oxygen concentrations, a_t represents the number of tips per unit mass of the extension zones. The parameter a_t is described as a function of μ (see [1, 10] for details concerning the morphological model). The kinetic expressions and the model parameters are presented in Appendices A.1 - A.2.

Specific rate of enzyme production. Enzyme production in filamentous fungi is a classical example of growth-associated product formation. The enzyme production is subject to glucose (substrate) inhibition and oxygen limitation:

$$r_{ps} = \left(\frac{\mu_0 s}{K_s + s + \frac{s^2}{K_I}} + k_c \frac{s}{s + K_{cor}} \right) \frac{DO}{DO + K_{DO}} \tag{5.14}$$

A Haldane expression is used to describe the substrate inhibition. The parameter k_c quantifies the constitutive level of enzyme production at high

glucose concentrations (during the batch phase).

The specific rate of dissolved oxygen consumption is expressed as:

$$r_{DO} = Y_{XO}\frac{q_2}{x_t} + Y_{PO}r_{ps}\frac{x_a}{x_t} + m_o\frac{DO}{DO + K_{DO}} \tag{5.15}$$

where Y_{XO} and Y_{PO} are the yield coefficients of dissolved oxygen consumption for growth and enzyme production, respectively, and m_o is the maintenance coefficient that represents the oxygen consumption of the biomass.

The specific rate of substrate consumption is expressed as:

$$r_s = Y_{XS}\frac{q_2}{x_t} + Y_{PS}r_{ps}\frac{x_a}{x_t} + m_s\frac{DO}{DO + K_{DO}} \tag{5.16}$$

where Y_{XS} and Y_{PS} are the yield coefficients of substrate consumption for growth and enzyme production, respectively, and m_s is the maintenance coefficient (based on the total amount of biomass).

The oxygen uptake rate is modeled as:

$$OUR = \lambda r_{DO} x_t V \sigma \tag{5.17}$$

where σ is the solubility of oxygen in water while λ is a proportionality constant.

The carbon evolution rate is computed as:

$$CER = Y_{XC} q_2 \tag{5.18}$$

where Y_{XC} is the yield coefficient of carbon dioxide formation by the microorganisms.

5.2.2 Mass balance equations

Morphological states x_e, x_a and x_h

$$\begin{aligned} \dot{x}_e &= q_1 - \tfrac{F}{V}x_e, \quad x_e(0) = x_{e0} \\ \dot{x}_a &= q_2 - q_1 - q_3 - \tfrac{F}{V}x_a, \quad x_a(0) = x_{a0} \\ \dot{x}_h &= q_3 - \tfrac{F}{V}x_h, \quad x_h(0) = x_{h0} \end{aligned} \tag{5.19}$$

Glucose concentration s

$$\dot{s} = -r_s x_t + \frac{F}{V}(s_f - s), \quad s(0) = s_0 \tag{5.20}$$

Enzyme concentration p

$$\dot{p} = r_{ps} x_a - \tfrac{F}{V} p, \quad p(0) = p_0 \tag{5.21}$$

Dissolved oxygen concentration DO

$$\dot{DO} = -r_{DO} x_t + k_L a(DO^* - DO) - \frac{F}{V} DO, \quad DO(0) = DO_0 \tag{5.22}$$

Carbon dioxide concentration n_{CO_2}

$$\dot{n}_{CO_2} = CER, \quad n_{CO_2}(0) = n_{CO_2,0} \tag{5.23}$$

Volume V

$$\dot{V} = F - F_{evap}, \quad V(0) = V_0 \tag{5.24}$$

In these equations, F represents the substrate feeding rate, s_f is the substrate concentration in the feed, F_{evap} is the evaporation rate, $k_L a$ the specific gas-liquid mass transfer coefficient for oxygen, and DO^* the oxygen saturation concentration.

5.2.3 Oxygen transfer

A linear empirical relationship between $k_L a$ and viscosity is given in [14]:

$$k_L a = c_0 - c_1 \eta \tag{5.25}$$

where η represents the on-line measurement of viscosity, and c_0 and c_1 are linear regression coefficients.

Also, a linear empirical relationship is used to describe the viscosity as a function of total biomass and dissolved oxygen:

$$\eta = \eta_0 + a_X x_t - a_{DO} DO \tag{5.26}$$

where η_0, a_X, and a_{DO} are linear regression coefficients.

The model parameters were fitted and validated on experimental data from Novozymes [14]. Their numerical values are given in Appendix A.2.

5.2.4 State-space model used for preferential estimation

The model of the filamentous fungal fermentation presented before can be rewritten in the state-space form:

$$\begin{aligned} \dot{x} &= f(x,u,\pi), \qquad x(0) = x_0 \\ y &= g(x,u,\pi) \\ z &= Lx \end{aligned} \tag{5.27}$$

where

$$\begin{aligned} x &= \left[\begin{array}{cccccccc} x_e & x_a & x_h & s & p & DO & n_{CO_2} & V \end{array}\right]^T \\ u &= F \\ y &= \left[\begin{array}{ccccc} DO & V & OUR & CER & \eta \end{array}\right]^T \\ z &= \left[\begin{array}{cc} x_t & p \end{array}\right] \\ L &= \left[\begin{array}{cccccccc} 1 & 1 & 1 & 0 & 0 & 0 & 0 & 0 \\ 0 & 0 & 0 & 0 & 1 & 0 & 0 & 0 \end{array}\right] \end{aligned}$$

$f(x,u,\pi)$ are the nonlinear state equations given by (5.19) - (5.24). The first two elements of the measurement vector y are simply two elements of x, while the last three are given by (5.17), (5.18) and (5.26). Hence the measurement model $g(x,u,\pi)$ is also nonlinear. The values of the parameters π are given in Table A.1. The preferred variables are chosen to be x_t and p, and they are given by a linear relationship, using the projection matrix L.

5.3 Observer design

The observers discussed in the previous chapters are implemented, that is a P^y and a $P^yP^zI^z$ observer tuned in the preferential way. Since the model

(5.27) is nonlinear and described in continuous time, approximations have to be made in order to use the linear and discrete observers proposed in this thesis. To minimize the errors induced by these approximations, the nonlinear continuous model is used for prediction between two fast sampling instants, while the update with measurements is made at the discrete sampling instants. This continuous-discrete update will be detailed in the next subsections.

In order to quantify the performance of these observers, they should be compared to some benchmark observer. In the previous chapters, the KF-ZOH and KF-Integral-Switch observers were used as benchmarks. To implement these observers, the same continuous-discrete update is used to ensure a fair comparison. As will be discussed in the next subsection, proper tuning of the KF-ZOH is extremely time consuming, while a simple tuning based on an educated guess provides unsatisfactory results. Hence, the benchmark observers based on the KF are not appropriate for this particular case study due to the overwhelming amount of computation required for their tuning. This confirms one of the advantages of the observer structures proposed in this thesis, i.e. their straightforward structure that yields a computationally less expensive tuning and implementation.

5.3.1 Extended Kalman filter based on y_k and z_l measurements – EKF-ZOH

Filter structure

The EKF is the extension of the linear Kalman filter to nonlinear systems by a LTV approximation based on Taylor series expansion [32]. When a continous nonlinear model and discrete measurements are available, the continuous-discrete extended Kalman filter can be used [15]. In addition, the z_l measurements are also used. Since these measurements are available infrequently, they are extrapolated to the fast time scale by a zero-order hold approximation. As a consequence, an augmented measurement matrix $\mathcal{H}$ and a measurement noise covariance $\mathcal{R}$ are introduced. The filter equations are:

- *Prediction in continuous time.* The prediction of the state and co-

variance values to the time instant $t = (k+1)t_k$ is carried out by integrating the continuous nonlinear model (5.27) and the continuous version of the covariance propagation equation [32], within the time interval $kt_k \leq t \leq (k+1)t_k$:

$$\begin{aligned} \dot{\hat{x}}^- &= f(\hat{x}^-, u, \pi), \qquad \hat{x}^-(kt_k) = \hat{x}_k \\ \dot{P}^- &= AP^- + P^-A^T - P^-\mathcal{H}^T\mathcal{R}^{-1}\mathcal{H}P^- + Q, \qquad P^-(kt_k) = P_k \end{aligned} \tag{5.28}$$

where

$$\begin{aligned} A &= \left.\frac{\partial f(x,u,\pi)}{\partial x}\right|_{\hat{x}^-,u} \\ \mathcal{H} &= \begin{bmatrix} \left.\frac{\partial g(x,u,\pi)}{\partial x}\right|_{\hat{x}^-,u} \\ L \end{bmatrix} \\ \mathcal{R} &= \begin{bmatrix} R & 0 \\ 0 & Z \end{bmatrix} \end{aligned}$$

- *Correction in discrete time.* The predictions $\hat{x}^-_{k+1}$ at $t = (k+1)t_k$ given by the continuous model are corrected by the measurements at iteration k, using the discrete Kalman filter equations:

$$\begin{aligned} \hat{x}_{k+1} &= \hat{x}^-_{k+1} + \mathcal{K}^y_k \begin{bmatrix} y_k - \hat{y}_k \\ z_k - \hat{z}_k \end{bmatrix}, \qquad \hat{x}_0 = \mathrm{E}(x_o) \\ \hat{y}_k &= g(\hat{x}_k, u_k, \pi) \\ \hat{z}_k &= L\hat{x}_k \\ z_k &= \begin{cases} z_l & if \quad \frac{k+1}{r} \in \mathcal{N} \\ z_{k-1} & otherwise \end{cases} \\ \mathcal{K}^y_k &= P^-_k\mathcal{H}^T_k\left(\mathcal{H}_kP^-_k\mathcal{H}^T_k + \mathcal{R}\right)^{-1} \\ P_k &= \left(I_n - \mathcal{K}^y_k\mathcal{H}_k\right)P^-_k \end{aligned} \tag{5.29}$$

where

$$\mathcal{H}_k = \begin{bmatrix} \left.\frac{\partial g(x,u,\pi)}{\partial x}\right|_{\hat{x}_k,u_k} \\ L \end{bmatrix}$$

The advantage of the above observer is the use of the nonlinear continuous model equations $f(x,u,\pi)$ for prediction, without discretization and linearization. However, since the covariance propagation as well as the correction steps are based on the linearized Kalman filter, linearization errors are introduced by this structure. In addition, errors associated with the ZOH extrapolation of the z_l measurement are also introduced.

Filter tuning

In order to initialize the EKF-ZOH, it is necessary to determine the initial values $\mathrm{E}(x_o)$, the measurement noise covariance matrices R and Z, the process noise covariance Q and the initial estimation error covariance P_0. The initial concentrations were provided by Novozymes along with the measured data, while R and Z could be inferred from the measurements. In general, the determination of Q and P_0 is not straightforward, since they express the confidence of the user in the model [32]. To ensure a fair comparison of EKF-ZOH with the P^y and $P^y P^z I^z$ observers that are tuned based on experimental data, it was attempted to tune Q and P_0 of the EKF-ZOH observer based on experimental data. All information available about the system, that is measurements of the both outputs y_k and preferred variables z_l from Experiment I (Figure 5.1), are used to determine Q and P_0 through the following optimization problem:

$$\begin{aligned} \min_{\mathrm{diag}(Q),\,\mathrm{diag}(P_0)} \quad J = \; & \frac{1}{N_y}\sum_k \mathrm{E}\left((y_k-\hat{y}_k)^T W_y (y_k-\hat{y}_k)\right) + \\ & \frac{1}{N_z}\sum_l \mathrm{E}\left((z_l-\hat{z}_l)^T W_z (z_l-\hat{z}_l)\right) \\ s.t. \quad & (5.28)-(5.29) \end{aligned} \tag{5.30}$$

where N_y and N_z are the number of data points available for the outputs and preferred variables, respectively. W_y and W_z are diagonal weighting

matrices for y and z, respectively. In order to decrease the number of decision variables involved, Q and P_0 are taken to be diagonal.

Since the estimation error in all the measured variables is minimized and there are measurements available at two time scales, it is necessary to make the total MSEs in y and z comparable. Hence, the respective quantities are divided by the number of available data points at each time scale. Additionally, the errors are weighted to compute the total MSEs.

5.3.2 Proportional observer based on y_k measurements – P^y

Observer structure

The observer structure from Section 3.2 is used. The continuous-discrete update discussed previously is used here as well:

- *Prediction in continuous time*

  $kt_k \leq t \leq (k+1)t_k$

$$\dot{\hat{x}}^- = f(\hat{x}^-, u, \pi), \qquad \hat{x}^-(kt_k) = \hat{x}_k \tag{5.31}$$

- *Correction in discrete time*

  $t = (k+1)t_k$

$$\begin{aligned} \hat{x}_{k+1} &= \hat{x}^-_{k+1} + K^y(y_k - \hat{y}_k) \qquad \hat{x}_0 = \mathrm{E}(x_o) \\ \hat{y}_k &= g(\hat{x}_k, u_k, \pi) \\ \hat{z}_l &= L\hat{x}_{lr} \end{aligned} \tag{5.32}$$

In contrast to the EKF-ZOH, neither linearization nor extrapolation is required by the above structure.

Observer tuning

The tuning parameters are K^y. As in Optimization problem (3.17), only the error in the preferred variables z is minimized by considering the gain matrix K^y as the decision variable. Data from Experiment I is used to evaluate the objective function:

$$\begin{aligned} \min_{K^y} \quad & J = \sum_l \mathrm{E}\left((z_l - \hat{z}_l)^T W_z (z_l - \hat{z}_l)\right) \\ s.t. \quad & (5.31) - (5.32) \end{aligned} \tag{5.33}$$

5.3.3 Proportional - Proportional Integral observer based on y_k and z_l measurements – $P^y P^z I^z$

Observer structure

The observer structure from Section 4.1 is used. The continuous-discrete update is used:

- *Prediction in continuous time*

  $kt_k \leq t \leq (k+1)t_k$

$$\dot{\hat{x}}^- = f(\hat{x}^-, u, \pi), \qquad \hat{x}^-(kt_k) = \hat{x}_k \tag{5.34}$$

- *Correction in discrete time*

  $t = (k+1)t_k$

$$\begin{aligned} \hat{x}_{k+1} &= \hat{x}^-_{k+1} + K^y(y_k - \hat{y}_k) + K^\beta \beta_k + c_k K^{z,x}(z_l - \hat{z}_l), && \hat{x}_0 = \mathrm{E}(x_o) \\ \beta_{k+1} &= \beta_k + c_k K^{z,\beta}(z_l - \hat{z}_l), && \beta_0 = 0 \\ \hat{y}_k &= g(\hat{x}_k, u_k, \pi) \\ \hat{z}_l &= L\hat{x}_{lr} \\ c_k &= \begin{cases} 1 & if \quad \frac{k+r-\theta}{r} \in \mathcal{N} \\ 0 & otherwise \end{cases} \end{aligned} \tag{5.35}$$

There is neither linearization nor extrapolation in the above structure.

Observer tuning

The tuning parameters are K^y, K^β and $K^z = \begin{bmatrix} K^{z,x} \\ K^{z,\beta} \end{bmatrix}$. The tuning procedure proposed in Section 4.5 cannot be applied since the model process

considered here is nonlinear. As a consequence, it is proposed to use all the gain matrices as decision variables in the optimization problem:

$$\begin{aligned} \min_{K^y, K^\beta, K^z} \quad & J = \sum_l \mathrm{E}\left((z_l - \hat{z}_l)^T W_z (z_l - \hat{z}_l)\right) \\ s.t. \quad & (5.34) - (5.35) \end{aligned} \tag{5.36}$$

Data from Experiment I is used.

5.4 Experimental results

In order to compare the performance of the various observers, the sum of the total MSEs $\Sigma_{\Pi_{e_y}}$ and $\Sigma_{\Pi_{e_z}}$ for the output and preferred variables, respectively, are computed. These quantities are computed using the weighting matrices W_y and W_z. Note that the mean and variance values used in Section 2.7 cannot be computed, since only one experiment for a given set of initial conditions and inputs is available.

5.4.1 Model open-loop prediction capability

The prediction capability of the open-loop nonlinear model (5.27) on the data from Experiment I is presented in Figure 5.3. It can be seen that, although there are some inaccuracies in the dissolved oxygen and total biomass, the model is able to follow the dynamics of the plant. This good performance is due to the fact that the same operating conditions, except for the feed rate, were used in Experiment I as in the experiments used for model fitting and validation.

However, in Experiment II, the initial substrate concentration is reduced by a factor of 11, which is a major perturbation. Consequently, the open-loop prediction is much less accurate, as shown in Figure 5.4. This can be explained as follows. With so much less substrate to consume in the initial batch phase, the development of the biomass is greatly affected. Not only less biomass is formed, which is rather well predicted by the model, but the fraction of active biomass is also smaller. This leads to reduced enzyme production and different oxygen consumption. Even the evaporation rate is

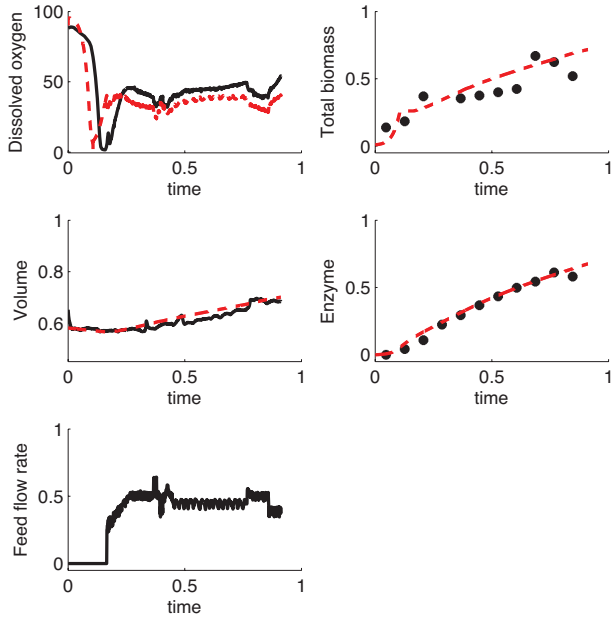

Figure 5.3: Open-loop model prediction for Experiment I. Plant – solid line and dots (black); Model – dashed line (red).

different, thus leading to a greater volume than predicted.

Hence, for the operating conditions of Experiment II, there is an important plant-model mismatch that can be interpreted as a source of deterministic disturbances. In order to improve the estimation accuracy of the preferred variables, the observers discussed previously are applied.

5.4.2 EKF-ZOH

The observer (5.28) - (5.29) is tuned by solving Optimization problem (5.30) based on data from Experiment I. Unfortunately, solving this optimization problem using the available MATLAB code would have taken several weeks

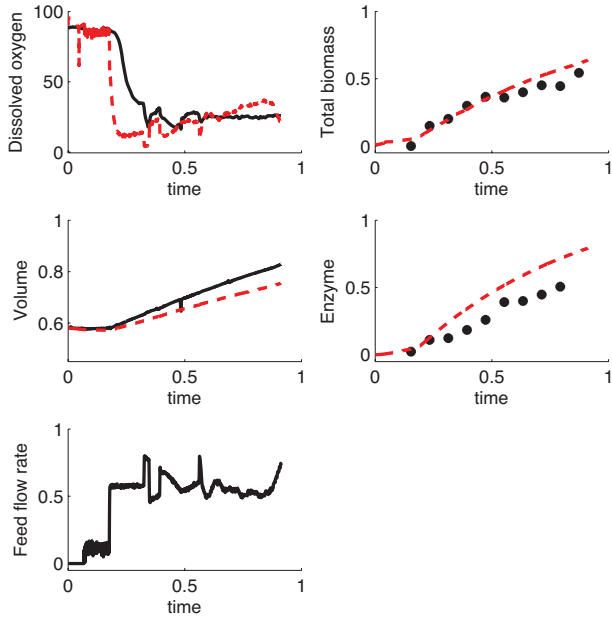

Figure 5.4: Open-loop model prediction for Experiment II. Plant – solid line and dots (black); Model – dashed line (red).

Table 5.1: Comparison of observer performances for Experiments I and II.

	$\Sigma_{\Pi_{e_y}}$	$\Sigma_{\Pi_{e_z}}$	$\Sigma_{\Pi_{e_y}}$	$\Sigma_{\Pi_{e_z}}$
Experiment	I	I	II	II
Model prediction	$7.4876 \cdot 10^2$	2.8420	$3.5293 \cdot 10^3$	$1.1391 \cdot 10^1$
EKF-ZOH	$2.3449 \cdot 10^3$	$7.0788 \cdot 10^{-1}$	$1.8329 \cdot 10^3$	3.7070
$P^y - K^y$	$6.5604 \cdot 10^3$	$4.6949 \cdot 10^{-1}$	$5.3314 \cdot 10^4$	$2.1889 \cdot 10^1$
$P^y - K^y - retuned$	–	–	$1.3913 \cdot 10^4$	$5.7903 \cdot 10^{-1}$
I^z	$6.7082 \cdot 10^2$	2.2161	$5.9265 \cdot 10^3$	4.1978
$I^z - L^T$	$1.6562 \cdot 10^3$	1.9057	$4.2074 \cdot 10^3$	2.1323

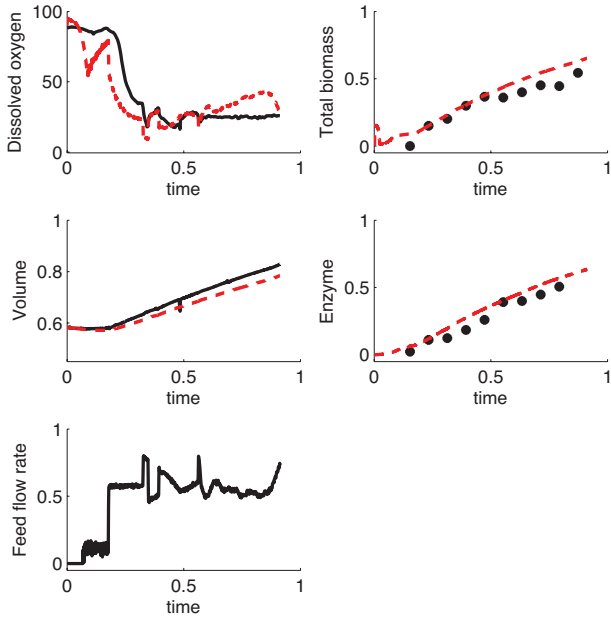

Figure 5.5: Estimates given by the EKF-ZOH for Experiment II. Plant – solid line and dots (black); EKF-ZOH observer – dashed line (red).

of computational time. Hence, this tuning method was abandoned. It was observed that the computationally most expensive step is the evaluation of the jacobians, which is repeated at each time instant. To ease the computational burden, constant jacobians are used in the tuning of the filter. The so-obtained Q and P_0 matrices are then implemented in the EKF-ZOH that updates the jacobians at each time instant. This observer is applied to data from Experiment II (Figure 5.5). The results presented in Table 5.1 show that, compared to the open-loop model prediction, the EKF-ZOH provides much better estimates. However, its tuning is not straightforward.

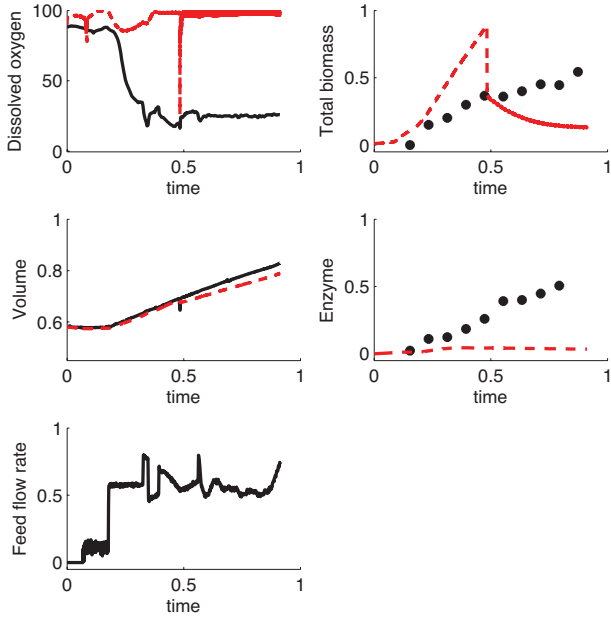

Figure 5.6: Estimates given by the $P^y - K^y$ observer for Experiment II. Plant – solid line and dots (black); P^y observer – dashed line (red).

5.4.3 P^y

The observer (5.31)-(5.32) is tuned by solving Optimization problem (5.33) based on data from Experiment I. As in Section 3.2.6, this observer is labeled $P^y - K^y$. As shown in Table 5.1, the estimation accuracy of the preferred variables is improved, while that of the outputs deteriorates. Then, the same observer is applied to the data from Experiment II, with the results presented in Figure 5.6 and Table 5.1. It can be seen that this observer is inappropriate for Experiment II. This can be explained by the presence of deterministic disturbances in Experiment II which are 'unfamiliar' to the observer gains obtained based on data from Experiment I.

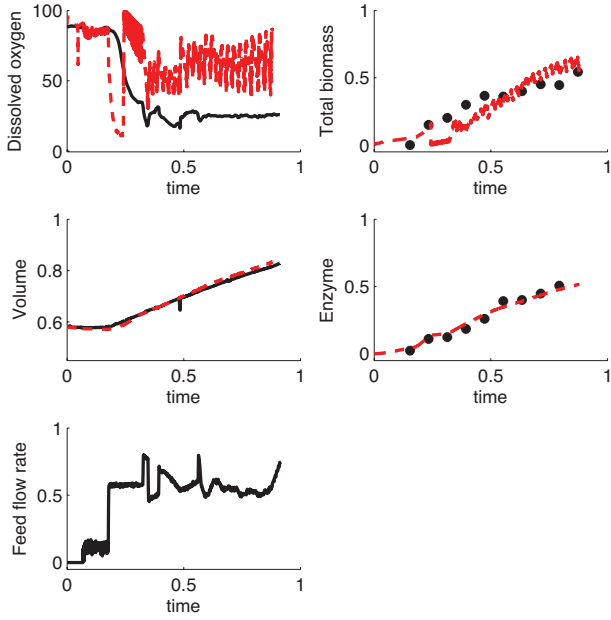

Figure 5.7: Estimates given by the $P^y - K^y - retuned$ observer for Experiment II. Plant – solid line and dots (black); $P^y - K^y - retuned$ observer – dashed line (red).

Hence, for Experiment II, it is proposed to repeat the optimization (5.33) online, each time a new z measurement becomes available. The results obtained with the retuned $P^y - K^y$ observer are presented in Figure 5.6 and Table 5.1. The biomass concentration is estimated less accurately at the beginning when only a few data points are available for tuning, but the estimates improve later on. Additionally, the continuously retuned and, thus, changing gains result in a non-smooth behavior. Nevertheless, a particularly good estimate is obtained for the enzyme concentration, which explains the smallest error in the z estimates in Table 5.1.

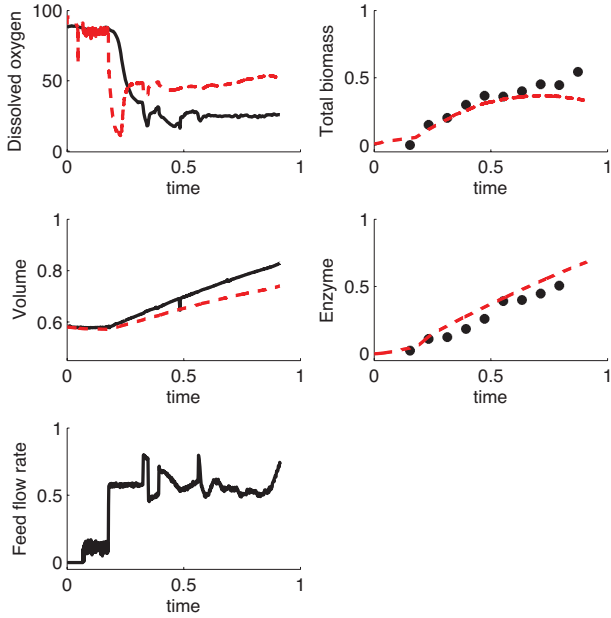

Figure 5.8: Estimates given by the I^z observer for Experiment II. Plant – solid line and dots (black); I^z observer – dashed line (red).

5.4.4 $P^y P^z I^z$

In Section 5.3.3 it is proposed to tune the observer (5.34) - (5.35) by solving Optimization problem (5.36) based on data from Experiment I. However, as seen in the previous subsection, a proportional observer with a gain matrix K^y that is tuned based on data from Experiment I is inappropriate for Experiment II, due to the change in the deterministic disturbances. Hence, retuning is needed. But, since the main advantage of an integral observer is its ability to cope with varying disturbances, the tuning of the $P^y P^z I^z$ observer is not repeated online for the conditions of Experiment II. Hence, it is better to leave out the P^y term by choosing $K^y = 0_{n \times p}$.

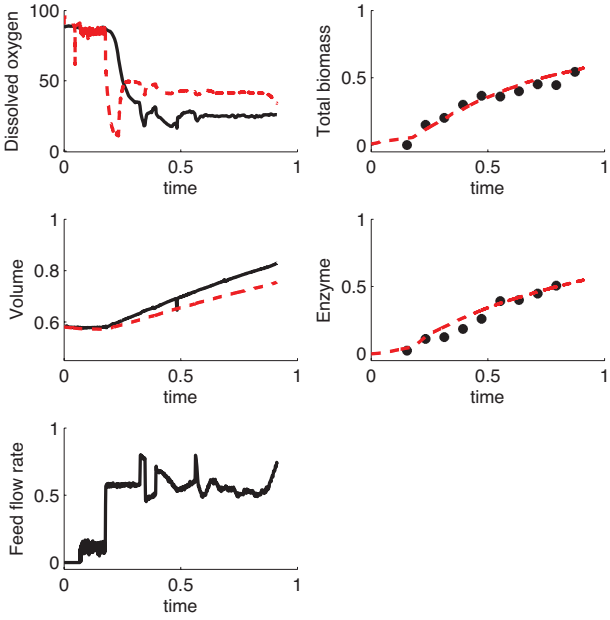

Figure 5.9: Estimates given by the $I^z - L^T$ observer for Experiment II. Plant – solid line and dots (black); $I^z - L^T$ observer – dashed line (red).

Additionally, it was seen in Section 4.6 that simple manual tuning of the $P^y P^z I^z$ observer is able to provide good estimates. By fixing $K^z = \begin{bmatrix} K^{z,x} \\ -K^{z,\beta} \end{bmatrix} = \begin{bmatrix} 0_{n\times m} \\ -I_m \end{bmatrix}$ and by an appropriate choice of K^β, results similar to those of the $P^y P^z I^z$ observer tuned in the preferential way are obtained. Note that by using $K^{z,x} = 0_{n\times m}$ the P^z term is also eliminated. A nonzero $K^{z,\beta}$ is needed for the integral term to work. As a consequence, the gain matrices $K^y = 0_{n\times p}$, $K^{z,x} = 0_{n\times m}$ and $K^{z,\beta} = I_n$ are used for this application as well. This tuning corresponds to a simple I^z observer. Optimization problem (5.36) reduces to:

$$\begin{aligned} \min_{K^\beta} \quad & J = \sum_l \mathrm{E}\left((z_l - \hat{z}_l)^T W_z (z_l - \hat{z}_l)\right) \\ s.t. \quad & (5.34) - (5.35) \\ & K^y = 0_{n\times p}, \quad K^{z,x} = 0_{n\times m}, \quad K^{z,\beta} = I_n \end{aligned} \tag{5.37}$$

The performance of the I^z observer is not fully satisfactory (Table 5.1 and Figure 5.8). A possible cause might be the higher number of parameters to tune ($n \cdot m = 16$ in the matrix K^β) than the number of measured data points available in Experiment I (11, see Figure (5.3)). As a consequence, the optimal values of these gains cannot be found.

Thus, it is proposed to reduce the number of tuning knobs even further. Simple intuition suggests the use of the integral states β to correct only the preferred variables. In other words, the gain matrix K^β could have the sparse structure of L^T, that is, all elements in K^β that correspond to a zero element in L^T should also be fixed to zero. Hence, Optimization problem (5.37) becomes:

$$\begin{aligned} \min_{k_1^\beta,\ldots,k_4^\beta} \quad & J = \sum_l \mathrm{E}\left((z_l - \hat{z}_l)^T W_z (z_l - \hat{z}_l)\right) \\ s.t. \quad & (5.34) - (5.35) \\ & K^y = 0_{n\times p}, \quad K^{z,x} = 0_{n\times m}, \quad K^{z,\beta} = I_n \\ & K^\beta = \begin{bmatrix} k_1^\beta & 0 \\ k_2^\beta & 0 \\ k_3^\beta & 0 \\ 0 & 0 \\ 0 & k_4^\beta \\ 0 & 0 \\ 0 & 0 \\ 0 & 0 \end{bmatrix} \end{aligned} \tag{5.38}$$

The resulting observer is denoted as $I^z - L^T$ and the results are shown in Table 5.1 and Figure 5.9. Its performance is the second best after the retuned $P^y - K^y$ observer. However, it provides smoother estimates,

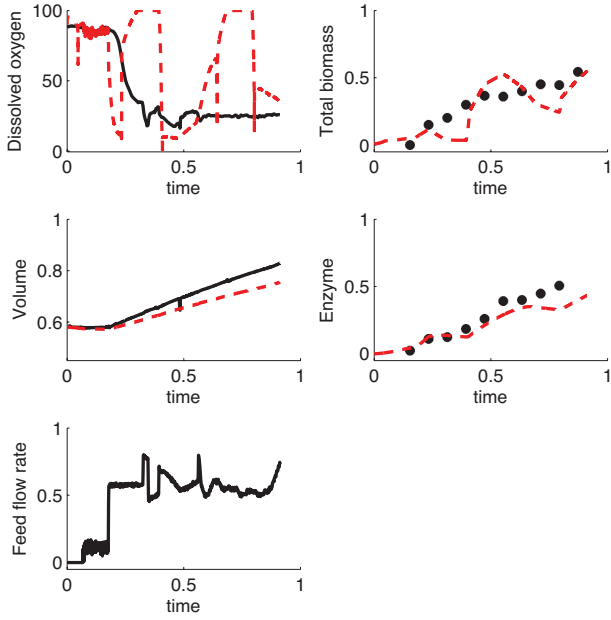

Figure 5.10: Estimates given by the $I^z - L^T$ observer with manual tuning for Experiment II. Plant – solid line and dots (black); $I^z - L^T$ observer with manual tuning – dashed line (red).

with a simple off-line tuning. Note that manual tuning of the knobs, e.g. $k_1^\beta = \cdots = k_4^\beta = 0.01$, yields an oscillatory behavior (Figure 5.10), thus demonstrating the usefulness of the calibration-based tuning given by (5.38).

5.5 Discussion

The concept of preferential estimation has been illustrated through the experimental case study of a pilot-scale fed-batch filamentous fungal fermentation. The objective is to estimate accurately the biomass and product concentrations for which only rare (r = 72) measurements are available.

Several observer structures have been implemented and their performance compared. The results confirm the insights gained from the theoretical developments in the previous chapters.

A proportional observer tuned in the preferential way $P^y - K^y$ is not able to compensate for the bias caused by deterministic disturbances not present in the tuning data. Hence, although the $P^y - K^y$ observer improves the estimation performance in Experiment I, it is not able to do so in Experiment II. However, on-line retuning of the $P^y - K^y$ observer based on data from Experiment II can eliminate the bias. The price to pay is a high computational load and a non-smooth estimate due to the continuously varying observer gain.

An integral observer can provide good estimates without being retuned. Additionally, these estimates are smoother. It was observed that the simple structure I^z can already provide improved estimation performance compared to open-loop model prediction. In this particular case, by simplifying the observer structure further and by updating only the preferred variables, even better results can be obtained ($I^z - L^T$ observer). This can be explained by the low number of data points available for tuning, which does not allow for good tuning of the numerous parameters of the full K^β gain matrix. The tuning of the $I^z - L^T$ observer is the most straightforward. However, a simple educated guess of the integral gain may not be sufficient. It is important to use the available data for calibration-based observer tuning.

The performance of the integral observers is not significantly better than that of a Kalman filter. This can be explained by the presence of a time-varying gain in the EKF-ZOH, due to the use of a time-varying linear model. By re-evaluating the jacobians using the current estimates, which are based on the z measurements, the gain of the EKF-ZOH is 'adapted' to the disturbance. In this particular case this adaptation is sufficient for bias elimination, hence, extending the Kalman filter with integrators is not needed. However, the tuning of such a filter is very time consuming, and for this case study some ad-hoc approximations had to be introduced to ease the computational burden (constant jacobians for tuning). On the contrary, using the same implementation and code, the tuning of integral observers is fast, which is an additional advantage of their simple structure.

Thus, simple guidelines for implementing preferential estimation can be

given:

1. Use an I^z term, possibly with the simplest structure $I^z - L^T$.
2. Tune the observer by a calibration-based approach, using experimental data.
3. If the resulting I^z observer is under-performing, introduce additional proportional terms, P^y and/or P^z, and repeat the calibration.

Chapter 6

Conclusions

6.1 Summary

This thesis has introduced the concept of preferential estimation. The problem of estimating accurately a subset of states has been treated in the literature either by reducing the order of the estimator to that of the subset, or by estimating all the states as accurately as possible, including the subset of interest. The novelty of preferential estimation is to use a full-order estimator to estimate the preferred subset accurately, without paying any attention to the complementary subset. This way, errors induced by order reduction are avoided.

It is shown that preferential estimation reduces or eliminates the effect of deterministic disturbances through the use of infrequent measurements of the preferred variables. The following observer structures have been proposed and studied:

- P^y

  This is the classical observer structure containing a term proportional to the frequent output measurements. Theoretical results show its ability to eliminate the effect of a constant deterministic disturbance in the preferred variables by appropriate choice of the gain K^y. The gains can be determined by numerical optimization based on the infrequent measurements of the preferred variables, thus leading to a calibration-based tuning. Since, in general, there are not enough degrees of freedom for simultaneous bias elimination and noise filtering, the P^y observer finds a compromise between the two objectives.

The advantage of this observer is its simplicity, since it contains the smallest number of tuning parameters. The disadvantage is that the observer has to be retuned for each disturbance d_k.

- $P^y P^z I^z$

  In order to have an observer that can adapt to variations of the deterministic disturbance, an integral term based on the infrequent measurement is introduced. Additionally, a term proportional to the infrequent measurements is also introduced to ensure stability of the structure. It is shown that the stability of the observer is the condition for eliminating bias in the preferred variables, for any value of the piecewise-constant disturbance $\tilde{d}$. An analytical method for choosing the observer gains is presented. Since this observer contains more tuning parameters than needed for bias elimination, the additional degrees of freedom can be used to minimize variance. These additional parameters are found via numerical optimization based on the infrequent measurements, that is, the same calibration-based tuning approach as for the P^y observer.

  The advantage of this observer is that the integral state can follow the variations of the disturbances. Nevertheless, there is no proof that the $P^y P^z I^z$ observer can eliminate bias for an arbitrary continuously-varying deterministic disturbance. However, as a rule of thumb, this observer reduces the effect of time-varying disturbances provided the observer dynamics are significantly faster than the disturbance dynamics.

Both observer structures have been applied to a pilot-scale fed-batch filamentous fungal fermentation. The experimental results show that retuning of the P^y observer is indeed necessary when the deterministic disturbances change. In contrast, such retuning is not necessary when using an integral observer. Also, it is demonstrated that a properly tuned integral observer is able to compensate for time-varying deterministic disturbances. The observer gains can be determined efficiently by the proposed calibration-based tuning. However, the noise filtering capabilities of these observers could not be assessed due to the limited amount of experimental data available.

6.2 Perspectives

The problem of preferential estimation involves three major components: the plant, the observer and the disturbances. The discussions in this thesis are limited to only some particular cases of these components: linear time-invariant plant, P^y or $P^yP^zI^z$ observers and constant or piecewise-constant disturbances. Hence, the logical continuation of the work carried out here is to extend this study to more general cases of the components of the PE problem.

- **Nonlinear plants.** The theoretical results of this thesis should be extended, first to linear and time-varying plants and, next, to nonlinear plants. A great amount of work has been carried out and reported in the literature on observers for nonlinear systems [24]. The concepts developed in this thesis could be combined with the nonlinear techniques already available.

- P^yI^z **observer.** In Sections 4.6 and 5.4.4, a particular tuning of the $P^yP^zI^z$ observer is used, with the choice of the gain matrix $K^z = \begin{bmatrix} K^{z,x} \\ -K^{z,\beta} \end{bmatrix} = \begin{bmatrix} 0_{n\times m} \\ -I_m \end{bmatrix}$, which can be interpreted as dropping the P^z term in the observer. The resulting P^yI^z observer was successfully applied, and even an I^z observer worked satisfactorily. Hence, the use of these observers for PE should be analyzed in more detail. Some results have shown that a P^yI^z observer is able to eliminate bias for single-output and mono-dimensional z plants [13]. It is desirable to extend these results to multi-output and multi-dimensional z systems as well.

- **Time-varying disturbances.** As a rule of thumb, integral observers can cope with time-varying disturbances, provided their dynamics are faster than the disturbance dynamics. This rule of thumb should be quantified. First, this would involve characterization of the disturbance. So far, only zero-order dynamics, i.e. constant disturbances, have been considered. Higher-order dynamics could be considered, and a relationship between the parameters of the disturbance model and the poles of the integral observers could be determined.

Appendix A

Kinetic expressions, model parameters and notations used in the fed-batch filamentous fermentation model

A.1 Kinetic expressions

$$k_1 = \frac{k_{bran} \cdot 10^4}{\frac{\pi}{4}(d \cdot 10^{-4})^2(1-w)f\rho} \tag{A.1}$$

$$a_t = \left(\frac{1}{2}\left(\frac{1}{2}d \cdot 10^{-4}\right)^3 \frac{4\pi}{3}(1-w)\rho\right)^{-1} \tag{A.2}$$

$$k_2 = k_{tip,max} \cdot 10^{-4}\frac{\pi}{4}\left(d \cdot 10^{-4}\right)^2 (1-w)f\rho \tag{A.3}$$

$$d = \frac{1.1 + \sqrt{1.21 + \frac{135 k_{tip,max} f s x_e}{(s+K_{s2})(x_e+x_a+x_h)}}}{2} \tag{A.4}$$

A.2 Model parameters

Table A.1: Model parameter values

Parameter	Value	Measurement unit
a_{DO}	0.04	kg/(m s %)
a_x	0.094	kg DW kg/(g m s)
c_0	67.2	h^{-1}
c_1	4.3816	m s/(kg h)
DO^*	100	%
η_0	4.185	kg/(m s)
f	80	%
F_{evap}	1.25	L/h
k_3	0.08	h^{-1}
k_{bran}	0.0017	tip / (μm h)
k_c	8	FAU kg DW/(L g h)
K_{cor}	10^{-6}	g/L
K_I	$1.5 \cdot 10^{-3}$	g glucose/L
K_{DO}	2.5	%
K_S	0.0211	g glucose /L
K_{s1}	0.003	g glucose /L
K_{s2}	0.006	g glucose /L
$k_{tip,max}$	49	μm / (tip h)
λ	0.01	1 / L
m_o	0.01	% kg DW/(g h)
m_s	0.01	kg DW g glucose /(g L h)
μ_0	227	FAU kg DW/(L g h)
ρ	1	g/cm^3
s_f	430	g glucose / L
σ	1.16	mmol / L
w	0.67	g/kg DW
Y_{XS}	1.75	g glucose kg DW / L g
Y_{PS}	$1.88 \cdot 10^{-4}$	g glucose / FAU
Y_{XO}	57	% kg DW / g
Y_{PO}	35	% L / FAU
Y_{XC}	57	mmol kg DW / L g

A.3 Notations

a_t – number of tips per unit mass (tips/(kg DW))

a_{DO} – regression coefficient (kg/(m s %))

a_x – regression coefficient (kg DW kg/(g m s))

CER – Carbon Evolution Rate (mmol/(L h))

c_0 – regression coefficient (h^{-1})

c_1 – regression coefficient (m s/ (kg h))

d – hyphal diameter (μ m)

$\Delta[CO_2]$ – change in carbon dioxide concentration over the reactor (%)

$\Delta[O_2]$ – change in oxygen concentration over the reactor (%)

DO – dissolved oxygen concentration (%)

DO^* – dissolved oxygen concentration at equilibrium (%)

η – viscosity (kg/(m s))

η_0 – regression coefficient (kg/(m s))

f – fraction of the active region (%)

F – feed flow rate (L/h)

FAU – 1 FAU is the amount of enzyme that hydrolyzes 5.26 g starch/h at 30 °C

F_{evap} – evaporation rate (L/h)

k_1 – specific branching frequency (tips/(kg DW h))

k_2 – maximal tip extension rate (kg DW/(tips h))

k_3 – rate constant (h^{-1})

k_{bran} – specific branching frequency determined by image analysis (tip/(μ m h))

k_c – constitutive α-amylase production rate (FAU kg DW/(L g h))

K_{cor} – correction constant for product formation (g glucose/L)

K_{DO} – limit value of concentration of dissolved oxygen, below which oxygen limitation occurs (%)

K_I – Haldane parameter (g glucose/L)

k_La – specific gas-liquid mass transfer coefficient (1/(L h))

K_S – Haldane parameter (g glucose/L)

K_{s1} – saturation constant for branching (g glucose /L)

K_{s2} – saturation constant for tip extension (g glucose /L)

$k_{tip,max}$ – maximal tip extension rate determined by image analysis (μm / (tip h))

λ – proportionality coefficient (1/L)

m_o – maintenance coefficient (% kg DW/(g h))

m_s – maintenance coefficient (kg DW g glucose /(g L h))

μ_0 – Haldane parameter (FAU kg DW/(L g h))

n_{CO_2} – carbon dioxide concentration (mmol / L)

OUR – Oxygen Uptake Rate (mmol/(L h))

p – α-amylase concentration (FAU / L)

p_{ref} – reference pressure (atm)

q_1 – rate of branching (g/(kg DW h))

q_2 – growth rate of the active region (g/(kg DW h))

q_3 – rate of hyphal cell formation (g/(kg DW h))

R – universal gas constant (L atm/(mmol K))

r_{DO} – oxygen consumption rate (kg DW/(g h))

r_{ps} – specific α-amylase formation rate (FAU kg DW/(L g h))

r_s – substrate consumption rate (kg DW g glucose /(g L h))

ρ – hyphal density (g/cm^3)

s – substrate concentration (g glucose / L)

s_f – feed substrate concentration (g glucose / L)

σ – solubility of oxygen in water (mmol / L)

T_{ref} – reference temeprature (K)

V – volume (L)

w – hyphal water content (g/kg DW)

x_a – concentration of active region (g/kg DW)

x_e – concentration of extension zone (g/kg DW)

x_h – concentration of hyphal region (g/kg DW)

Y_{PO} – yield coefficient for oxygen consumption for product formation (% L / FAU)

Y_{XO} – yield coefficient for oxygen consumption for growth (% kg DW / g)

Y_{PS} – yield coefficient for substrate consumption for product formation (g glucose / FAU)

Y_{XS} – yield coefficient for substrate consumption for growth (g glucose kg DW / L g)

Y_{XC} – yield coefficient for carbon dioxide formation by the biomass (mmol kg DW / L g)

Bibliography

[1] T. Agger, B. Spohr, M. Carlsen, and J. Nielsen. Growth and product formation of aspergillus oryzae during submerged cultivations: Verification of a morphologically structured model using fluorescent probes. *Biotech. Bioeng.*, 57:321–329, 1998.

[2] M. Aldeen and H. Trinh. Reduced-order linear functional observer for linear systems. *IEE Proc.-Contr. Theory Appl.*, 146(5):399–405, 1999.

[3] A. Alessandri, M. Baglietto, and G. Battistelli. Robust receding-horizon state estimation for uncertain discrete-time linear systems. *Systems and Control Letters*, 54:627–643, 2005.

[4] D. Andrisani and C. F. Gau. Estimation using a multirate filter. *IEEE Trans. Autom. Contr.*, 32(7):653–656, 1987.

[5] O. Y. Bas, B. Shafai, and S. P. Linder. Design of optimal gains for the proportional integral kalman filter with application to single particle tracking. In *Conference on Decision and Control*, pages 4567–4571, Phoenix, Arizona, USA, 1999.

[6] G. Bastin and D. Dochain. *On-line Estimation and Adaptive Control of Bioreactors*. Elsevier, 1990.

[7] S. Beale and B. Shafai. Robust control system design with a proportional integral observer. *Int. J. Contr.*, 50:97–111, 1989.

[8] O. Bernard and J. L. Gouze. Closed loop observers bundle for uncertain biotechnological models. *J. Process Contr.*, 14:765–774, 2004.

[9] D. S. Bernstein and D. C. Hyland. The optimal projection equations for reduced-order state estimation. *IEEE Trans. Autom. Contr.*, AC-30(6):583–585, 1985.

[10] L. Bodizs, B. Srinivasan, and D. Bonvin. Optimal feeding strategy for bioreactors with biomass death. In *9th International Symposium on Computer Applications in Biotechnology*, Nancy, France, 2004.

[11] L. Bodizs, B. Srinivasan, and D. Bonvin. Preferential estimation via tuning of the Kalman filter. In *Dynamics and Control of Process Systems-7*, Cambridge, MA, USA, July 2004.

[12] L. Bodizs, B. Srinivasan, and D. Bonvin. Preferential estimation for uncertain linear systems at steady state: Application to filamentous fungal fermentation. In *Conference on Decision and Control*, Seville, Spain, 2005.

[13] L. Bodizs, B. Srinivasan, and D. Bonvin. Preferential estimation for uncertain linear systems. *Comp. Chem. Eng.*, 2007. submitted.

[14] Levente Bodizs, Mariana Titica, Nuno Faria, Bala Srinivasan, Denis Dochain, and Dominique Bonvin. Oxygen Control for an Industrial Pilot-Scale Fed-Batch Filamentous Fungal Fermentation. *J. Process Contr.*, 17(7):595–606, 2007.

[15] Ph. Bogaerts and A. Vande Wouwer. Parameter identification for state estimation - application to bioprocess software sensors. *Chem. Eng. Science*, 59:2465–2476, 2004.

[16] R. G. Brown and P. Y. C. Hwang. *Introduction to Random Signals and Applied Kalman Filtering.* John Wiley, 2nd edition, 1992.

[17] E. Bullinger and F. Allgower. An adaptive high-gain observer for nonlinear systems. In *Conference on Decision and Control*, pages 4348–4353, San Diego, California, USA, 1997.

[18] K. K. Busawon and P. Kabore. On the design of integral and proportional integral observers. In *American Control Conference*, pages 3725–3729, Chicago, Illinois, USA, 2000.

[19] C. T. Chen. *Linear System Theory and Design.* Oxford University Press, 1999.

[20] J. Chen, R. J. Patton, and H. Y. Zhang. Design of unknown input observers and robust fault detection filters. *Int. J. Contr.*, 63(1):85–105, 1996.

[21] J. A. D'Appolito and C. E. Hutchinson. A minimax approach to the desing of low sensitivity state estimators. *Automatica*, 8:599–608, 1972.

[22] M. Darouach. Existence and design of functional observers for linear systems. *IEEE Trans. Autom. Contr.*, 45(5):940–943, 2000.

[23] Ph. de Valliere and D. Bonvin. Application of estimation techniques to batch reactors - II. Experimental studies in state and parameter estimation. *Comp. Chem. Eng.*, 13:11–20, 1989.

[24] D. Dochain. State and parameter estimation in chemical and biochemical processes : A tutorial. *J. Process Contr.*, 13:801–818, 2003.

[25] F. J. Doyle. Nonlinear inferential control for process applications. *J. Process Contr.*, 8:339–353, 1998.

[26] M. Farza, K. Busawon, and H. Hammouri. Simple nonlinear observers for on-line estimation of kinetic rates in bioreactors. *Automatica*, 34(3):301–318, 1998.

[27] R. A. Fisher. On an absolute criterion for fitting frequency curves. *Messenger of Math.*, 41:155, 1912.

[28] B. Friedland. Treatment of bias in recursive filtering. *IEEE Trans. Autom. Contr.*, 14:359–367, 1969.

[29] K. F. Gauss. *Theory of Motion of the Heavenly Bodies*. Dover, New York, 1963.

[30] A. M. Gibon-Fargeot, H. Hammouri, and F. Celle. Nonlinear observers for chemical reactors. *Chem. Eng. Science*, 49(14):2287–2300, 1994.

[31] J. L. Gouze, A. Rapaport, and M. Z. Hadj-Sadok. Interval observers for uncertain biological systems. *Ecological Modelling*, 133:45–56, 2000.

[32] M. S. Grewal and A. P. Andrews. *Kalman Filtering. Theory and Practice*. Prentice Hall, 1993.

[33] Y. Guan and M. Saif. A novel approach to the design of unknown input observers. *IEEE Trans. Autom. Contr.*, 36(5):632–635, 1991.

[34] D. Haessig and B. Friedland. Separate-bias estimation with reduced-order Kalman filters. *IEEE Trans. Autom. Contr.*, 43:983–987, 1998.

[35] J. Hahn and T. F. Edgar. An improved method for nonlinear model reduction using balancing of empirical gramians. *Comp. Chem. Eng.*, 26:1379–1397, 2002.

[36] R. E. Helmick, K. M. Nagpal, and C. S. Sims. Reduced-order estimation. Part 2. Smoothing. *Int. J. Contr.*, 45(6):1889–1898, 1987.

[37] C. Herwig. *On-Line Exploitation Tools for the Quantitative Analysis of Metabolic Regulations in Microbial Cultures*. PhD thesis, # 2484, Ecole Polytechnique Federale de Lausanne.

[38] M. Hou and P. C. Muller. Design of observers for linear systems with unknown inputs. *IEEE Trans. Autom. Contr.*, 37(6):871–875, 1992.

[39] M. Hou, A. C. Pugh, and P. C. Muller. Disturbance decoupled functional observers. *IEEE Trans. Autom. Contr.*, 44(2):382–386, 1999.

[40] D. C. Hyland and D. S. Bernstein. The optimal projection equations for fixed-order dynamic compensation. *IEEE Trans. Autom. Contr.*, AC-29(11):1034–1037, 1984.

[41] D. C. Hyland and D. S. Bernstein. The optimal projection equations for model reduction and the relatinoships among the methods of Wilson, Skelton, and Moore. *IEEE Trans. Autom. Contr.*, AC-30(12):1201–1211, 1985.

[42] The MathWorks Inc. *Matlab: Control System Toolbox User's Guide*. http://www.mathworks.com/access/helpdesk/help/toolbox/control/index.html.

[43] Wolfram Research Inc. *Mathematica: Control System Professional Documentation*. http://documents.wolfram.com/ applications/control/index.html.

[44] A. A. Jalali, C. S. Sims, and P. Famouri. *Reduced Order Systems*. Lecture Notes in Control and Information Sciences. Springer, 2006.

[45] A. H. Jazwinski. *Stochastic Processes and Filtering Theory*. Academic Press, 1970.

[46] T. Kailath. *Linear Systems*. Prentice Hall, 1980.

[47] T. Kailath, A. H. Sayed, and B. Hassibi. *Linear Estimation*. Prentice Hall, 2000.

[48] R.E. Kalman. A new approach to linear filtering and prediction problems. *Transaction of the ASME-Journal of Basic Engineering*, pages 35–45, 1960.

[49] J. Kautsky, N. K. Nichols, and P. Van Dooren. Robust pole assignment in linear state feedback. *Int. J. Contr.*, 41(5):1129–1155, 1985.

[50] Z. J. Li, V. Shukla, A. P. Fordyce, A. G. Pedersen, K. S. Wenger, and M. R. Marten. Fungal morphology and fragmentation behavior in fed-batch *Aspergillus oryzae* fermentation at the production scale. *Biotech. Bioeng.*, 70:300–312, 2000.

[51] L. Ljung. *System Identification - Theory for the User*. Prentice Hall, 1999.

[52] D. G. Luenberger. *Introduction to Dynamic Systems*. John Wiley, New York, 1979.

[53] D. G. Luenberger. Observing the state of a linear system. *IEEE Transactions on Military Electronics*, April 1964.

[54] W. Marquardt. Fundamental modeling and model reduction for optimization based control of transient processes. In *Chemical Process Control-6*, Tucson, Arizona, 2001.

[55] H. Martens and T. Naes. *Multivariate Calibration*. John Wiley, 1989.

[56] P. S. Maybeck. *Stochastic Models, Estimation and Control*, volume 1. Academic Press, 1979.

[57] M. McIntyre, C. Muller, J. Dynesen, and J. Nielsen. Metabolic engineering of the morphology of *Aspergillus*. *Adv. Biochem. Eng./Biotech.*, 73:104–128, 2001.

[58] J. M. Mendel. *Lessons in Digital Estimation Theory*. Prentice-Hall, 1986.

[59] A. Moser. *Bioprocess Technology. Kinetics and Reactors.* Springer-Verlag, 1988.

[60] K. M. Nagpal, R. E. Helmick, and C. S. Sims. Reduced-order estimation. Part 1. Filtering. *Int. J. Contr.*, 45(6):1867–1888, 1987.

[61] J. Nielsen and J. Villadsen. *Bioreaction Engineering Principles*. Plenum Press, New York, 1994.

[62] H. H. Niemann, J. Stoustrup, B. Shafai, and S. Beale. LTR design of proportional-integral observers. *Int. J. Rob. Nonlin. Contr.*, 5:671–693, 1995.

[63] S. Niwa, T. Masuda, and Y. Sezaki. Kalman filter with time-variable gain for a multisensor fusion system. In *IEEE International Conference on Multisensor Fusion*, pages 56–61, Taipei, Taiwan, 1999.

[64] B. A. Ogunnaike and W. H. Ray. *Process Dynamics, Modeling, and Control*. Oxford University Press, 1994.

[65] R. J. Patton and J. Chen. Optimal unknown input distribution matrix selection in robust fault diagnosis. *Automatica*, 29(4):837–841, 1993.

[66] A. G. Pedersen. k_La characterization of industrial fermentors. In 4^{th} *International Conference on Bioreactor and Bioprocess Fluid Dynamics*, Edinburgh, UK, 1997.

[67] M. Pottmann, B. A. Ogunnaike, and J. S. Schwaber. Development and implementation of a high-performance sensor system for an industrial polymer reactor. *Ind. Eng. Chem. Res.*, 44:2606–2620, 2005.

[68] J. K. Rasmussen and S. B. Jorgensen. Experimental investigation of data-driven modelling for control of fed-batch cultivation. In *IFAC World Congress*, Prague, Czech Republic, 2005.

[69] A. V. Sebald and A. H. Haddad. Robust state estimation in uncertain systems: Combined detection-estimation with incremental MSE criterion. *IEEE Trans. Autom. Contr.*, 22:821–825, 1977.

[70] D. E. Seborg, T. F. Edgar, and D. A. Mellichamp. *Process Dynamics and Control*. Wiley, 1989.

[71] C. S. Sims and J. L. Melsa. Specific optimal estimation. *IEEE Trans. Autom. Contr.*, AC-14:183–186, 1969.

[72] H. W. Smith and E. J. Davison. Design of industrial regulators: Integral feedback and feedforward control. *Proc. IEE*, 119:1210–1216, 1972.

[73] H. W. Sorenson. *Kalman Filtering: Theory and Application*. IEEE Press, 1985.

[74] M. Soroush. Nonlinear state-observer design with application to reactors. *Chem. Eng. Science*, 52:387–404, 1997.

[75] M. Soroush. State and parameter estimations and their applications in process control. *Comp. Chem. Eng.*, 23:229–245, 1998.

[76] B. Srinivasan and D. Bonvin. Real-time optimization of batch processes by tracking the necessary conditions of optimality. *Ind. Eng. Chem. Res.*, 46(2):492–504, 2007.

[77] B. Srinivasan, D. Bonvin, E. Visser, and S. Palanki. Dynamic optimization of batch processes: II. Role of measurements in handling uncertainty. *Comp. Chem. Eng.*, 27:27–44, 2003.

[78] R. Suzuki, T. Kudou, M. Ikemoto, M. Minami, and N. Kobayashi. Linear functional observer design for unknown input system and its application to disturbance attenuation problems. In *IEEE Conference on Control Applications*, pages 388–393, Toronto, Canada, 2005.

[79] R. H. C. Takahashi and P. L. D. Peres. Unknown input observers for uncertain systems: A unifying approach and enhancements. In *Conference on Decision and Control*, pages 1483–1488, Kobe, Japan, 1996.

[80] S. Tatiraju, M. Soroush, and R. Mutharasan. Multirate nonlinear state and parameter estimation in a bioreactor. *Biotech. Bioeng.*, 63:22–32, 1999.

[81] S. Tatiraju, M. Soroush, and B. A. Ogunnaike. Multirate nonlinear state estimation with application to a polymerization reactor. *AIChE J.*, 45:769–780, 1999.

[82] C. C. Tsui. A new design approach to unknown input observers. *IEEE Trans. Autom. Contr.*, 41(3):464–468, 1996.

[83] N. Wiener. *The Extrapolation, Interpolation and Smoothing of Stationary Time Series*. Wiley, New York, 1949.

[84] N. Zambare, M. Soroush, and M. C. Grady. Real-time multirate state estimation in a pilot-scale polymerization reactor. *AIChE J.*, 48:1022–1033, 2002.

[85] N. Zambare, M. Soroush, and B. A. Ogunnaike. A method of robust multirate state estimation. *J. Process Contr.*, 13:337–355, 2003.

[86] S. Y. Zhang. Generalized functional observer. *IEEE Trans. Autom. Contr.*, 35(6):733–737, 1990.

Curriculum vitae and list of publications

Bódizs Levente Csaba grew up in Suplacu de Barcău, BH, Romania in 1978. He received his diploma in chemical engineering at Universitatea Babeş-Bolyai, Cluj-Napoca, Romania in 2001. His diploma work was supervised by Dr. Zoltán K. Nagy and focused on black-box modeling and model predictive control. He joined the Laboratoire d'Automatique at EPFL in 2002 as a PhD student, under the supervision of Prof. Dominique Bonvin. His research is focused on control, optimization and state estimation in chemical and biochemical processes.

Publications

Journal Papers

1. L. Bodizs, B. Srinivasan, and D. Bonvin. Preferential estimation for uncertain linear systems. *Comp. Chem. Eng.*, 2007. submitted.

2. L. Bodizs, M. Titica, N. Faria, B. Srinivasan, D. Dochain, and D. Bonvin. Oxygen control for an industrial pilot-scale fed-batch filamentous fungal fermentation. *J. Process Contr.*, 17(7):595–606, 2007.

3. D. Bonvin, L. Bodizs, and B. Srinivasan. Optimal grade transition for polyethylene reactors via NCO tracking. *Chem. Eng. Res. Des.*, 83(A6):692–697, 2005.

Conference Papers

1. G. Goffaux, L. Bodizs, A. Vande Wouwer, Ph. Bogaerts, and Dominique Bonvin. Parameter identification to enforce practical observability of nonlinear systems. In *10th International Symposium on Computer Applications in Biotechnology*, Cancun, Mexico, 2007.

2. L. Bodizs, B. Srinivasan, and D. Bonvin. Preferential estimation for uncertain linear systems at steady state: Application to filamentous fungal fermentation. In *Conference on Decision and Control*, Seville, Spain, 2005.

3. L. Bodizs, N. Faria, M. Titica, B. Srinivasan, H. Jorgensen, D. Bonvin, and D. Dochain. Industrial experience with oxygen control of fed-batch filamentous fungal fermentation. In *IFAC World Congress*, Prague, Czech Republic, 2005.

4. D. Bonvin, L. Bodizs, and B. Srinivasan. Optimal grade transition for polyethylene reactors via NCO tracking. In *7th World Congress of Chemical Engineering*, Glasgow, Great Britain, 2005.

5. L. Bodizs, D. Bonvin, and B. Srinivasan. Run-to-run optimization of filamentous fungal fermentation. In *15th International Conference on Control Systems and Computer Science*, Bucharest, Romania, 2005.

6. L. Bodizs, B. Srinivasan, and D. Bonvin. Optimal feeding strategy for bioreactors with biomass death. In *9th International Symposium on Computer Applications in Biotechnology*, Nancy, France, 2004.

7. M. Titica, L. Bodizs, F. Lei, B. Srinivasan, D. Dochain, and D. Bonvin. Modeling and optimization of fed-batch filamentous fungal fermentation. In *BatchPro Symposium*, pages 55–65, Poros, Greece, 2004.

8. L. Bodizs, B. Srinivasan, and D. Bonvin. Preferential estimation via tuning of the Kalman filter. In *Dynamics and Control of Process Systems-7*, Cambridge, MA, USA, July 2004.

9. Z. Nagy, L. Bodizs, R. Findeisen, M. Diehl, F. Allgower, S. Agachi, H. G. Bock, and J. P. Schloder. A comparison of first principles and neural network model based nonlinear predictive control of a distillation column. In *AIChE Annual Meeting*, page 257h, Los Angeles, CA, USA, November 2000.

10. Z. Nagy, S. Agachi, and L. Bodizs. Adaptive neural network model based nonlinear predictive control of a fluid catalytic cracking unit. In Pierucci S., editor, *European Symposium on Computer Aided Process Engineering-10 (ESCAPE-10)*, pages 235–240, Florence, Italy, May 2000. Elsevier Science.